Synthetic, Kinetic and Mechanistic Studies in Early Transition Metal Systems.

I. α- and β-Hydrogen Elimination Reactions in Derivatives of Permethyltitanocene, -Zirconocene, and -Hafnocene

II. The Reactions of Aluminum Alkyls with Derivatives of Permethylniobocene

Thesis by

Christine McDade

In Partial Fulfillment of the Requirements

for the Degree of

Doctor of Philosophy

California Institute of Technology

Pasadena, California

1985

(Submitted October 23, 1984)

For Scott,

who believes

ACKNOWLEDGMENTS

This is probably the hardest part of the thesis to write, for, while the compounds described herein have been formed under vacuum and in inert atmospheres, the science that surrounds them certainly has not. The primary scientific interactions have been with that boisterous bunch known as the Bercaw group. Members of the Collins, Grubbs, and Gray groups have also provided valuable information and insight. The truly cooperative nature of the entire Chemistry Department is greatly appreciated.

The technical assistance of many individuals has been invaluable. Kevin Ott and Doug Meinhart were helpful in explaining the idiosyncracies of the JEOL. Bill Croasmun, Lucianno Mueller and other members of the Southern California Regional NMR Facility were always willing to answer queries. Al Sylwester and Burt Leland showed me the ropes of the FTIR. The assistance from members of the Mechanical, Electrical, and Glass Shops in addition to the Chemistry staff, especially Pat Anderson, is greatly appreciated.

I would like to thank Dot Lloyd for her excellent typing of this thesis.

Enthusiastic coworkers and special friends have made life in Southern California enjoyable. I'd like to thank Dean, Tippy, Wendy, Rocco, Marty and Dai for being cheerful linemates. My membership in the illustrious group the POC provided many memorable experiences and a few good philosophical arguments. Some great dinners and good bridge were had in the company of Eric, Julie, Lisa, Jim, and Maile. Layne and Laurie and Wendy and John have also been good friends.

Financial support has been provided by the National Science Foundation and the Tyler Foundation. Financial support as well as advice, friendship and

encouragement were provided by John Bercaw. His enthusiasm is infectious.

Finally, I would like to thank my family and Scott's for their love and support and their frequent admonitions to "not work too hard."

ABSTRACT

The thermal decomposition of $Cp^*_2Ti(CH_3)_2$ ($Cp^* \equiv \eta^5$-C_5Me_5) in toluene solution follows cleanly first-order kinetics and produces a single titanium product $Cp^*(C_5Me_4CH_2)Ti(CH_3)$ concurrent with the evolution of one equivalent of methane. Labeling studies using $Cp^*_2Ti(CD_3)_2$ and $(Cp^*\text{-}\underline{d}_{15})_2Ti(CH_3)_2$ show the decomposition to be intramolecular and the methane to be produced by the coupling of a methyl group with a hydrogen from the other $TiCH_3$ group. Activation parameters, $\Delta H^{\ddagger}$ and $\Delta S^{\ddagger}$, and kinetic deuterium isotope effects have been measured. The alternative decomposition pathways of α-hydrogen abstraction and α-hydrogen elimination, both leading to a titanium-methylidene intermediate, are discussed.

The insertion of unactivated acetylenes into the metal-hydride bonds of $Cp^*_2MH_2$ (M = Zr, Hf) proceeds rapidly at low temperature to form mono- and/or bisinsertion products, dependent upon the steric bulk of the acetylene substituents. $Cp^*_2M(H)(C(Me)=CHMe)$, $Cp^*_2M(H)(CH=CHCMe_3)$, $Cp^*_2M(H)(CH=CHPh)$, $Cp^*_2M(CH=CHPh)_2$, $Cp^*_2M(CH=CHCH_3)_2$ and $Cp^*_2Zr(CH=CHCH_2CH_3)_2$ have been isolated and characterized. To extend the study of unsaturated-carbon ligands, $Cp^*_2M(C\equiv CCH_3)_2$ have been prepared by treating $Cp^*_2MCl_2$ with $LiC\equiv CCH_3$. The reactivity of many of these complexes with carbon monoxide and dihydrogen is surveyed. The mono(2-butenyl) complexes $Cp^*_2M(H)(C(Me)=CHMe)$ rearrange at room temperature, forming the crotyl-hydride species $Cp^*_2M(H)(\eta^3\text{-}C_4H_7)$. The bis(propenyl) and bis(1-butenyl) zirconium complexes $Cp^*_2Zr(CH=CHR)_2$ (R = CH_3, CH_2CH_3) also rearrange, forming zirconacyclopentenes. Labeling

studies, reaction chemistry, and kinetic measurements, including deuterium isotope effects, demonstrate that the unusual β-hydrogen elimination from an sp^2-hybridized carbon is the first step in these latter rearrangements but is not observed in the former. Details of these mechanisms and the differences in reactivity of the zirconium and hafnium complexes are discussed.

The reactions of hydride- and alkyl-carbonyl derivatives of permethylniobocene with equimolar amounts of trialkylaluminum reagents occur rapidly producing the carbonyl adducts $Cp^*_2Nb(R)(COAlR'_3)$ (R = H, CH_3, CH_2CH_3, CH_2CH_2Ph, C(Me)=CHMe; R' = Me, Et). The hydride adduct $Cp^*_2NbH_3 \cdot AlEt_3$ has also been formed. In solution, each of these compounds exists in equilibrium with the uncomplexed species. The formation constants for $Cp^*_2Nb(H)(COAlR'_3)$ have been measured. They indicate the steric bulk of the Cp* ligands plays a deciding factor in the isolation of the first example of an aluminum Lewis acid bound to a carbonyl-oxygen in preference to a metal-hydride. Reactions of $Cp^*_2Nb(H)CO$ with other Lewis acids and of the one:one adducts with H_2, CO and C_2H_4 are also discussed.

$Cp^*_2Nb(H)(C_2H_4)$ also reacts with equimolar amounts of trialkylaluminum reagents, forming a one:one complex that ^1H NMR spectroscopy indicates contains a $Nb\text{-}CH_2CH_2\text{-}Al$ bridge. This adduct also exists in equilibrium with the uncomplexed species in solution. The formation constant for $Cp^*_2\overset{+}{Nb}(H)(CH_2CH_2\bar{A}lEt_3)$ has been measured. Reactions of $Cp^*_2Nb(H)(C_2H_4)$ with other Lewis acids and the reactions of $Cp^*_2\overset{+}{Nb}(H)(CH_2CH_2\bar{A}lEt_3)$ with CO and C_2H_4 are described, as are the reactions of

$Cp^*_2Nb(H)(CH_2{=}CHR)$ (R = Me, Ph), $Cp^*_2Nb(H)(CH_3C{\equiv}CCH_3)$ and $Cp^*_2Ti(C_2H_4)$ with $AlEt_3$.

TABLE OF CONTENTS

TABLE OF CONTENTS (continued)

LIST OF FIGURES

LIST OF FIGURES (continued) Page

LIST OF TABLES

LIST OF SCHEMES

ABBREVIATIONS

Anal.	elemental analysis
atm	atmosphere
br	broad
Bu	butyl, C_4H_{10}
c	central
Calcd.	calculated
CH_2CH_2Ph	phenethyl
Cp	cyclopentadienyl anion, $(\eta^5\text{-}C_5H_5)^-$
Cp*	pentamethylcyclopentadienyl anion, $(\eta^5\text{-}C_5(CH_3)_5)^-$
d	doublet
δ	NMR peak position in ppm relative to TMS as 0
DME	dimethoxyethane
Et	ethyl, $-CH_2CH_3$
eq	equation
equiv	equivalent
Fig	Figure
HOMO	highest occupied molecular orbital
h	hour
Hz	Hertz, cycles$\cdot s^{-1}$
IR	infrared spectroscopy
J	spin-spin coupling constant
k	rate constant
K	equilibrium constant

ABBREVIATIONS (continued)

κ	transmission coefficient
L	ligand
lit	literature
LUMO	lowest unoccupied molecular orbital
m	multiplet (NMR) or medium (IR)
M	metal
Me	methyl, $-CH_3$
min	minute
mL	milliliter
MO	molecular orbital
mw	molecular weight
n	normal
NMR	nuclear magnetic resonance
NOE	nuclear Overhauser enhancement
o	outer
pet. ether	40-60°C petroleum ether
Ph	phenyl, $-C_6H_5$
ppm	parts per million
Pr	propyl, $-C_3H_5$
q	quartet
R	alkyl group
s	second or singlet (NMR) or strong (IR)
sec	second

ABBREVIATIONS (continued)

t	triplet
$\underline{t}$	tertiary
T	temperature
TMS	tetramethylsilane
$t_{½}$	half-life
ν	IR stretching frequency
w	weak (IR)

CHAPTER I

A Kinetic and Mechanistic Study of the Thermolysis of Bis(pentamethylcyclopentadienyl)dimethyltitanium(IV). Evidence for α-Hydrogen Abstraction.[1]

Introduction

The organometallic chemistry of titanium(IV) provides many examples of isolable, yet thermally and photolytically unstable compounds containing Ti-C σ bonds.[2,3] Moderately stable compounds of the types TiR_4 ($R = CH_2C_6H_5$, C_6H_5, $CH_2C(CH_3)_3$, CH_2SiR_3), $TiRX_3$, $TiRX_3 \cdot L$, and $TiRX_3 \cdot L_2$ (R = alkyl, alkenyl, alkynyl, aryl; X = halide, alkoxide, amide; L = oxygen, sulfur, nitrogen, or phosphorus base) have been isolated. Evolution of RH usually accompanies decomposition, although in no case has the mechanism been fully investigated. Alkyl and aryl derivatives of dicyclopentadienyltitanium(IV) are generally more stable species, and their decomposition pathways have been more extensively studied.[4] Dvorak and coworkers have shown that the thermal decomposition of $(\eta^5\text{-}C_5H_5)_2Ti(C_6H_5)_2$ probably proceeds *via* an benzyne intermediate $[(\eta^5\text{-}C_5H_5)_2Ti(C_6H_4)]$ generated by *ortho*-hydrogen abstraction from the other phenyl group.[5]

The related compound, $(\eta^5\text{-}C_5H_5)_2Ti(CH_3)_2$ (**1**), decomposes even at room temperature, rapidly in light and more slowly in the dark.[6,7] The mechanism(s) of the decomposition of **1** have proven difficult to establish, however. Van Leeuwen *et al.* have shown by chemically induced dynamic nuclear polarization (CIDNP) studies of photochemically initiated reactions of $(\eta^5\text{-}C_5H_4Me)_2Ti(CH_3)_2$ that homolysis of the $Ti\text{-}CH_3$ bond does occur.[8] Similar studies of the pathway for the thermal decomposition of **1** are not as conclusive. The favored mechanisms involve loss of the methane *via* α-H abstraction by the other methyl group or *via* α-H elimination and subsequent reductive elimination of CH_4.[9-11] The thermal decomposition of

1 is complicated by the apparent two-stage nature of the reaction in solution: α-H abstraction yielding CH_4 and a dark solution, followed by solid-catalyzed α-H abstraction coupled with ring-hydrogen abstraction. Furthermore, there is evidence for yet another minor pathway that results in ethane production in both solution- and solid-state decompositions.[9b] Due to these complicating features, a kinetic study of the decomposition of 1 has not been feasible. In view of the increasing interest in the nature of these proposed α-H abstraction and α-H elimination processes, for example as regards their possible participation in Ziegler-Natta polymerization of olefins[12] and in the synthesis of "Tebbe's reagent" $(\eta^5\text{-}C_5H_5)_2\text{-}TiCH_2\cdot ClAl(CH_3)_2$ from $(\eta^5\text{-}C_5H_5)_2TiCl_2$ and $Al(CH_3)_3$,[13] a system more amenable to kinetic studies is clearly desirable.

The bis(pentamethylcyclopentadienyl) analogue of 1, $Cp^*_2Ti(CH_3)_2$ (2) [$Cp^* \equiv \eta^5\text{-}C_5(CH_3)_5$], has been reported to be much more stable.[14] Upon heating to 110°C in toluene solution 2 decomposes to form quantitatively a turquoise compound of known composition, $(\eta^5\text{-}C_5H_5)(C_5Me_4CH_2)TiCH_3$ (3), concurrent with the evolution of 1 equivalent of methane (eq. 1).

$$\underset{\mathbf{2}}{Cp^*_2Ti(CH_3)_2} \xrightarrow{\Delta} \underset{\mathbf{3}}{Cp^*(C_5Me_4CH_2)Ti(CH_3)} + CH_4 \qquad (1)$$

Preliminary experiments indicated that cleanly first-order kinetic results could be expected from this thermal decomposition. A kinetic and mechanistic study of the thermal decomposition of 2 involving rate

measurements taken over a range of temperatures and isotopic ^{2}H substitutions are reported herein.

Results

The thermal decomposition of $Cp^*_2Ti(CH_3)_2$ (**2**) and its deuterated analogues $Cp^*_2Ti(CD_3)_2$ (**4**) and $(Cp^*\text{-}\underline{d}_{15})_2Ti(CH_3)_2$ (**5**) in toluene solution were followed by ^1H and ^2H NMR at 98.3, 115.5, and 127.2°C. The reaction kinetics, as measured by loss of starting dimethyl compound relative to an internal ferrocene reference with time, consistently proved to be cleanly first order for greater than three half-lives. A representative plot is presented in Figure 1. The observed rate constants are summarized in Table I. Attempts to determine the rate by measuring the increase in integrated

Table I. Summary of Rate Constants for the Thermolysis of $Cp^*_2Ti(CH_3)_2$ (**2**) and Its Deuterated Analogues.

Temp, °C	$Cp^*_2Ti(CH_3)_2$ (**2**)	$Cp^*_2Ti(CD_3)_2$ (**4**)	$(Cp^*\text{-}\underline{d}_{15})_2Ti(CH_3)_2$ (**5**)
98.3	0.378(18)[a]	0.128(6)	0.382(18)
115.5	2.05(10)	0.683(32)	1.93(9)
127.2	6.07(29)	2.17(12)	5.78(27)

$\underline{k}_H/\underline{k}_D^6 = 2.92(10)$; $\underline{k}_H/\underline{k}_D^{30} = 1.03(4)$

[a]Units of 10^{-4} s^{-1} for all values of $\underline{k}_{obsd}$. The entry in parentheses is the error estimated to be one standard deviation based on repetition of the experiments. The standard deviation calculated from an analysis of residuals for any single experiment was always much smaller.

intensity of the product Ti-CY_3 (Y = H or D) resonance, even when not complicated by the presence of more than one isotopic substitution pattern

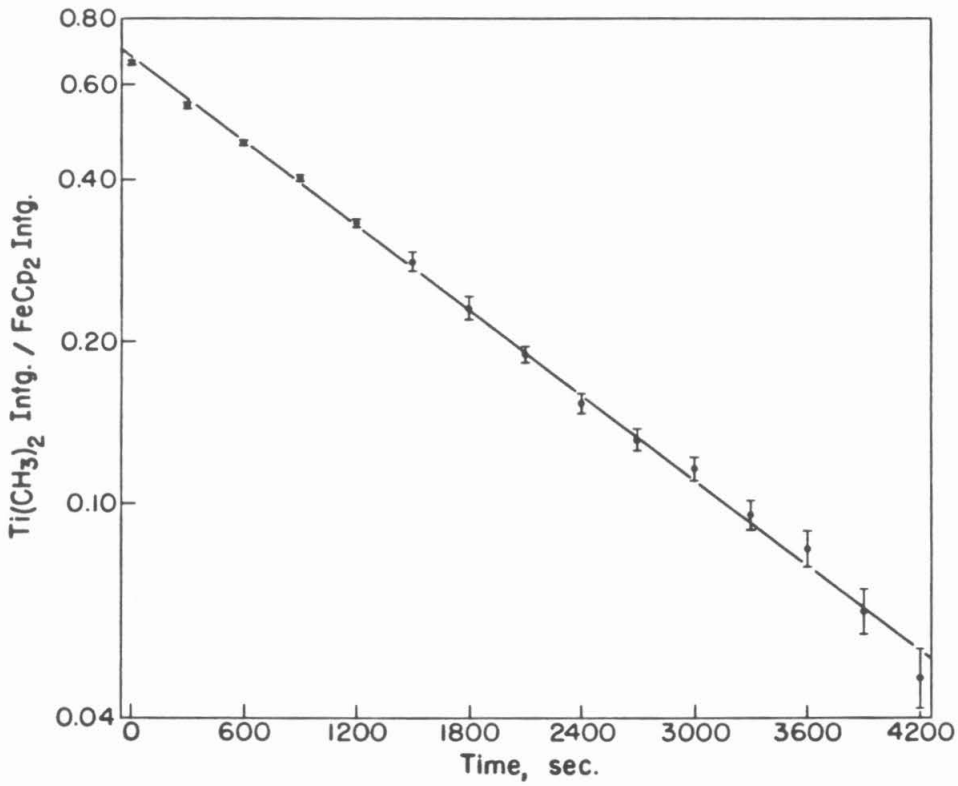

Figure 1. Representative Plot of Data from a Kinetic Run: The Thermolysis of $Cp^*_2Ti(CH_3)_2$ (2) at 127.2°C.

(vide infra), gave non-first-order plots. Rather, the plots are indicative of a subsequent, slower first-order reaction[15] in which the turquoise product **3** apparently decomposes slowly at the elevated temperatures used (eq. 2), although no new signals were observed in the NMR spectrum.

$$Cp^*_2Ti(CH_3)_2 \xrightarrow[-CH_4]{\Delta} Cp^*(C_5Me_4CH_2)TiCH_3 \xrightarrow{\Delta} ? \qquad (2)$$

Verification of the intramolecular nature of the decomposition of **2** is provided by crossover experiments. A toluene solution of $Cp^*(C_5Me_4CH_2)$-$TiCH_3$ (**3**) and $Cp^*_2Ti(CD_3)_2$ (**4**) (1:1) was heated in a sealed NMR tube at 110°C for 2 h, the time scale of most of the kinetics experiments. No evidence for Ti-CH_3 exchange was found. In fact, the ^2H NMR spectrum (observed at 76.8 MHz) for this experiment was identical with that found for the thermolysis of **4** alone (vide infra). A 1:1 toluene solution of Cp^*_2Ti-$(CH_3)_2$ (**2**) and $Cp^*_2Ti(CD_3)_2$ (**4**) was also heated at 110°C, but for 24 h, at which time most of **4** had reacted. Again this sample showed no evidence of isotope or methyl group exchange during the course of the thermolysis. The methane and titanium products were those produced by the independent thermolyses of **2** and **4**; no significant amount of CH_3D or CD_3H, expected from an exchange, was seen (vide infra).

The isotopic labeling of the thermolysis products from the decomposition of $Cp^*_2Ti(CD_3)_2$ (**4**) and $(Cp^*\text{-}\underline{d}_{15})_2Ti(CH_3)_2$ (**5**) was examined by ^1H (90- and 500.1-MHz) and ^2H (76.8-MHz) NMR, in which the upfield shifts caused by increasing deuterium substitution in CY_4 and Ti-CY_3 are clearly,

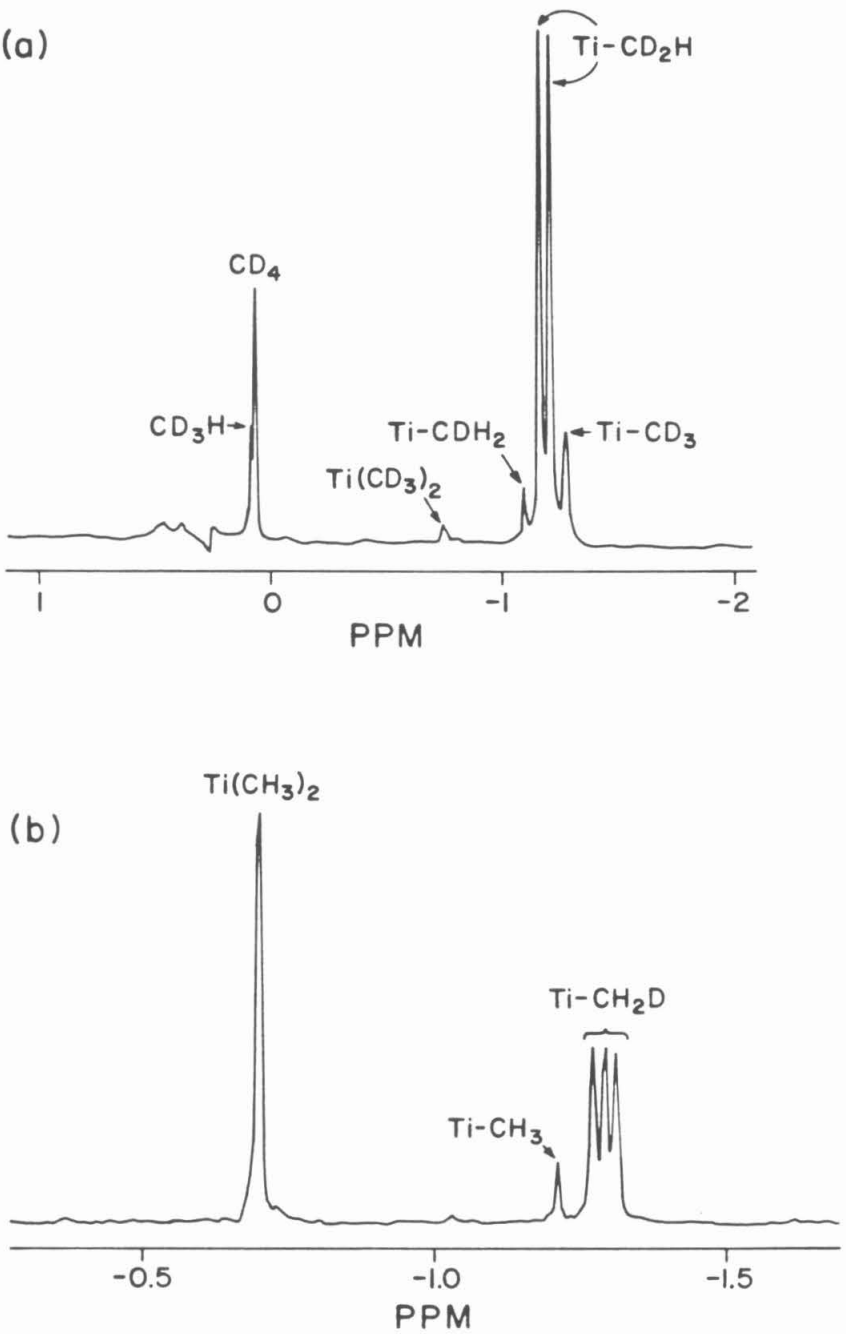

Figure 2. NMR Spectra of the Titanium-Methyl Region During Thermolysis of **4** and **5**. (a) Proton decoupled ^{2}H NMR spectrum (76.8 MHz) near the end of the thermolysis of **4**. Note the diastereotopic deuteria in $(Ti\text{-}CD_2H)$. (b) ^{1}H NMR spectrum (90 MHz) during the thermolysis of **5**.

although not base line, resolved (Fig. 2). $Cp^*(C_5Me_4CH_2)Ti(CD_2H)$ (**6**) and CD_4 are the major products from the thermolysis of **4**. $Cp^*(C_5Me_4CH_2)Ti(CDH_2)$ (**7**) and CD_3H are also observed. The product ratios were quantified by peak area determinations. As can be seen from Scheme I and Table II, the observed values agree very well with those expected for an α-abstraction or α-elimination mechanism in which the leaving methyl group couples with a hydrogen from the other $Ti-CH_3$ group only. Note that a small amount (2%) of $Cp^*(C_5Me_4CH_2)Ti(CD_3)$ (**8**) is also observed. This product is most consistent with abstraction of a ring hydrogen by a CD_3 moiety to yield CD_3H and **8**. Thus, a ring abstraction mechanism

Scheme I. Statistical Product Distribution for Thermolysis of **4** (97.0% Deuteration of $Ti-CH_3$ Groups; $Cp^* \equiv \eta^5-C_5(CH_3)_5$; $Fv^* \equiv C_5(CH_3)_4CH_2$).

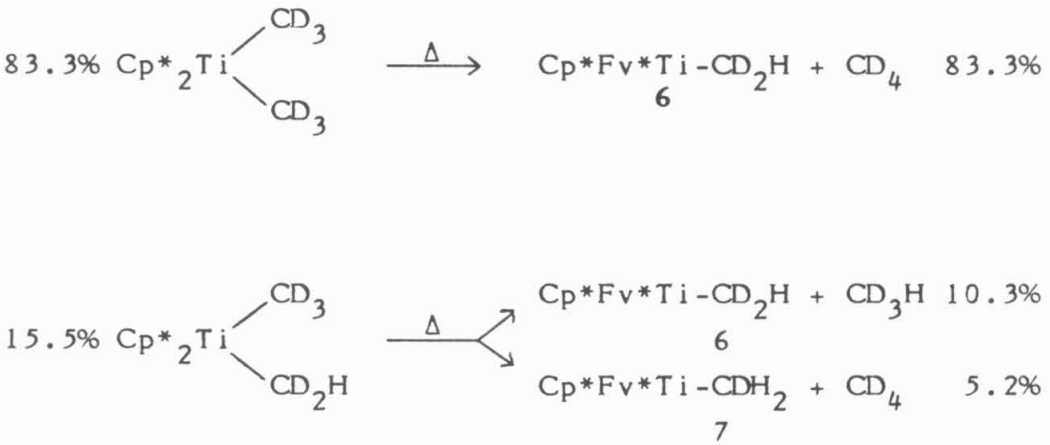

Table II. Observed Labeling Patterns and Theoretical Expectations for the Thermolyses of $Cp^*_2Ti(CD_3)_2$ (**4**) and $(Cp^*\text{-}\underline{d}_{15})_2Ti(CH_3)_2$ (**5**).

		Observed	Expected[a]
$Cp^*_2Ti(CD_3)_2$ (4)	CD_4	91(3)	88
97.0%	CD_3H	9(3)	10
	$TiCD_2H$	95(3)	94
	$TiCDH_2$	4(3)	5
	$TiCD_3$	2(1)	0
$(Cp^*\text{-}\underline{d}_{15})_2Ti(CH_3)_2$ (5)	CH_4	100(1)	100
96.9%	$TiCH_2D$	96(1)	96
	$TiCH_3$	4(1)	3

[a]Expected values are probability calculations based on the known isotopic purity of the starting compounds and calculated based on Schemes I and II. The observed isotope effect for compound **4**, if included in the calculation, does not produce significantly different values for the expected product ratio.

appears accessible in this system but represents only a very minor decomposition pathway. This will be considered further in the Discussion.

The ^1H and ^2H NMR spectra of the products of the thermolysis of $(Cp^*\text{-}\underline{d}_{15})_2Ti(CH_3)_2$ (**5**) show only CH_4 and the Ti-containing products, $(Cp^*Fv^*\text{-}\underline{d}_n)Ti(CH_2D)$ (**9**) ($Fv^* \equiv C_5(CY_3)_4CY_2$) and $(Cp^*Fv^*\text{-}\underline{d}_n)Ti(CH_3)$ (**10**) (Fig. 2) in the expected ratio (Scheme II and Table II). To the limits of detection inherent in NMR spectroscopy, an α-abstraction or α-elimination mechanism appears to be the only one operative; there is no

Scheme II. Statistical Product Distribution for Thermolysis of **5** [96.9% Deuteration of η^5-$C_5(CH_3)_5$ Groups; Cp* ≡ η^5-$C_5(CH_3)_5$; Fv* ≡ $C_5(CH_3)_4CH_2$]

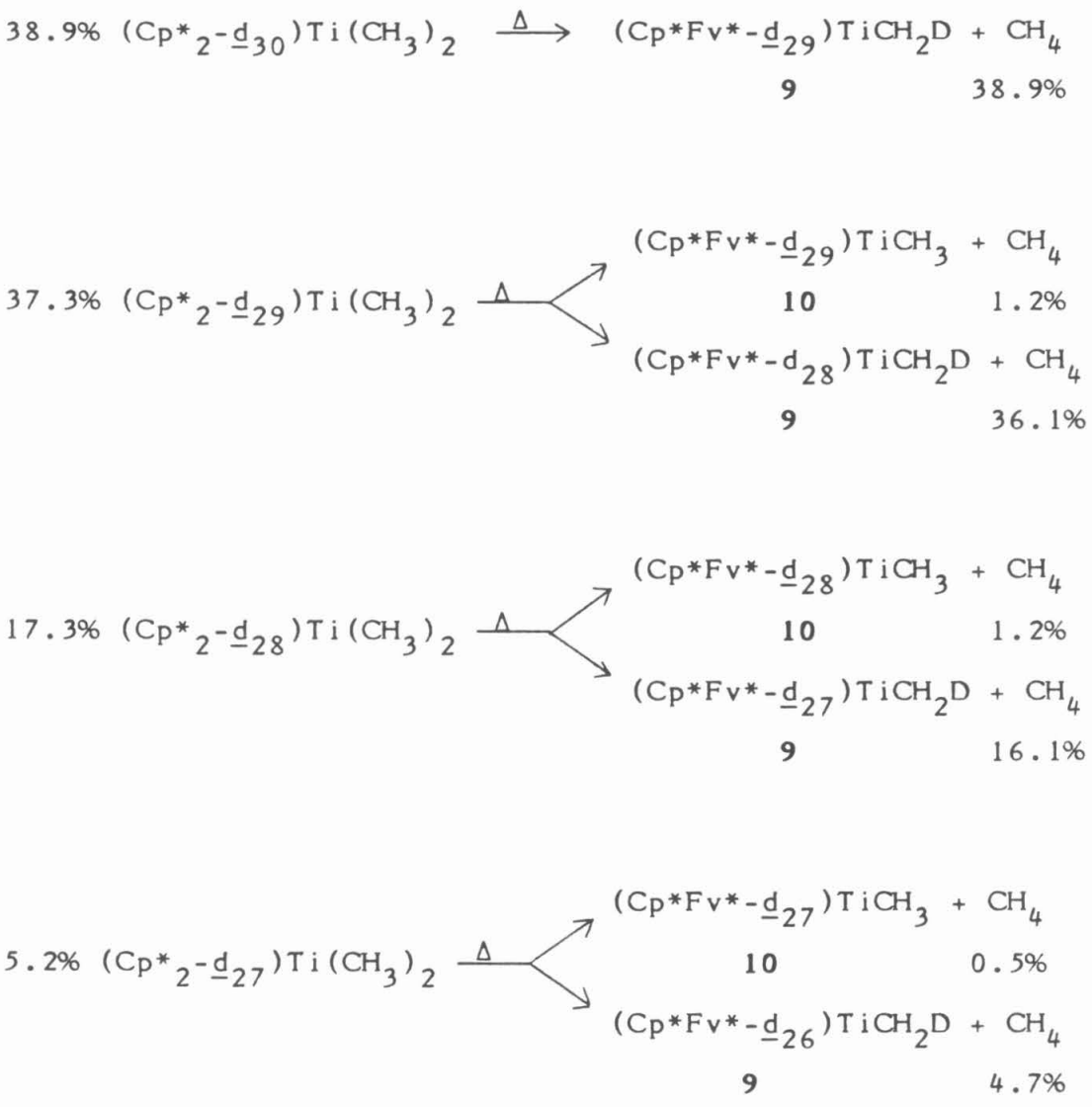

evidence for a ring-abstraction mechanism for **5**.

Returning to the kinetic data in Table I, there is a definite deuterium isotope effect on the thermolysis of $Cp^*_2Ti(CD_3)_2$ (**4**) ($\underline{k}_H/\underline{k}_D{}^6$ = 2.92 (10)), indicating that a methyl C-H bond is being broken in the transition state of the rate-determining step. In contrast, there is no significant isotope effect observed in the thermolysis of $(Cp^*\text{-}\underline{d}_{15})_2Ti(CH_3)_2$ (**5**) ($\underline{k}_H/\underline{k}_D{}^{30}$ = 1.03 (4)). Thus, while the isotopic labeling indicates a ring methyl carbon-hydrogen bond is broken in the formation of the titanium product, this must occur after the rate-determining step.

An Arrhenius plot produced from the data of the thermolysis of $Cp^*_2Ti(CH_3)_2$ (**2**) correlates very well with the expected straight line (r^2 = 1.000) (Fig. 3) and yields values at 98.3°C of 27.62 (28) kcal·mol^{-1} and 2.85 (71) eu for $\Delta H^{\ddagger}$ and $\Delta S^{\ddagger}$, respectively.

The structure of the turquoise product **3** is also of interest. Mass spectral and proton NMR data had suggested structures A and B, which may be thought of as related by resonance or, in MO theory, by assuming overlap

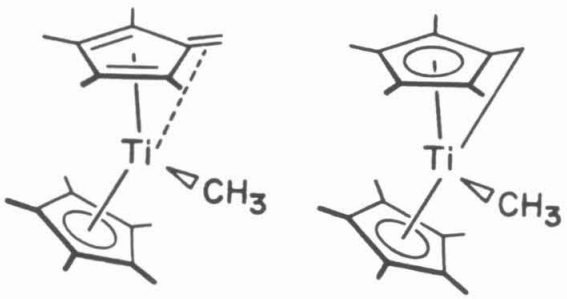

A B

of Ti atomic orbitals with those of the methyl-substituted fulvene ligand.[14] An attempt to determine an X-ray structure was unsuccessful; the crystal

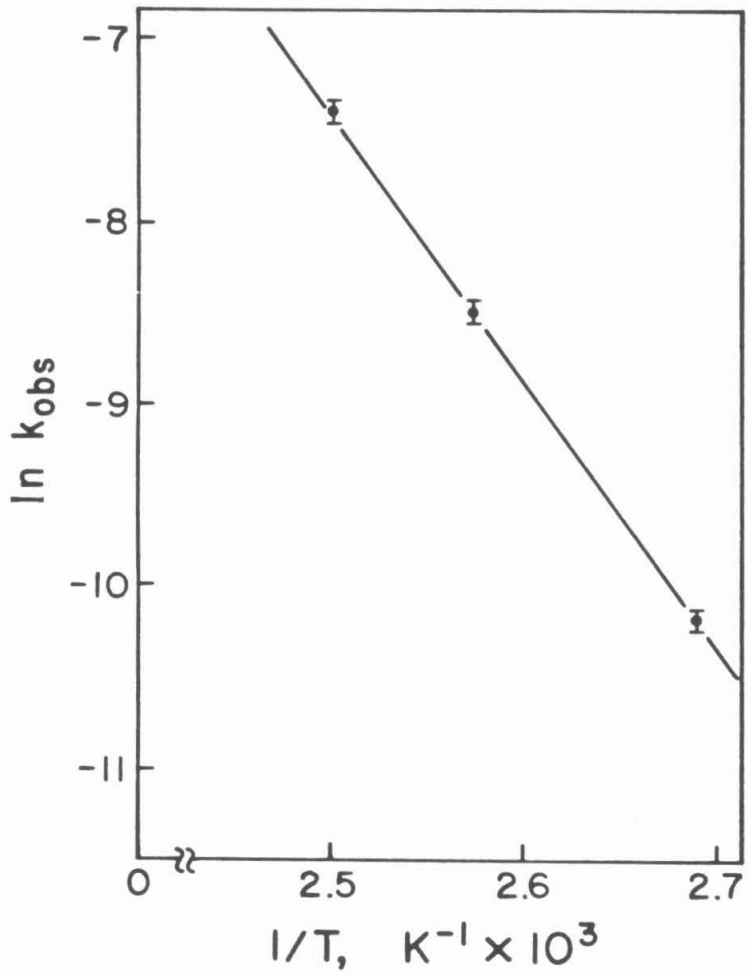

Figure 3. Arrhenius Plot for the Thermolysis of $Cp^*_2Ti(CH_3)_2$ (**2**).

was disordered.[16] However, infrared and ^{13}C and ^{1}H NMR data support A as the preferred structure. An olefinic C-H stretch at 3040 cm^{-1} is observed in the IR spectrum of **3**.[14] The ^{1}H spectrum at 500.1 MHz shows two doublets with coupling constant $^{2}J_{HH}$ = 4 Hz assigned to the diasteriotopic hydrogens of the CH_2 group. This coupling constant is more consistent with the geminal sp^2 hydrogens of structure A, normally 0-3 Hz, than with the geminal sp^3 hydrogens of structure B, normally 12-15 Hz. The gated carbon spectrum at 126.8 MHz is the most telling, however. The carbon of the CH_2 group resonates at δ 73.9 with a $^{1}J_{CH}$ = 150 Hz, values most consistent with sp^2 hybridization at carbon. The NMR data for **3** are similar to those observed for the terminal carbon atoms of the butadiene ligand in (η^4-butadiene)Ti(COT),[17,18] and (η^4-butadiene)$ZrCp_2$.[19] Note also that the σ-bound CH_3 carbon is present as a further check. It resonates further upfield (δ 41.4) with a one-bound coupling constant of 119 Hz, consistent with other observations of sp^3-carbon atoms σ bound to a metal.[20,21].

Discussion

The labeling and crossover experiments detailed above clearly show the thermal decomposition of $Cp^*_2Ti(CH_3)_2$ (**2**) occurs primarily *via* a pathway in which one of the titanium-methyl groups obtains a hydrogen from its neighboring $Ti-CH_3$ group to form methane and the reactive $(Cp^*_2Ti{=}CH_2)$ species; this rearranges to **3** *via* hydrogen migration from a ring methyl group to the methylidene ligand (Scheme III). Evidence for direct abstraction of a hydrogen from a ring-methyl group by the departing $Ti-CH_3$ group is seen only in the thermolysis of $Cp^*_2Ti(CD_3)_2$ (**4**), where this process is a very minor pathway that produces only 2% of the final product. Since a moderate, positive kinetic isotope effect slowing the rate of the principal process by a factor of three is operative in the thermolysis of **4**, it is observed that the direct ring hydrogen abstraction mechanism becomes competitive with the α-hydrogen abstraction/elimination mechanism only when the rate of the latter process is significantly slowed. Indeed, no ring-hydrogen abstraction is observed for **5**, which decomposes at the same rate as **2**.

It must be pointed out that our data do not allow us to choose between a formal α-abstraction mechanism and a formal α-elimination mechanism mediated by the titanium methylidene hydride species **12** (Scheme III). The latter possibility would require generation of an unusual d^0 methylidene species, for which the $Ti{=}CH_2$ π-bonding might resemble the $Zr{=}C{=}O$ π-bonding described for a related complex, $Cp^*_2ZrH_2(CO)$.[22] Note that both mechanisms postulate the intermediacy of a titanium-methylidene species **11**, consistent with previous suggestions in the literature.[9-11,13c]

Scheme III. Alternate Mechanisms for the Thermal Decomposition of $Cp^*_2Ti(CH_3)_2$

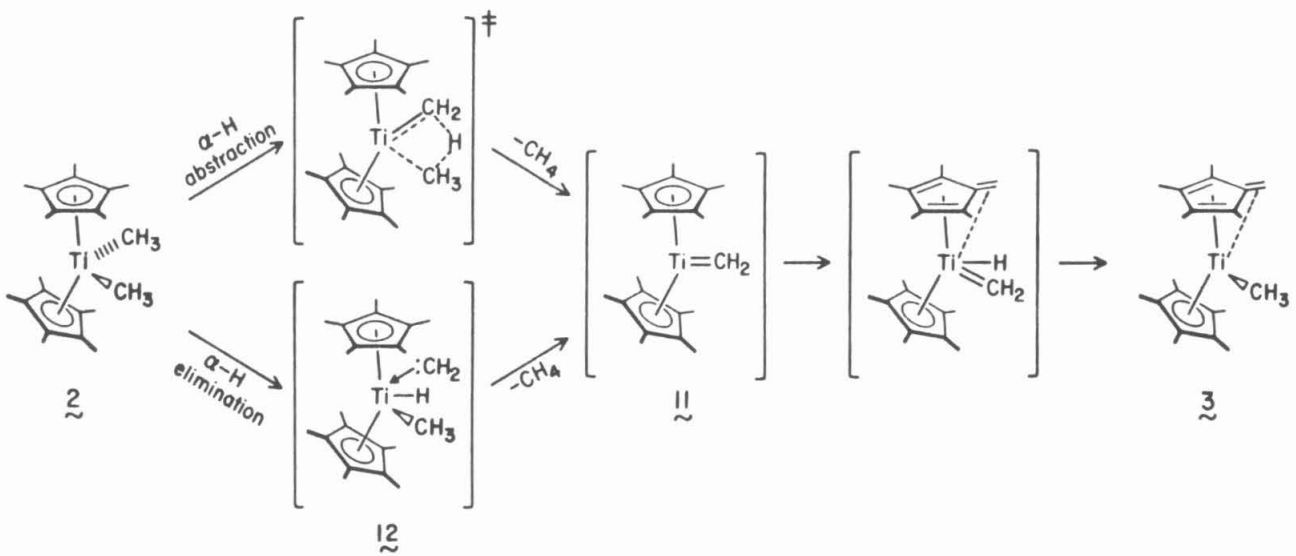

Any mechanism not mediated by this species can be excluded by the results of our labeling studies. Although a titanium-methylidene species analogous to **11** has never been directly observed, "Tebbe's Reagent", $Cp_2TiCH_2AlClMe_2$ is one example in which such a titanium-methylidene complex has apparently been sufficiently stabilized by coordination for isolation as an adduct.[13a,b] Grubbs and coworkers have further postulated that formation of titanacycles from Tebbe's Reagent and olefins results from the olefin trapping the reactive (Cp_2TiCH_2) fragment, which has been freed from $AlMe_2Cl$.[13d,e]

Attempts to trap our proposed methylidene intermediate **11** with $AlMe_2Cl$ were unsuccessful. Adding $AlMe_2Cl$ to a toluene solution of $Cp^*(C_5Me_4CH_2)Ti(CH_3)$ (**3**) in an attempt to revert it to **11** leads only to decomposition of **3**. When $AlMe_2Cl$ is added to a toluene solution of $Cp^*_2Ti(CH_3)_2$ (**2**), a loose complex is formed as proposed by Tebbe et al. for the reaction of $Cp_2Ti(CH_3)_2$ (**1**) with $AlMe_3$,[13a] so the usual thermolysis pathways are apparently prevented from operating. A reaction did occur, and methane was produced during the thermolysis; however, NMR spectra of the resultant mixtures were not readily interpretable.

Returning to the mechanism of formation of the methylidene intermediate **11**, it is striking to note the similarity of the activation energy of this process (E_a = 28 kcal·mol^{-1}) to that found by other researchers investigating the thermolysis of Cp_2TiR_2. Waters and coworkers[4] found activation energies of 20-29 kcal·mol^{-1} for the thermal decomposition of various $Cp_2Ti(R)Cl$ species. Boekel and coworkers[23] found similar values for the thermolysis of $Cp_2Ti(aryl)_2$. Waters and coworkers[4] emphasize that

these values are consistent with a published Ti-C σ-bound strength of 31 kcal·mol^{-1} and propose a caged radical mechanism.[24a] However, they neglect an earlier report of the dissociation energy of the Ti-CH_3 bond as 60 kcal·mol^{-1}.[24b] This value seems more reasonable and would discount near complete homolysis of the Ti-C bond in the transition state for these systems.

The observed activation energy thus indicates that no Ti-C or C-H bond is completely broken in the transition state of the rate-determining step. The rate-determining step, according to Scheme III, must either be methane formation (for the α-abstraction mechanism) or a 1,2-H shift to the titanium center (for the α-elimination mechanism). The observed isotopic effects yield little additional information that would allow a differentiation between these two plausible alternatives. The lack of a significant $\underline{k}_H/\underline{k}_D$[30] indicates that ring methyl C-H moieties are not an integral feature of the transition state. A similar conclusion was also reached by Boekel and coworkers in their thermolysis of $Cp_2Ti(aryl)_2$.[23] The value of $\underline{k}_H/\underline{k}_D^6 = 2.9$ is not particularly helpful either. The observed value results from a compound that is isotopically labeled in all titanium-methyl positions, so secondary effects are included. Further, the transition state is undoubtedly bent, which precludes extracting much information from the value, even if it represented only a primary kinetic isotope effect.[25,26] It is interesting to note, however, that the value of $\underline{k}_H/\underline{k}_D^6$, to the limits of our experimental error, does not vary with temperature. This suggests the isotope effect is not due to zero-point energy differences but rather is found in the pre-exponential, or entropy, term. This feature may, in turn, indicate a loosely

bound hydrogen in the transition state of the rate-determining step,[26,27] more in accord with the α-abstraction mechanism.

Conclusion

As expected, the thermal decomposition of $Cp^*_2Ti(CH_3)_2$ (**2**) proceeds cleanly with first-order loss of **2** over a 30° range of temperatures. Deuterium labeling studies and crossover experiments utilizing $Cp^*_2Ti(CD_3)_2$ (**4**) and $(Cp^*\text{-}\underline{d}_{15})_2Ti(CH_3)_2$ (**5**) demonstrate that the decomposition is unimolecular and proceeds <u>via</u> an α-hydrogen abstraction or α-hydrogen elimination mechanism. The highly reactive titanium-methylidene species **11** (Scheme III) is proposed to be a key intermediate. Thus, activation parameters and kinetic data obtained in this study are relevant to the further understanding of the possible role of such species in olefin metathesis and Ziegler-Natta polymerization.

Experimental Section

General Considerations. All manipulations were performed using glovebox or high vacuum line techniques. Solvents were purified by vacuum transfer first from $LiAlH_4$ and then from "titanocene".[14] NMR solvents were purified by vacuum transfer from activated molecular sieves (4A, Linde) and then from "titanocene". Hydrogen, deuterium, and nitrogen gases were passed over MnO on vermiculite and activated molecular sieves.[28]

^1H, ^2H, and ^{13}C NMR spectra were obtained using JEOL FX-90Q and Bruker WM-500 spectrometers. Kinetic data were obtained using the JEOL STACK*WAIT program and a thermostated probe. An example of a typical experiment is given below. Infrared spectra were recorded on a Beckman 4240 spectrophotometer.

Procedures. (1) $Cp^*_2Ti(CH_3)_2$ (2) and $Cp^*(C_5Me_4CH_2)Ti(CH_3)$ (3). Compounds **2** and **3** were prepared as previously reported.[14] They were refrigerated under N_2 until use. ^1H (500.1-MHz) and ^{13}C (125.8-MHz) spectra were obtained for **3**: ^1H data (C_6D_6, ppm relative to Me_4Si at δ 0.00) 1.77 (s, 15, Cp*), 2.03, 1.67, 1.43, 1.26 (all s, all 3, $C_5\underline{Me}_4CH_2$), 1.14, 1.92 (d,d, 1,1, $^2J_{HH}$ = 4 Hz, $C_5Me_4C\underline{H}_2$), -1.10 (s, 3, $TiC\underline{H}_3$); ^{13}C data (C_6D_6, ppm relative to C_6D_6 at δ 128.0) 118.3 (s, $\underline{C}_5Me_5$), 12.1 (q, $^1J_{CH}$ = 125 Hz, $C_5\underline{Me}_5$), 119.6, 123.9, 125.0, 126.0, 130.1 (all s, $\underline{C}_5Me_4CH_2$), 10.6, 11.1, 11.2, 14.7 (all q, $^1J_{CH}$ = 126 Hz, $C_5\underline{Me}_4CH_2$), 73.9 (t, $^1J_{CH}$ = 150 Hz, $C_5Me_4\underline{C}H_2$), 41.4 (q, $^1J_{CH}$ = 119 Hz, $Ti\underline{C}H_3$).

(2) $Cp^*_2Ti(CD_3)_2$ (4). Compound **4** was prepared in the same manner as $Cp^*_2Ti(CH_3)_2$ above, except that $LiCD_3$ (97% isotopically pure, Stohler) was added to $Cp^*_2TiCl_2$ in place of $LiCH_3$.[14] The orange crystals were

refrigerated under N_2 until use.

(3) $(Cp^*\text{-}\underline{d}_{15})_2Ti(CH_3)_2$ (5). Compound **5** was prepared from the titanium-ethylene species $Cp^*_2Ti(C_2H_4)$[29] as follows. D_2O was heated throughout a large glass bomb and a portion of the vacuum line in order to replace H^+ by D^+ at glass sites. $Cp^*_2Ti(C_2H_4)$ (1.20 g, 3.5 mmol) and toluene (20 mL) were placed in the bomb, which was then evacuated. Deuterium gas ($\sim$1.5 atm, 97% isotopically pure) was admitted to the bomb and the orange-red solution was allowed to stir at room temperature for $\sim$10 h. The bomb was evacuated, refilled with D_2, and allowed to stir five more times. After the last evacuation, DCl was admitted and the purple-red solution stirred at room temperature for 24 h. The toluene was pumped away and purple-red solid $(Cp^*\text{-}\underline{d}_{15})_2TiCl_2$ was washed out of the bomb with $CHCl_3$. The solution was evaporated to dryness and the brown solid was purified by Soxhlet extraction as previously described for $Cp^*_2TiCl_2$.[14] The yield of $(Cp^*\text{-}\underline{d}_{15})_2TiCl_2$ was 1.35 g (91%; total isotopic purity = 96.9%). The infrared spectrum (KBr pellet) of $(Cp^*\text{-}\underline{d}_{15})_2TiCl_2$, when contrasted with that of $Cp_2^*TiCl_2$, showed the expected shift to lower frequencies of the C-H(D) stretch: IR data (KBr, cm^{-1}): 2238 (m), 2192 (m), 2060 (m), 1487 (m), 1473 (m), 1099 (s), 1069 (m), 1039 (s), 829 (m), 752 (w), 680 (w), 396 (s), 358 (s), 331 (s).

$(Cp^*\text{-}\underline{d}_{15})_2TiCl_2$ (1.01 g, 2.4 mmol) was then reacted with $LiCH_3$ as described previously for $Cp^*_2Ti(CH_3)_2$.[14] Yield of $(Cp^*\text{-}\underline{d}_{15})_2Ti(CH_3)_2$ (**5**) was 0.61 g (66.8%) of orange-yellow needles. The compound was refrigerated under N_2 until use.

(4) Kinetic Measurements of Thermal Decomposition. The rates of

decomposition were followed by monitoring the decrease in integrated intensity of the $TiCH_3$ or $TiCD_3$ peak of the starting dimethyltitanocene relative to an internal, nonreacting standard of $FeCp_2$ (recrystallized from benzene) or C_6D_6, respectively. FT NMR spectra were recorded automatically at pre-set time intervals by using the JEOL FX-90Q STACK*WAIT routine. Standard ^1H and ^2H NMR accumulation parameters were used, and ^2H NMR spectra were ^1H decoupled.[30] Reaction temperatures were maintained by the JEOL probe temperature controller and were observed to be constant to within 0.4°C by measurement of the peak separation of ethylene glycol both before and after thermolyses.

A typical ^1H NMR experiment involved 40 mg of $Cp^*_2Ti(CH_3)_2$ or $(Cp^*\text{-}\underline{d}_{15})_2Ti(CH_3)_2$ and 15 mg of $FeCp_2$ dissolved in 0.3 mL of toluene-$\underline{d}_8$. A typical ^2H NMR experiment involved a similar amount of $Cp^*_2Ti(CD_3)_2$ and ~1 equiv of C_6D_6 dissolved in 0.3 mL of toluene-$\underline{d}_0$. In both cases, 2-3 atm of N_2 was sealed into the NMR tube to prevent the toluene from refluxing at the elevated temperatures used in this study.

As the decomposition progressed, the Ti-C(H or D)$_3$ resonance of the starting material lost intensity, and plots of the decay of the ratio of the methyl integration/reference compound integration as a function of time showed first-order behavior for greater than three half-lives. In experiments that were followed further, no deviation from first-order behavior was found even beyond five half-lives. As expected, the rate of decomposition was independent of the concentration of the dimethyl species over a five-fold range.

The values given in Table I are derived from the slopes of the semilog

plots. The error represents one standard deviation estimated by repetition of the experiments. An analysis of residuals for a single determination always gave a smaller estimate of the error.

An Arrhenius plot of $\underline{k}$ vs. 1/T was constructed. For the thermal decomposition of $Cp^*_2Ti(CH_3)_2$ (**2**), a least-squares fit of the data to the Arrhenius equation $\underline{k}_{obsd} = \ln A - \underline{E}_a/RT$ gives values of ln A = 28.24 and $\underline{E}_a/R = 1.427 \times 10^4$ or $A = 1.833 \times 10^{12}$ s^{-1} and $\underline{E}_a = 28.36$ kcal·mol^{-1}. $\Delta H^{\ddagger}$ and $\Delta S^{\ddagger}$ were calculated from the usual equations ($\Delta H^{\ddagger} = \underline{E}_a - RT$ and $\Delta S^{\ddagger} = R \ln (hA/\underline{k}T)$) and are presented in the body of this paper. The error for these last two values represents one standard deviation estimated from changes in the values of $-\underline{E}_a/R$ and ln A when the $\underline{k}_{obsd}$ values are varied within their error limit. Analysis of residuals for the line gave much smaller estimates.

(5) Crossover Experiments. NMR tubes containing approximately equal amounts of $Cp^*_2Ti(CH_3)_2$ (**2**) and $Cp^*_2Ti(CD_3)_2$ (**4**) or $Cp^*(C_5Me_4CH_2)Ti(CH_3)$ (**3**) and $Cp^*_2Ti(CD_3)_2$ (**4**) in toluene solution were sealed under vacuum and heated to check for any evidence of methyl exchange or any other result which might indicate intermolecular reaction. Results were negative, as discussed in the body of the chapter.

(6) Analysis of Isotopic Labeling in Thermolysis Products from $Cp^*_2Ti(CD_3)_2$ (4) and $(Cp^*\text{-}\underline{d}_{15})_2Ti(CH_3)_2$ (5). Proton-decoupled ^2H (76.8 MHz) and ^1H (90 MHz) NMR spectra of thermolyzed samples of **4** and **5**, respectively, were taken and the region of interest -- from $\delta \sim 0.2$ for the methanes to $\delta \sim -1.1$ for the titanium methyl peaks -- was expanded so that couplings and peak overlap could be clearly seen. Each

spectrum was copied and peak areas determined by a cut-and-weigh procedure. Values given in Table II are the average from several determinations and the errors given are one standard deviation (n - 1 weighting).

(7) Attempted Trapping of Titanium-Carbene Species 11. In the first of two experiments conducted, a roughly stoichiometric amount of $AlMe_2Cl$ was added to a yellow-orange toluene-$\underline{d}_8$ solution of $Cp^*_2Ti(CH_3)_2$ (**2**) (32 mg, 87 μmol) and $FeCp_2$ (140 μmol). The color changed immediately to an opaque red-orange. The tube was sealed under N_2. Red-orange crystals were noted after 1 h at room temperature. The ^1H NMR spectrum showed only resonances that could be assigned to the Cp* and methyl hydrogens. The latter appeared at δ 0.22, midway between the methyl resonances of $Cp^*_2Ti(CH_3)_2$ (**2**) (δ 0.69) and $AlMe_2Cl$ (δ -0.38). Subsequent thermolysis of this tube in the JEOL FX-90Q at 127.2°C resulted in uninterpretable ^1H NMR spectra. Methane (δ 0.18) was produced, but other resonances were not clearly resolved.

The second experiment involved adding an excess of $AlMe_2Cl$ to a turquoise toluene-$\underline{d}_8$ solution of $Cp^*(C_5Me_4CH_2)Ti(CH_3)$ (**3**) and $FeCp_2$ ($\sim$1:1). The color changed immediately to a green-brown solution which contained dark solid material. The tube was sealed under N_2. No ^1H NMR spectrum could be observed for this reaction mixture, however, suggesting the presence of paramagnetic products.

References and Notes

(1) This chapter includes previously published results. McDade, C.; Green, J. C.; Bercaw, J. E. Organometallics **1982**, 1, 1629-1634.

(2) Cotton, F. A. Chem. Rev. **1955**, 551-594.

(3) Wailes, P. C.; Coutts, R. S. P.; Weigold, H. "Organometallic Chemistry of Titanium, Zirconium, and Hafnium"; Academic Press: New York, 1974.

(4) Waters, J. A.; Vickroy, V. V.; Mortimer, G. A. J. Organomet. Chem. **1971**, 33, 41-52 and references contained therein.

(5) Dvorak, J.; O'Brien, R. J.; Santo, W. J. Chem. Soc., Chem. Commun. **1970**, 411-412.

(6) Piper, T. S.; Wilkinson, G. J. Inorg. Nucl. Chem. **1956**, 3, 104-124.

(7) Clauss, K.; Bestian, H. Liebigs Ann. Chem. **1962**, 654, 8-19.

(8) Van Leeuwen, P. W. N. M.; Van der Heijden, H.; Roobeek, C. G.; Frijns, J. H. G. J. Organomet. Chem. **1981**, 209, 169-182.

(9) (a) Erskine, G.J.; Wilson, D. A.; McCowan, J. D. J. Organomet. Chem. **1976**, 114, 119-125. (b) Erskine, G. J.; Hartgerink, J.; Weinberg, E. L.; McCowan, J. D. Ibid. **1979**, 170, 51-61.

(10) Alt, H. G.; DiSanzo, F. P.; Rausch, M. D.; Uden, P. C. J. Organomet. Chem. **1976**, 107, 257-263.

(11) Chang, B.-H.; Tung, H.-S.; Brubaker, C. H. Inorg. Chem. Acta **1981**, 51, 143-148.

(12) Ivin, K. J.; Rooney, J. J.; Stewart, C. D.; Green, M. L. H.; Mahtab, R. J. Chem. Soc., Chem. Commun. **1978**, 604-606.

(13) (a) Tebbe, F. N.; Parshall, G. W.; Reddy, G. S. J. Am. Chem. Soc.

1978, 100, 3611-3613. (b) Tebbe, F. N.; Parshall, G. W.; Ovenall, D. W. Ibid. **1979**, 101, 5074-5075. (c) Grubbs, R. H.; Miyashita, A. Ibid. **1978**, 100, 7418-7420. (d) Howard, T. R.; Lee, J. B.; Grubbs, R. H. Ibid. **1980**, 102, 6878-6880. (e) Lee, J. B.; Gadja, G. J.; Schaefer, W. P.; Howard, T. R.; Ikariya, T.; Straus, D. A.; Grubbs, R. H. Ibid. **1981**, 103, 7358-7361.

(14) (a) Bercaw, J. E.; Marvich, R. H.; Bell, L. G.; Brintzinger, H. H. J. Am. Chem. Soc. **1972**, 94, 1219-1238. (b) Bercaw, J. E.; Brintzinger, H. H. Ibid. **1971**, 93, 2045-2046.

(15) Moore, J. W.; Pearson, R. G. "Kinetics and Mechanism: A Study of Homogeneous Chemical Reactions", 3rd ed.; Wiley: New York, 1981; pp 290-296.

(16) A communication of the structure of a related species has appeared in the literature. Bis(μ-oxo)(η^1,η^5-1,2,3,4-tetramethyl-5-methylene-1,3-cyclopentadiene)bis[(methylcyclopentadienyl)titanium] is proposed to have a truly methylenic bridge to the second titanium. However, the authors present insufficient NMR and no IR data for the compound that would allow us to compare our results. Bottomley, F.; Lin, I. J. B.; White, P. S. J. Am. Chem. Soc. **1981**, 103, 703-704.

(17) Jolly, P. W.; Mynot, R. Adv. Organomet. Chem. **1981**, 19, 257-304.

(18) Fulvene has the following chemical shifts in $CDCl_3$:

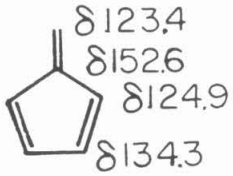

Hollenstein, R.; Philipsborn, W. V.; Vogeli, R.; Neuenschwander, M. Helv. Chim. Acta **1973**, 56, 847-860.

(19) Erker, G.; Wicher, J.; Engel, K.; Rosenfeld, F.; Dietrich, W. J. Am. Chem. Soc. **1980**, 102, 6346-6348.

(20) (a) Cohen, S. A. Ph.D. Thesis, California Institute of Technology, 1982. (b) McLain, S. J.; Wood, C. D.; Schrock, R. R. J. Am. Chem. Soc. **1977**, 99, 3519-3520.

(21) Manriquez, J. M.; McAllister, D. R.; Sanner, R. D.; Bercaw, J. E. J. Am. Chem. Soc. **1978**, 100, 2716-2724.

(22) Marsella, J. A.; Curtis, C. J.; Bercaw, J. E.; Caulton, K. G. J. Am. Chem. Soc. **1980**, 102, 7244-7246.

(23) Boekel, C. P.; Teuben, J. H.; de Liefde Meijer, H. J. J. Organomet. Chem. **1975**, 102, 161-165.

(24) (a) Chirkov, N. M. Kinet. Catal. **1970**, 11, 269-278. (b) Tel'noi, V. I.; Rabinovich, I. B.; Tikhonov, V. D.; Latyaeva, V. N.; Vyshinskaya, L. I.; Razuvaev, G. A. Dokl. Akad. Nauk. SSSR **1967**, 174, 1374-1376.

(25) It is interesting to note that our measured $k_H/k_D^6 = 2.9$ from the thermolysis of **2** and **4** is equivalent to that found for the formation of Tebbe Reagent through competition studies involving Cp_2TiCl_2 and equal amounts of $Al(CH_3)_3$ and $Al(CD_3)_3$. Ott, K.; Grubbs, R. H. Personal communication.

(26) O'Ferrall, R. A. M. J. Chem. Soc. B **1970**, 785-790.

(27) Lewis, G. S.; Grinstein, R. H. J. Am. Chem. Soc. **1962**, 84, 1158-1161 and references contained therein.

(28) Brown, T. L.; Dickerhoff, D. W.; Bafus, D. A.; Morgan, G. L. Rev.

Sci. Instrum. **1962**, 33, 491-492.

(29) Cohen, S. A.; Auburn, P. R.; Bercaw, J. E. J. Am. Chem. Soc. **1983**, 105, 1136-1143.

(30) The integration is not affected since the quadrupolar ^{2}H nuclei are not subject to nuclear Overhauser enhancement. Elvidge, J. A. "Isotopes: Essential Chemistry and Applications"; Elvidge, J. A., Jones, J. R., Eds.; The Chemical Society: London, 1979; pp 123-194.

CHAPTER II

Synthesis and Reactivity of Alkenyl and Alkynyl Derivatives of Permethylzirconocene and Permethylhafnocene. Rearrangements of Alkenyl Derivatives Involving β-Hydrogen Elimination from an sp^2-Hybridized Carbon[1]

Introduction

The reactions of unsaturated hydrocarbons with transition metal compounds are of fundamental importance in organometallic chemistry.[2] Insertion of olefins and acetylenes into metal-hydrogen and metal-carbon bonds are requisite steps in industrially important processes such as isomerization, hydrogenation, and polymerization as well as in stoichiometric transformations for organic synthesis. Whereas the reactions of late transition metal hydrides with acetylenes have been extensively documented,[3,4] less is known concerning the reactions of early transition metal hydrides with acetylenes or the chemistry available to the resultant alkenyl insertion products.

Labinger and Schwartz have described the cis addition of Zr-H to terminal and internal acetylenes and, together with Negishi, have documented its synthetic utility.[5,6] Wailes, Weigold, and Bell briefly reported on the reactions of $[(\eta^5\text{-}C_5H_5)_2ZrHCl]_x$ and $[(\eta^5\text{-}C_5H_5)_2ZrH_2]_x$ with acetylenes.[7] However, some of the products obtained, including the bis-(alkenyl) derivatives, were not completely characterized. Bis(alkynyl) derivatives of zirconocene and hafnocene have also been described only briefly.[8] Most recently, Erker and coworkers have systematically studied the alkenyl derivatives of $[(\eta^5\text{-}C_5H_5)_2ZrCl]$ and have reported some binuclear compounds containing an unusual bridging alkenyl ligand.[9]

During the course of our work with bis(pentamethylcyclopentadienyl) derivatives of zirconium and hafnium we have noted that $Cp^*_2MH_2$ ($Cp^* \equiv \eta^5\text{-}C_5Me_5$; M = Zr, Hf) reacts with terminal olefins to afford very stable, monomeric, alkyl hydride derivatives.[10] Preliminary evidence

indicated that analogous alkenyl derivatives are even more robust; $Cp^*_2Hf(H)(CH{=}CHCMe_3)$, obtained from $Cp^*_2HfH_2$ and $HC{\equiv}CCMe_3$, is stable for days at 125°C.[11] Our studies on the formation and reactivity of these alkenyl hydride and the related bis(alkenyl) derivatives of permethylzirconocene and permethylhafnocene, obtained *via* insertion of unactivated acetylenes into metal-hydrogen bonds, are reported herein.

While the hafnium derivatives do prove relatively thermally stable, the zirconium analogues rearrange readily under mild conditions. The 2-butenyl hydride derivative isomerizes to an η^3-crotyl hydride species. The bis-(alkenyl) derivatives rearrange to afford zirconacyclopentenes. The mechanisms of these transformations are explored and the latter transformation is shown to involve a rare example of β-hydrogen elimination from an sp^2-hybridized carbon.[12]

To further extend this study of unsaturated-carbon ligands, the reactivity of these compounds with carbon monoxide and dihydrogen is examined. Additionally, the bis(propynyl) derivatives of permethyl-zirconocene and permethylhafnocene are synthesized and the extent of their reactivity is explored.

Results

Synthesis and Characterization of Alkenyl Derivatives of Permethylzirconocene and Permethylhafnocene. The reactions of $Cp^*_2MH_2$ (M = Zr (**1a**),[10c] Hf (**1b**)[13]) with unactivated alkynes occur rapidly at room temperature in toluene, benzene, or petroleum ether solutions. The course of these reactions is highly dependent on the nature of the alkyne substituent(s). t-Butylacetylene adds to an M-H bond of $Cp^*_2MH_2$ (**1a** and **1b**) in a cis manner to afford the monoinsertion products $Cp^*_2M(H)(CH{=}CHCMe_3)$ (**2a** and **2b**) (eq. 1), isolable as colorless, crystalline

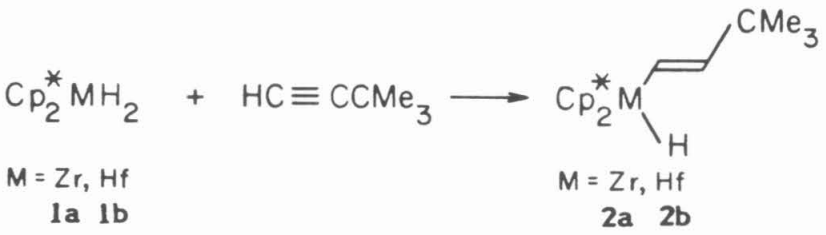

(1)

solids.[14] The trans configuration about the double bond is supported by the large value of $^3J_{HH}$ for the vinylic protons (21 Hz for **2a** and **2b**) (Table I). On the other hand, the reactions of **1a** and **1b** with the less sterically demanding phenylacetylene yield mixtures of the mono- and bisinsertion products, $Cp^*_2M(H)(CH{=}CHPh)$ (**3a** and **3b**) and $Cp^*_2M(CH{=}CHPh)_2$ (**4a** and **4b**) (eq. 2). These have been characterized by NMR spectroscopy only, and also show large coupling of the vinylic protons ($^3J_{HH}$ = 20 Hz).[15] With an even smaller substituent, methyl, on the acetylene, **1a** and **1b** react to form only the bisinsertion products $Cp^*_2M(CH{=}CHCH_3)_2$ (**5a** and **5b**) (eq. 3). As before,

Table I. NMR[a] and IR[b] Spectroscopic Data

Compound	IR	NMR (Chemical Shift, Multiplicity, Coupling Constants) Assignment	^{1}H	^{13}C
$Cp^*_2Zr(H)(CH{=}CHCMe_3)$ (2a)[c]		$C_5(\underline{CH_3})_5$	1.85 s	
		$ZrCH{=}CHC(CH_3)_3$	6.60 dd J = 21 1,5	
		$ZrCH{=}\underline{CH}C(CH_3)_3$	4.28 dd J = 21, 2.2	
		$ZrCH{=}CHC(\underline{CH_3})_3$	1.17 s	
		$Zr{-}\underline{H}$	5.73 s, br	
$Cp^*_2Hf(H)(CH{=}CHCMe_3)$ (2b)[d]	ν(C=C) 1560	$C_5(\underline{CH_3})_5$	1.91 s	12.0 q J = 126
	ν(Hf-H) 1625	$\underline{C}_5(CH_3)_5$		116.5 s
		$Hf\underline{CH}{=}CHC(CH_3)_3$	5.80 d J = 21	191.9 dd J = 117, 10
		$HfCH{=}\underline{CH}C(CH_3)_3$	4.81 d J = 21	140.1 d J = 146
		$HfCH{=}CHC(\underline{CH_3})_3$	1.09 s	30.1 q J = 122
		$HfCH{=}CH\underline{C}(CH_3)_3$		38.1 s
		$Hf{-}\underline{H}$	12.83 s, br	
$Cp^*_2Zr(CH{=}CHCH_3)_2$ (5a)[e,f]	ν(C=C) 1570	$C_5(\underline{CH_3})_5$	1.76 s	11.8 q J = 125
		$\underline{C}_5(CH_3)_5$		117.9 s
		$ZrCH{=}CHCH_3$	5.83 dq J = 18, 1.5	191.5 dq J = 114, 6
		$ZrCH{=}\underline{CH}CH_3$	5.21 dq J = 18, 5.5	130.4 dq J = 148, 8
		$ZrCH{=}CH\underline{CH_3}$	1.90 dd J = 5.5, 1,5	25.3 qdd J = 124, 12, 8
$Cp^*_2Hf(CH{=}CHCH_3)_2$ (5b)[f]	ν(C=C) 1571	$C_5(\underline{CH_3})_5$	1.79 s	
		$Hf\underline{CH}{=}CHCH_3$	5.56 dq J = 18, 1.5	
		$HfCH{=}\underline{CH}CH_3$	5.24 dq J = 18, 5.5	
		$HfCH{=}CH\underline{CH_3}$	1.88 dd J = 5.5, 1.5	

Table I (continued)

Compound	IR	NMR (Chemical Shift, Multiplicity, Coupling Constants) Assignment	^{1}H	^{13}C
$Cp^*_2Zr(CH{=}CHCH_2CH_3)_2$ (6)		$C_5(\underline{CH_3})_5$	1.78 s	
		$ZrCH{=}CHCH_2CH_3$	5.85 d J = 19	
		$ZrCH{=}CHCH_2CH_3$	5.27 dt J = 19, 5.5	
		$ZrCH{=}CHCH_2CH_3$	2.13 qd J = 7, 5.5	
		$ZrCH{=}CHCH_2CH_3$	1.11 t J = 7	
$Cp^*_2Zr(H)(C(CH_3){=}CHCH_3)$ (7a)[e,f]	ν(C=C) 1513	$C_5(\underline{CH_3})_5$	1.83 s	12.0 q J = 126
	ν(Zr–H) 1565	$\underline{C}_5(CH_3)_5$		114.7 s
		$Zr\underline{C}(CH_3){=}CHCH_3$		191.0 s
		$ZrC(\underline{CH_3}){=}CHCH_3$	2.26 s, br	11.4 q J = 120
		$ZrC(CH_3){=}C\underline{H}CH_3$	1.71 d J = 4.5	17.5 qd J = 121, 16
		$ZrC(CH_3){=}\underline{CH}CH_3$	3.65 m	86.5 dqd J = 120, 11, 5.5
		Zr–H	4.29 d J = 4.0	
$Cp^*_2Hf(H)(C(CH_3){=}CHCH_3)$ (7b)[e,f]	ν(C=C) 1486	$C_5(\underline{CH_3})_5$	1.90 s[g]	11.9 q J = 126[g]
	ν(Hf–H) 1568		1.91 s[h]	13.2 q J = 126[h]
	ν(Hf–D) 1123	$\underline{C}_5(CH_3)_5$		115.1 s
				116.6 s
		$Hf\underline{C}(CH_3){=}CHCH_3$		198.6 s
				201.7 s
		$HfC(\underline{CH_3}){=}CHCH_3$	2.14 s, br	9.9 q J = 126
			0.94 s, br	11.7 q J = 126
		$HfC(CH_3){=}C\underline{H}CH_3$	1.73 d J = 5.8	19.2 qd J = 124, 13.5
			1.73[i]	30.7 q J = 125
		$HfC(CH_3){=}\underline{CH}CH_3$	3.80 m	93.6 d J = 130
			4.89 m	125.8 d J = 143
		Hf–H	9.59 d J = 3.4	
			12.04 s	

Table I (continued)

Compound	IR	NMR (Chemical Shift, Multiplicity, Coupling Constants) Assignment	^{1}H	^{13}C
$Cp^*_2\overline{ZrCH_2CH(CH_3)CH=C(CH_3)}$ (8)[e, f]	ν(C=C) 1554	$C_5(\underline{CH_3})_5$	1.80 s	12.0 q J = 126
			1.83 s	11.4 q J = 126
		$\underline{C}_5(CH_3)_5$		118.2 s
				118.4 s
		$ZrCH(H)CH(CH_3)$	0.02 ddd J = 13, 7.9, 2.4	53.3 t J = 122
		$ZrCH(\underline{H})CH(CH_3)$	1.27 dd J = 13, 8.8	
		$ZrCH(H)\underline{CH}(CH_3)$	2.33 m	32.2 d J = 122
		$ZrCH(H)CH(\underline{CH_3})$	1.22 d J = 6.6	26.7 qd J = 123, 12
		$ZrC(CH_3)=\underline{CH}$	6.07 d J = 1.5	138.0 d J = 139
		$ZrC(\underline{CH_3})=CH$	1.69 s	29.1 q J = 124
		$ZrC(CH_3)=CH$		193.6 s
$Cp^*_2\overline{ZrCH_2CH(CH_3)C(CH_3)=CH}$ (9)[e, f, j]	ν(C=C) 1555	$C_5(\underline{CH_3})_5$	1.79 s	11.7 q J = 126
			1.83 s	11.7 q J = 126
		$\underline{C}_5(CH_3)_5$		118.0 s
				118.2 s
		$ZrCH(H)CH(CH_3)$	-0.17 dd J = 13, 7.4	57.7 t J = 119
		$ZrCH(\underline{H})CH(CH_3)$	1.35 dd J = 13, 8.8	
		$ZrCH(H)\underline{CH}(CH_3)$	2.51 m	41.6 dd J = 127, 10
		$ZrCH(H)CH(\underline{CH_3})$	1.24 d J = 7.0	26.5 qd J = 125, 5
		$ZrCH=C(CH_3)$	5.49 s	184.3 d J = 128
		$ZrCH=C(\underline{CH_3})$	1.80 s	27.3 q J = 120
		$ZrCH=\underline{C}(CH_3)$		151.3 s

Table I (continued)

Compound	IR	NMR (Chemical Shift, Multiplicity, Coupling Constants) Assignment	^{1}H	^{13}C
$Cp^*_2Zr(CH=CHCH_3)(C\equiv CCH_3)$ (11)[e,k]	ν(C=C) 1566	$C_5(\underline{CH_3})_5$	1.91 s	12.2 q J = 127
	ν(C≡C) 2095	$\underline{C}_5(CH_3)_5$		119.2 s
		$Zr\underline{CH}=CHCH_3$	5.98 dq J = 18.5, 1.	192.3 ddq J = 122, 6, 6
		$ZrCH=\underline{CH}CH_3$	5.49 dq J = 18.5, 6.0	130.1 ddq J = 152, 6, 6
		$ZrCH=CH\underline{CH_3}$	1.90 dd J = 6.0, 1.4	124.4 qdd J = 124, 12, 8
		$ZrC=C\underline{CH_3}$	1.77 s	5.8 q J = 127
		$ZrC\equiv\underline{C}CH_3$		110.6 q J = 10
		$Zr\underline{C}\equiv CCH_3$		140.3 q J = 4
$Cp^*_2Zr(CH=C(CH_3)CH(CH_3)_2)(C\equiv CCH_3)$[e,f]		$C_5(\underline{CH_3})_5$	1.04 s	12.2 q J = 127
		$\underline{C}_5(CH_3)_5$		119.3 s
		$Zr\underline{CH}=C(CH_3)CH(CH_3)_2$	4.81 s	187.6 d J = 106
		$ZrCH=C(\underline{CH_3})CH(CH_3)_2$	ℓ	11.3 q J = 125
		$ZrCH=C(CH_3)\underline{CH}(CH_3)_2$	2.77 sep. J = 7	36.5 d J = 132
		$ZrCH=C(CH_3)CH(\underline{CH_3})_2$	1.16 d J = 7	22.6 qd J = 125, 5
		$ZrCH=\underline{C}(CH_3)CH(CH_3)_2$		ℓ
		$ZrC\equiv C\underline{CH_3}$	ℓ	5.8 q J = 129
		$ZrC\equiv\underline{C}CH_3$		111.5 s
		$Zr\underline{C}\equiv CCH_3$		ℓ
$Cp^*_2\overline{ZrO(CH_3CH=CH)C=C(CH=CHCH_3)O}$ (14a)[e]	ν(C=C) 1636, 1523	$C_5(\underline{CH_3})_5$	1.85 s	10.8 q J = 126
		$\underline{C}_5(CH_3)_5$		121.8 s
		$ZrO\underline{C}CH=CHCH_3$		148.2 s
		$ZrOCCH=CHCH_3$	6.46 dq J = 14.6, 1.2	126.4 ddq J = 147, 7, 2
		$ZrOCCH=\underline{CH}CH_3$	5.96 dq J = 14.6, 7.0	117.5 ddq J = 156, 14, 7
		$ZrOCCH=CH\underline{CH_3}$	1.91 dd J = 17.0, 1.2	18.6 qdd J = 125, 12, 6

Table I. (continued)

Compound	IR	NMR (Chemical Shift, Multiplicity, Coupling Constants) Assignment	^{1}H	^{13}C
$Cp^*_2\overline{HfO(CH_3CH{=}CH)C{=}C(CH{=}CHCH_3)O}$ (14b)	ν(C=C) 1631, 1528	$C_5(\underline{CH_3})_5$	1.87 s	10.8
		$\underline{C}_5(CH_3)_5$		120.7
		$HfO\underline{C}CH{=}CHCH_3$		146.7
		$HfOC\underline{C}H{=}CHCH_3$	6.45 dq J = 15.0, 1.0	126.5
		$HfOCCH{=}\underline{C}HCH_3$	5.93 dq J = 15.0, 6.2	117.3
		$HfOCCH{=}C\underline{H}CH_3$	m	18.6
$Cp^*_2Zr(H)(\overline{OC{=}CHCH(CH_3)CH{=}C(CH_3)})$ (15) a b c d e f g		$C_5(\underline{CH_3})_5$	1.95 s	11.7 q J = 127
		$\underline{C}_5(CH_3)_5$		118.4 s
		a		138.7 s
		f		162.6 s
		b	4.95 m J = 1	107.5 d J = 162
		e	5.98 m J = 1	134.8 d J = 158
		d	1.18 d J = 7.5	12.6 q J = 127
		g	1.90 s	16.9 q J = 130
		c	3.06 qm J = 7.5, 1	41.2 d J = 124
		Zr-H	6.12 s	
$Cp^*_2Zr(H)(\overline{OC{=}CHCH(CH_3)C(CCH_3){=}CH})$ (16) a b c d e f g		$C_5(\underline{CH_3})_5$	1.93 s	11.7 q J = 126
		$\underline{C}_5(CH_3)_5$		118.3 s
		a		149.3 s
		e		162.0 s
		b	4.84 m J = 1	103.4 d J = 165
		g	5.77 s	128.8 d J = 160
		d	1.12 d J = 7.5	11.0 q J = 127
		f	1.68 s	14.6 q J = 126
		c	2.75 qd J = 7.5, 1	46.0 d J = 122
		Zr-H	6.28 s	

Table I. (continued)

Compound		NMR (Chemical Shift, Multiplicity, Coupling Constants) Assignment	^{1}H	^{13}C
$Cp^*_2Zr(H)(\eta^3\text{-}CH_2CHCHCH_3)$ (17a)[n]	ν(π-allyl) 1530	$C_5(\underline{CH_3})_5$	1.81 s	
	ν(Zr–H) 1575	$Zr(\eta^3\text{-}CH_2\underline{CH}CHCH_3)$	3.81 dt J = 16, 11	
		$Zr(\eta^3\text{-}\underline{CH_2}CHCHCH_3)$	0.80 - 2.80 m, br	
		$Zr(\eta^3\text{-}CH_2C\underline{H}CHCH_3)$		
		$Zr(\eta^3\text{-}CH_2CHC\underline{H}CH_3)$		
		Zr–H		
$Cp^*_2Hf(H)(\eta^3\text{-}CH_2CHCHCH_3)$ (17b)[o]		$C_5(\underline{CH_3})_5$	1.86 s	
		$Hf(\eta^3\text{-}CH_2\underline{CH}CHCH_3)$	3.75 dt J = 16.11	
		$Hf(\eta^3\text{-}\underline{CH_2}CHCHCH_3)$	0.80 - 2.90 m, br	
		$Hf(\eta^3\text{-}CH_2C\underline{H}CHCH_3)$		
		$Hf(\eta^3\text{-}CH_2CHC\underline{H}CH_3)$		
		Hf–H	4.24 s, br	

Table I. (continued)

Compound	IR	NMR (Chemical Shift, Multiplicity, Coupling Constants) Assignment	^{1}H	^{13}C
$Cp^*_2\overline{ZrCH_2CH(CH_2CH_3)C(CH_3)=C(CH_3)}$ (18)[e,f]	ν(C=C) 1554	$C_5(\underline{CH_3})_5$	1.79 s 1.84 s	11.3 q J = 126 11.9 q J = 126
		$\underline{C}_5(CH_3)_5$		118.6 s 118.7 s
		$ZrC\underline{H}(H)CH(CH_2CH_3)$	-0.13 dd J = 13, 7.5	54.7 td J = 117, 4
		$ZrCH(\underline{H})CH(CH_2CH_3)$	1.35 dd J = 13, 8.5	
		$ZrCH_2\underline{CH}(CH_2CH_3)$	m	32.0 dt J = 128, 2
		$ZrCH_2CH(\underline{CH_2}CH_3)$	m	11.1 t J = 126
		$ZrCH_2CH(CH_2\underline{CH_3})$	1.12 t J = 7.0	11.8 q J = 126
		$ZrC(CH_3)=C(\underline{CH_3})$	1.29 s	17.5 q J = 124
		$ZrC(\underline{CH_3})=C(CH_3)$	1.63 s	19.8 q J = 122
		$ZrC(CH_3)=\underline{C}(CH_3)$		185.7 s
		$ZrC(CH_3)=\underline{C}(CH_3)$		144.6 s
$Cp^*_2Zr(C\equiv CCH_3)_2$ (20a)	ν(C≡C) 2090	$C_5(\underline{CH_3})_5$	2.05 s	12.5
		$\underline{C}_5(CH_3)_5$		120.0
		$ZrC\equiv CC\underline{H}_3$	1.77 s	6.0
		$ZrC\equiv\underline{C}CH_3$		112.9
		$ZrC\equiv CCH_3$		40.9
$Cp^*_2Hf(C\equiv CCH_3)_2$ (20b)[p]	ν(C≡C) 2102	$C_5(\underline{CH_3})_5$	2.07 s	12.4
		$\underline{C}_5(CH_3)_5$		118.6
		$ZrC\equiv CC\underline{H}_3$	1.82 s	6.2
		$ZrC\equiv\underline{C}CH_3$		116.7
		$ZrC\equiv CCH_3$		149.8

[a] ^{1}H (90 MHz) and ^{13}C (22.5 MHz) NMR spectra taken in benzene-d_6 at ambient temperature unless otherwise noted. Chemical shifts are reported in δ relative to internal TMS or by reference to residual protons or carbons in the solvent. Coupling constants are reported in Hz. [b] IR spectra obtained in Njuol mulls unless otherwise noted. Values given in cm^{-1}. Complete spectra are reported in the Experimental section. [c] Reference 14. [d] ^{1}H and IR data from reference 11. [e] ^{13}C NMR spectrum obtained at 125 MHz. [f] ^{1}H NMR spectrum obtained at 500 MHz. [g] Major isomer (~90%). [h] Minor isomer (~10%). [i] Observed by integration of the ^{1}H-decoupled ^{2}H spectrum of 7b-d_6. [j] IR spectrum taken in C_6H_6. [k] ^{1}H data from reference 24. [l] These may not be definitively assigned: 1.79 s and 1.80 s for CH_3; 141.1 s and 147.6 s for quaternary carbons. [m] Not observed. [n] Reference 19. [o] Toluene-d_8. [p] IR spectrum taken in C_6D_6.

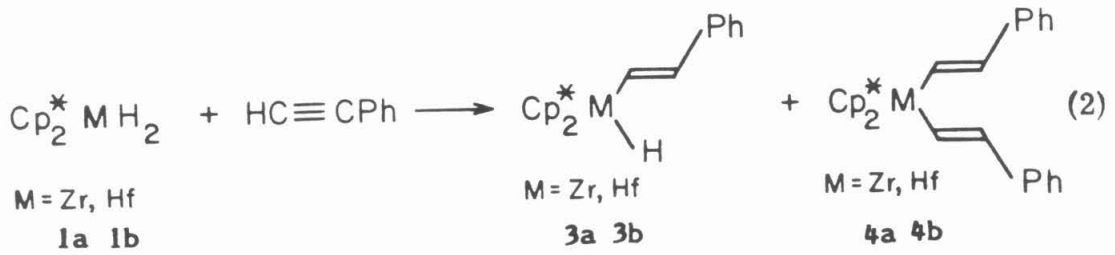

(2)

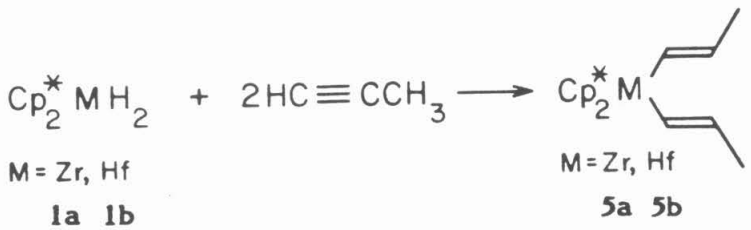

(3)

exclusively cis addition of the metal-hydride bond to the alkyne is observed, as judged by the magnitude of the vinylic H-H coupling ($^3J_{HH}$ = 18 Hz for **5a** and **5b**) (Table I).

Compound **5a** forms very rapidly -- the monoinsertion product is not observed, even by low temperature NMR spectrometry -- and is isolated as an off-white microcrystalline solid in good yield (66%) from -78°C petroleum ether solutions. The yield is quantitative by NMR, with the high solubility of these complexes reducing the isolated yields. Compound **5a** is stable at low temperature, but at room temperature rearranges in solution to form zirconacyclopentenes, as described in detail in the next section.

Infrared and nuclear magnetic resonance spectra are consistent with the formulation of **5a** as a bis(propenyl) complex: a C=C stretch of medium

intensity is observed at 1570 cm^{-1} and ^{13}C NMR data show the downfield shift and reduced ^{13}C-^{1}H coupling constant expected for the carbons nearest the Lewis acidic metal center[16] (δ 191.5 ppm, $^{1}J_{CH}$ = 114 Hz) and more typical sp^2-carbon values for the β-carbons[17] (δ130.4ppm, $^{1}J_{CH}$ = 148Hz). These assignments are supported by deuterium labeling experiments. By treating **1a** with 1-d-propyne and $Cp^*_2ZrD_2$ (**1a**-d_2) with perprotio propyne (eqs. 4 and 5), it is possible to specifically label the α and β positions.

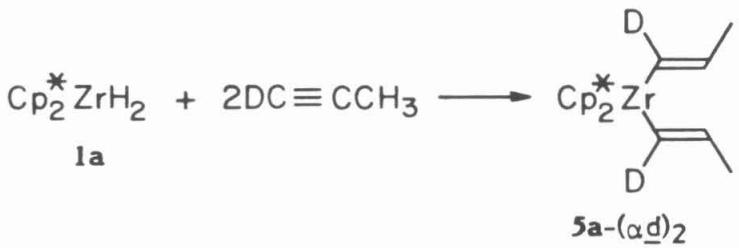

(4)

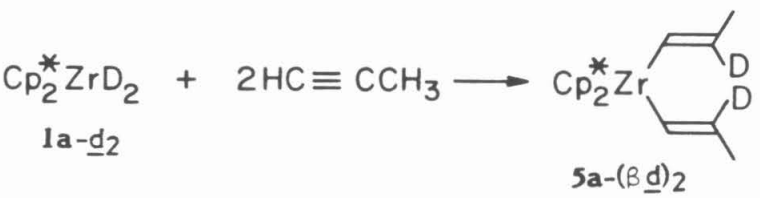

(5)

Compound **5b** can be isolated as a colorless microcrystalline solid in good yield (60%) from petroleum ether solutions. Its infrared and NMR data are analogous to that for the zirconium complex **5a** (Table I). However, ^{1}H NMR spectroscopy shows that an impurity, whose identity is unknown, comprises

approximately 10% of the isolated product.[18] Repeated recrystallization attempts have failed to further purify **5b**. Unlike **5a**, the hafnium complex **5b** is stable in solution at 80°C; no change is observed in the NMR spectrum for days at 80°C until decomposition begins. Moreover, the formation of **5b** is notably slower than that of its zirconium analogue **5a**. Signals assignable to the monoinsertion product $Cp^*_2Hf(H)(CH{=}CHCH_3)$ can be observed by ^1H NMR, even at room temperature. The insertion of propyne into the second Hf-H bond is still sufficiently fast, however, to preclude clean isolation of this intermediate, even when a single equivalent of propyne is utilized.

The reaction of $Cp^*_2ZrH_2$ (**1a**) with 1-butyne proceeds analogously to the reaction with propyne, yielding only the bisinsertion product $Cp^*_2Zr(CH{=}CHCH_2CH_3)_2$ (**6**) with no observation of the monoinsertion intermediate (eq. 6). Compound **6** is very soluble; its isolation as a pale

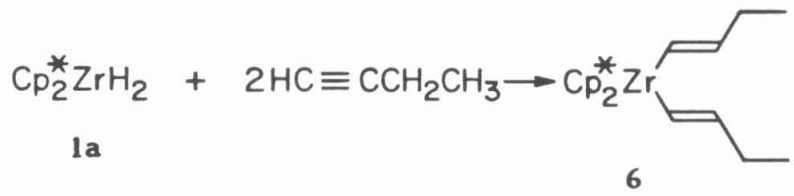

(6)

yellow solid requires evaporation of the solvent. The NMR data are again consistent with a <u>cis</u> addition of the Zr-H to the alkyne ($^3J_{HH}$ = 21.0 Hz) (Table I). As expected, the reactivity of the bis(butenyl)zirconium complex **6** is analogous to that of the bis(propenyl)zirconium complex **5a** (<u>vide infra</u>).

The reactions of $Cp^*_2MH_2$ (**1a** and **1b**) with 2-butyne, however, proceed quite differently, yielding only the monoinsertion products $Cp^*_2M(H)(C(CH_3){=}CHCH_3)$ (**7a** and **7b**) (eq. 7). The addition is assumed to

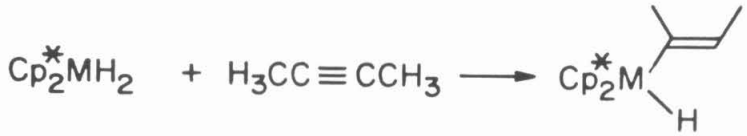

M = Zr, Hf
1a 1b

M = Zr, Hf
7a 7b

(7)

be cis by analogy to the preceding reactions; however, this assumption could not be confirmed by ^{1}H NMR spectrometry. Apparently the internal alkenyl ligand is sufficiently sterically demanding to prevent the insertion of a second molecule of 2-butyne. The reactions induced under more forcing conditions will be discussed in a subsequent section.

The ^{1}H and ^{13}C NMR data for compound **7b** (Table I) indicate that it exists in two isomeric forms in a 90:10 ratio at room temperature. The ratio decreases reversibly to 85:15 at 80°C. The ratio of isomers changes slightly (88:12) when the deuterated analogues $Cp^*_2Hf(D)(C(CH_3)=CDCH_3)$ (**7b**-d_2) and $Cp^*_2Hf(H)(C(CD_3)=CHCD_3)$ (**7b**-d_6) are formed from $Cp^*_2HfD_2$ (**1b**-d_2) and 2-butyne and $Cp^*_2HfH_2$ (**1b**) and 2-butyne-d_6, respectively.

The ^{1}H and ^{13}C NMR data for **7a** and the major isomer of **7b** (Table I) are unusual by comparison to the alkenyl derivatives with only H at the α position (**2a, 2b, 5a, 5b,** and **6**). The metal-hydride ^{1}H NMR signal is significantly farther upfield for **7a** and the major isomer of **7b** as compared to **2a** and **2b**. The metal-hydride resonance of the minor isomer of **7b**, in contrast, is very close to that of **2b**. Similarly, the ^{13}C NMR spectra for **7a** and the major isomer of **7b** show the β carbon resonance significantly up-

field with a large reduction in the coupling constant ($^1J_{CH}$ = 120 Hz for **7a**, 130 Hz for **7b**-major). The α carbon resonance for **7a** and **7b** and the β carbon resonance for **7b**-minor, in contrast, appear at positions similar to those of **2a**, **2b**, **5a**, **5b**, and **6**. The significance of these results will be considered further in the Discussion.

Reactivity of the Bis(alkenyl) Derivatives of Permethylzirconocene and Permethylhafnocene. Isomerization Reactions. The thermal stability of coordinatively unsaturated 16-electron compounds of the form $Cp^*_2MR_2$ (M = Zr, Hf; R = alkyl) is well documented.[10] The increased stability of an alkenyl-hydride over an alkyl-hydride complex had been noted.[11] Thus, it was surprising to observe that the bis(alkenyl) derivatives of permethylzirconocene were not stable at room temperature in hydrocarbon solutions, but rather rearranged to zirconacyclopentenes.

The bis(propenyl) compound, $Cp^*_2Zr(CH{=}CHCH_3)_2$ (**5a**), reacts at 24°C with a half-life of 9.1 h to form zirconacyclopentene **8** (eq. 8). Interestingly,

5a **8** (8)

this zirconacyclopentene **8** is also unstable, rearranging over weeks at room temperature and more rapidly at 78°C ($t_{½}$ = 6.5 h) to yield a second, isomeric, zirconacyclopentene **9** (eq. 9). Both products have been isolated as bright yellow, microcrystalline solids and have been characterized by infrared and NMR spectroscopies (Table I) and microanalyses. Deuterium labeling,

8 9 (9)

from the rearrangements of **5a**-(α-d)$_2$ and **5a**-(β-d)$_2$ (vide infra), has allowed unambiguous assignment of all resonances. As was noted for the previously described compounds, the ^{13}C NMR data are most useful. The position of the resonance of each carbon that is immediately adjacent to zirconium (e.g., δ 193.6 and 53.3 ppm in **8**) is shifted downfield relative to its next neighbor (δ138.0 and 32.2 ppm).[16]

Two alternate isomeric zirconacyclopentenes with a methyl group on the α sp^3-carbon are not observed. Their absence probably results from unfavorable steric interactions of the CH_3 group with the bulky Cp* ligands. Indeed, to our knowledge, no stable example of a metallacyclopentane or metallacyclopentene derivative of (Cp_2M) (M = Ti, Zr, Hf) with alkyl substitution at the sp^3-hybridized αcarbon has been isolated. Internal olefins isomerize to terminal olefins prior to coupling to form five-membered rings.[5a,19] Only Whitesides and coworkers have reported such a compound, $Cp_2\overline{TiCH(Me)(CH_2)_2CH_2}$, formed from the reaction of Cp_2TiCl_2 with 1,4-dilithiopentane, but they report its decomposition above -45°C.[20]

The overall reaction, then, involves the very rapid formation of an isolable kinetic product, the bis(propenyl) compound **5a**, that subsequently

rearranges to a second cleanly isolable kinetic product, the zirconacyclopentene **8**, which in turn forms the thermodynamic product, zirconacyclopentene **9** (eqs. 3, 8, and 9). Compound **9** is expected to be very stable, as numerous examples of related species have been reported in the literature.[21] Although zirconacyclopentene **8** can be cleanly isolated from petroleum ether solution, ^{1}H NMR spectra taken to follow the isomerization of **5a** in benzene-d_6 reveal that 11% of the thermodynamic product **9** is present in these solutions. Since rearrangement of **8** to **9** is slow at room temperature (vide supra), this observation suggests a common intermediate and allows us to calculate a transition state energy difference of 1.2(1) kcal·mol^{-1} in the formation of **8** and **9**.[22]

A mechanism that accounts for these observations is shown in Scheme I. The propyne coordination and insertion steps leading to **5a** must be rapid since no intermediates are detected even at -78°C. The common intermediate in the formation of zirconacyclopentenes **8** and **9** is the zirconium(II)-η^2-propyne species $(Cp^*_2Zr(HC{\equiv}CCH_3))$ (**10**), formed via β-hydrogen elimination from one of the propenyl ligands to yield the 18-electron intermediate $(Cp^*_2Zr(CH{=}CHCH_3)(H)(HC{\equiv}CCH_3))$ followed by reductive elimination of propene. The competition between faster insertion of propyne to generate **5a** and induced reductive elimination of propene yielding **10** is entirely analogous to the ethylene-induced reductive elimination of isobutane from $Cp^*_2Zr(H)(CH_2CHMe_2)$.[10c]

The zirconium-propyne intermediate **10** has precedent in the stable, isolated η^2-alkyne derivatives $Cp^*_2Ti(CH_3C{\equiv}CCH_3)$, $Cp^*_2Ti(PhC{\equiv}CPh)$, and $Cp^*_2Zr(PhC{\equiv}CPh)$.[23] Its intermediacy is also strongly suggested by the

Scheme I. Mechanism for the Formation and Rearrangements of **5a**, **8** and **9**.

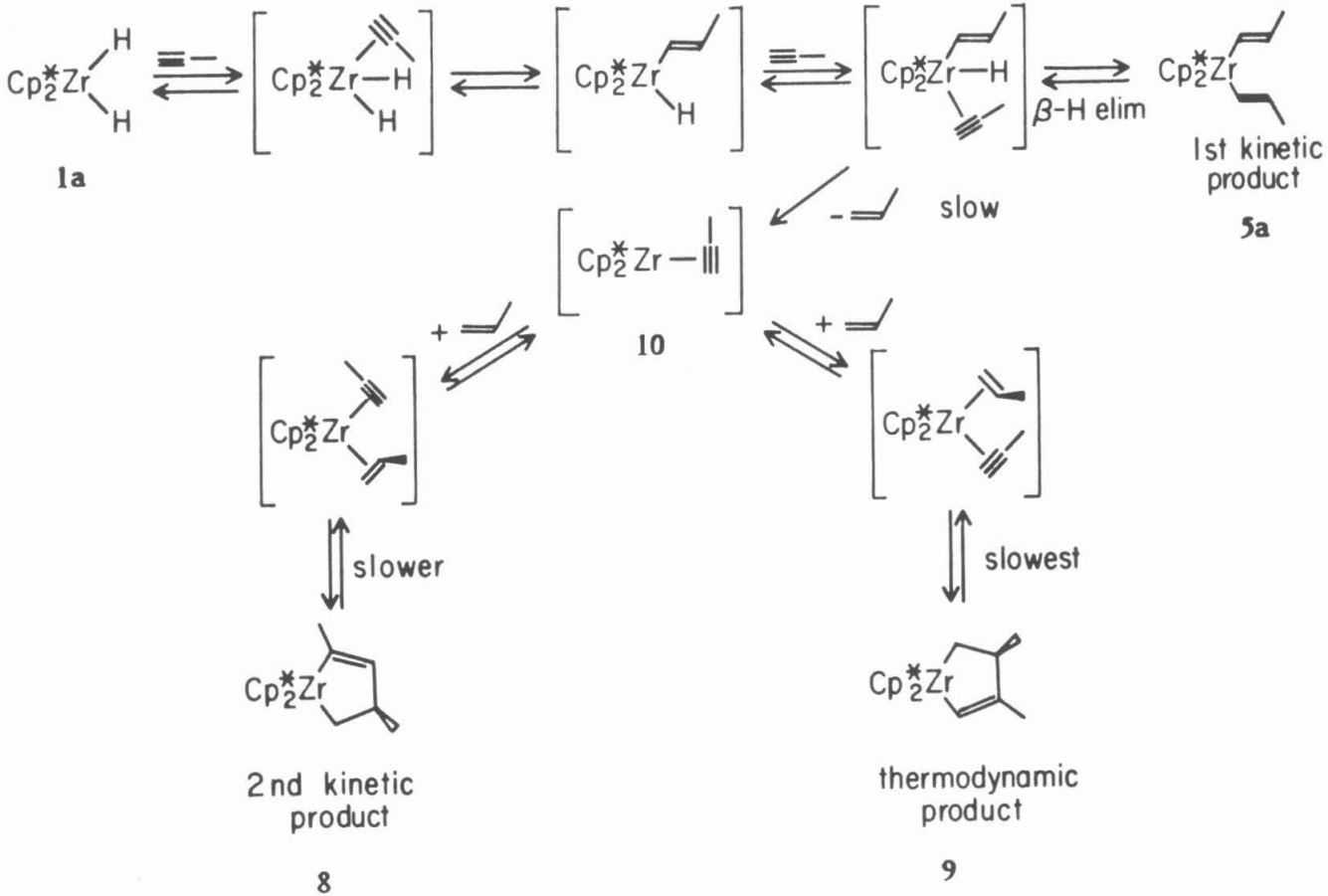

reactions of **5a** and **8** in the presence of excess alkyne. Both the bis(propenyl) compound **5a** and the kinetic metallacyclopentene **8** react with excess propyne (eqs. 10 and 11) to form the same propenyl-propynyl species **11** that is formed from the reaction of the known $\{Cp^*_2Zr(II)\}$ precursor $\{Cp^*_2ZrN_2\}_2N_2$ with propyne (eq. 12).[24] In contrast, the thermodynamic zirconacyclopentene **9** reacts quite differently with propyne (eq. 13), giving a product (identified by NMR) that does not arise from the intermediate **10** but rather from addition of propyne across the zirconium-sp^3-carbon bond in a

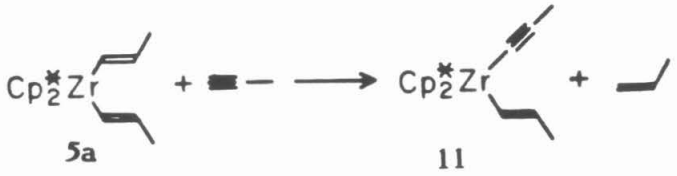

(10)

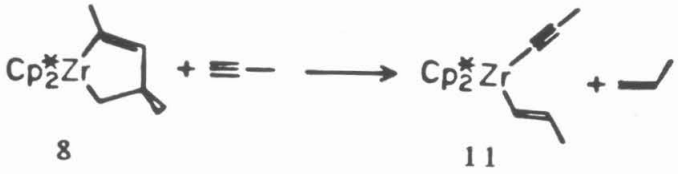

(11)

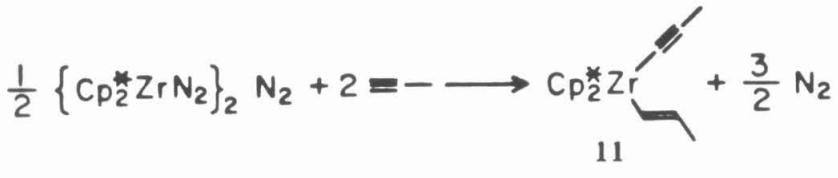

(12)

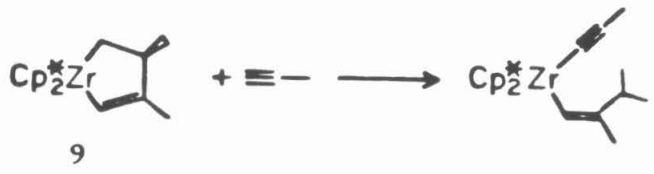

(13)

manner similar to the reactions of these complexes with H_2 (vide infra).

Studies with the deuterium-labeled compounds provide further support

for the proposed mechanism. $Cp^*_2Zr(CH{=}CDCH_3)_2$ (**5a**-(β-$\underline{d}$)$_2$) reacts in the presence of propyne to yield 1,2-dideuteriopropene and **11**-$\underline{d}_0$ according to Scheme II. The steps leading to the formation of the Zr(II) intermediate **10** are those of our proposed mechanism (Scheme I). The steps from the formation of **10** onward are those proposed for the reaction of $\{Cp^*_2ZrN_2\}_2N_2$ with propyne (eq. 12),[24] and hence any compound with access to intermediate **10** will follow the same path. The different reactivity of the thermodynamic zirconacyclopentene **9** suggests that **10** is not accessible from **9**, again speaking to the high thermodynamic stability of this zirconacyclopentene.

In the absence of propyne, **5a**-(β-$\underline{d}$)$_2$ yields the specifically labeled zirconacyclopentene (**8**-$\underline{d}_2$)$_A$ (eq. 14), the product expected for the reaction

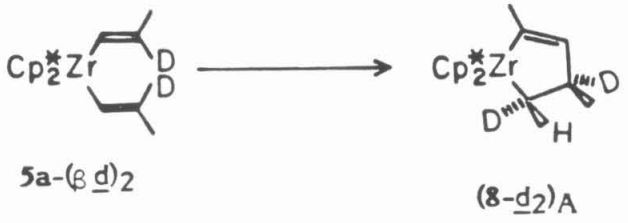

5a-(β $\underline{d}$)$_2$ (**8**-$\underline{d}_2$)$_A$ (14)

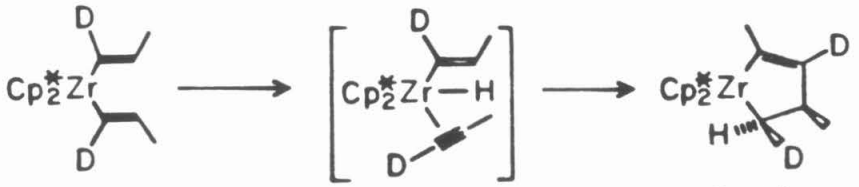

5a-(α-$\underline{d}$)$_2$ (**8**-$\underline{d}_2$)$_B$ (15)

of intermediate **10** with free cis-1,2-dideuteriopropene (Schemes I and II). Similarly, $Cp^*_2Zr(CD{=}CHCH_3)_2$ (**5a**-(α-$\underline{d}$)$_2$) yields the doubly labeled zirconacyclopentene (**8**-$\underline{d}_2$)$_B$ (eq. 15).

Scheme II. Mechanism for the Production of 1,2-Dideuteriopropene from **5a**-(β d)$_2$.

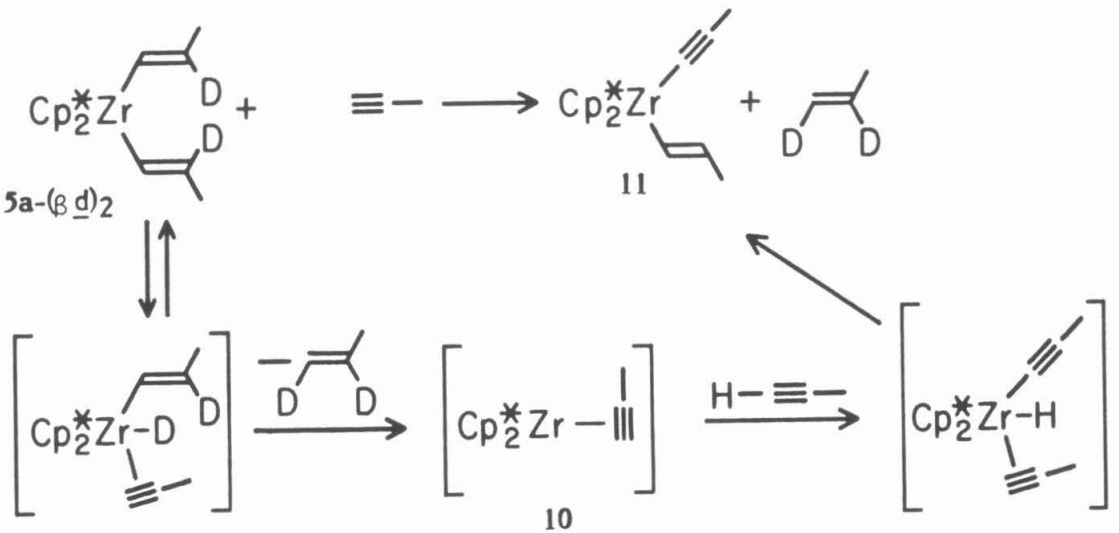

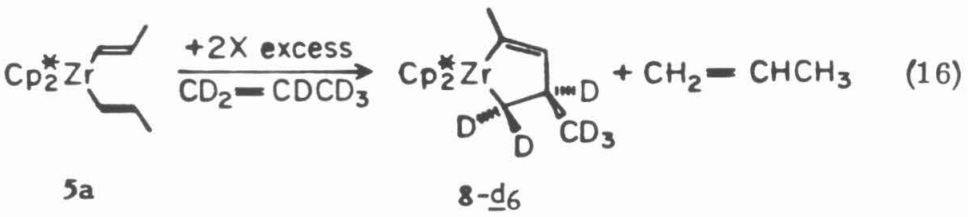

5a 8-$\underline{d}_6$

The products of the rearrangements of perprotio **5a** and **8** in the presence of propene-$\underline{d}_6$ indicate that propene is indeed released from the coordination sphere of zirconium. In the presence of a two-fold molar excess of propene-$\underline{d}_6$ at 24°C, **5a** yields **8** with propene-$\underline{d}_6$ incorporated in 90% of the product (eq. 16). At 78°C, **8** yields **9** with propene-$\underline{d}_6$ incorporated into 80% of the product (eq. 17). Propene-$\underline{d}_6$ is incorporated into zirconacyclopentene **8** faster than **8** isomerizes to **9**, as evidenced by liberation of 50% of the possible perprotio propene before 10% of **8** has

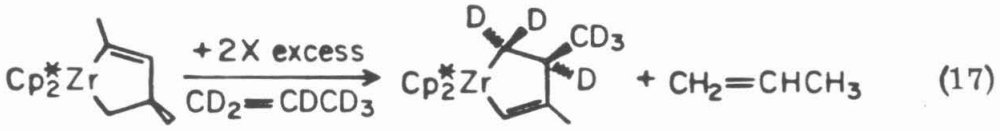

8 9-$\underline{d}_6$

rearranged to **9**. This result is consistent with the proposal of the common intermediate **10** reacting to produce the kinetic product **8** faster than the thermodynamic product **9**. No exchange of propene-$\underline{d}_6$ into **9** is observed even after one day at 80°C, again indicating that the reversion of **9** to **10** has a much higher activation barrier than that of **8** to **10**.

The availability of **5a**, **5a**-($\beta\underline{d}$)$_2$ and **5a**-($\alpha\underline{d}$)$_2$ has permitted measurements of the kinetics for the rearrangements of the bis(propenyl) complex **5a** and the zirconacyclopentene **8**, including deuterium isotope effects and activation barriers.[25] The isomerizations of **5a** to **8** and **8** to **9** were first-order in loss of **5a** and **8**, respectively, to three half-lives (Figs. 1 and 2). The isomerization of the bis(propenyl) complex **5a** to zirconacyclopentene **8** has a half-life of 9.1 h at 24°C, corresponding to k_{obs} = 2.1(2) x 10^{-5} sec^{-1} and $\Delta G^{\ddagger}$(297) K = 23.7(2) kcal·mol^{-1}. When deuterium replaces hydrogen in the β positions of **5a** the reaction is slowed significantly, yielding $\underline{k}_H/\underline{k}_D$ = 4.9(5). When deuterium replaces hydrogen in the α positions, however, the reaction rate is not significantly changed ($\underline{k}_H/\underline{k}_D$ = 1.03(10)). The magnitudes of these isotope effects indicate the β carbon-hydrogen bond is indeed being broken as **5a** rearranges.

Similarly, the isomerization of zirconacyclopentene **8** to zirconacyclopentene **9** has a half-life of 6.5 h at 78°C, corresponding to k_{obs} = 3.0(3) x 10^{-5} sec^{-1} and $\Delta G^{\ddagger}$ (351 K) = 27.9(3) kcal·mol^{-1}, comparable to the values found for the ring cleavage of zirconaindans.[21a] When (**8**-$\underline{d}_2$)$_A$ is thermolyzed the rearrangement proceeds slightly more slowly, yielding $\underline{k}_H/\underline{k}_D$ = 1.07(10). Although this value is not statistically different from unity, the direction (>1) is consistent with that expected for a rate-

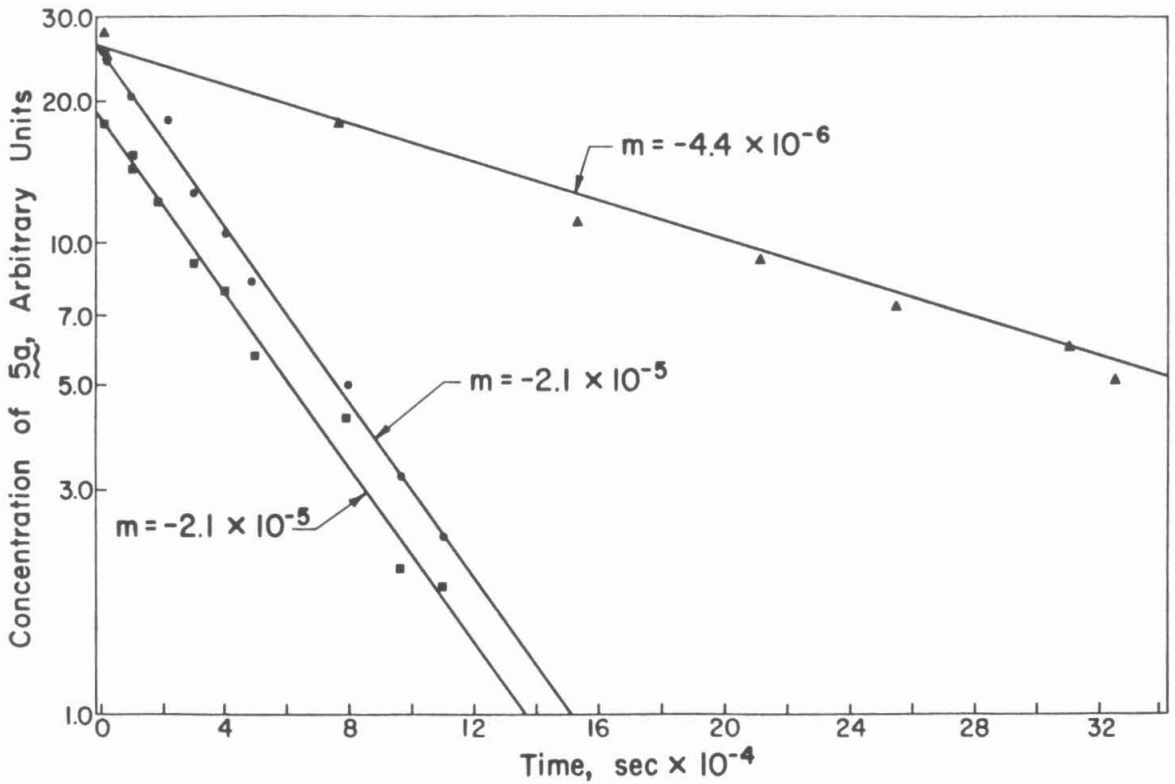

Figure 1. The Rearrangement of **5a:** Kinetic Plots Demonstrating the First-Order Loss of **5a** (●), **5a**-$(\alpha\underline{d})_2$ (■), and **5a**-$(\beta\underline{d})_2$ (▲) at 24°C. The loss of **5a**, **5a**-$(\alpha\underline{d})_2$, and **5a**-$(\beta\underline{d})_2$ was monitored by measuring the peak height of the Cp* resonance relative to the peak height of internal TMS.

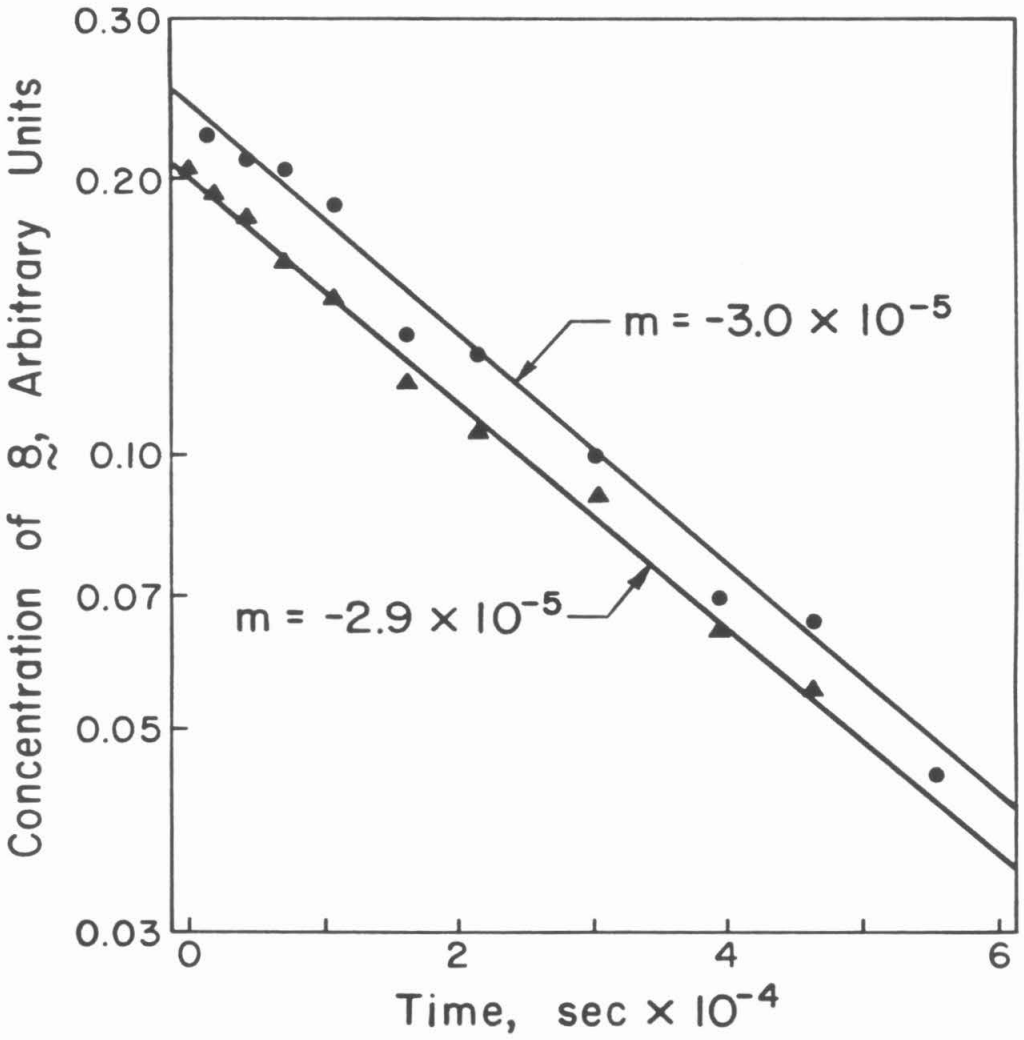

Figure 2. The Rearrangement of **8**: Kinetic Plots Demonstrating the First-Order Loss of **8** (●) and (**8**-$\underline{d}_2$)$_A$ (▲) at 78°C. The loss of **8** and (**8**-$\underline{d}_2$)$_A$ was monitored by measuring the peak height of the vinylic proton relative to the peak height of residual protons of C_6D_6.

determining ring cleavage in which a decrease in p-character ($sp^3 \rightarrow sp^2$) occurs for the carbons bearing the deuteriums.[27] Similar measurements were not undertaken for $(8\text{-}\underline{d}_2)_B$, since no NMR resonance is sufficiently isolated to monitor.

In order to ascertain whether free propene had any effect on the rate of isomerization of **5a**, zirconacyclopentene formation was monitored in the presence of 0, 2.1 and 9.7 molar equivalents of excess propene. In each case, the reaction is first-order in loss of the bis(propenyl) complex **5a** to three half-lives (Fig. 3). Significantly, the rate at 28°C did not change with increasing amounts of free propene, yielding $k_{obs} = 2.9 \times 10^{-5}$ sec^{-1} (no added propene), 3.3×10^{-5} sec^{-1} (2.1 molar equiv of propene), and 2.9×10^{-5} sec^{-1} (9.7 molar equiv of propene), for an average $k_{obs} = 3.0(2) \times 10^{-5}$ sec^{-1}. Thus, free propene is not involved in the rate-determining step, although the experiments utilizing propene-$\underline{d}_6$ (<u>vide supra</u>) show that propene is liberated in the formation of the zirconacyclopentenes **8** and **9**.

In contrast, the rate of isomerization of zirconacyclopentene **8** is found to increase linearly with the concentration of added propene (Figs. 4 and 5). The apparent rate constants, $k_{obs} = 5.9 \times 10^{-5}$ sec^{-1} (no added propene), 6.7×10^{-5} sec^{-1} (2.2 molar equiv of propene), and 8.7×10^{-5} sec^{-1} (8.3 molar equiv of propene), fit the equation $k_{obs} = k + k'[\text{propene}]$, where $k = 5.9(6) \times 10^{-5}$ sec^{-1} and $k' = 2.1(2) \times 10^{-5}$ $L \cdot mol^{-1} \cdot sec^{-1}$.[26b,28] Thus, free propene catalyzes (albeit rather poorly) the isomerization of zirconacyclopentene **8** to zirconacyclopentene **9**, and will therefore influence the results of the experiments conducted in the presence of propene-$\underline{d}_6$. However, the unimolecular transformation of **8** to **9**

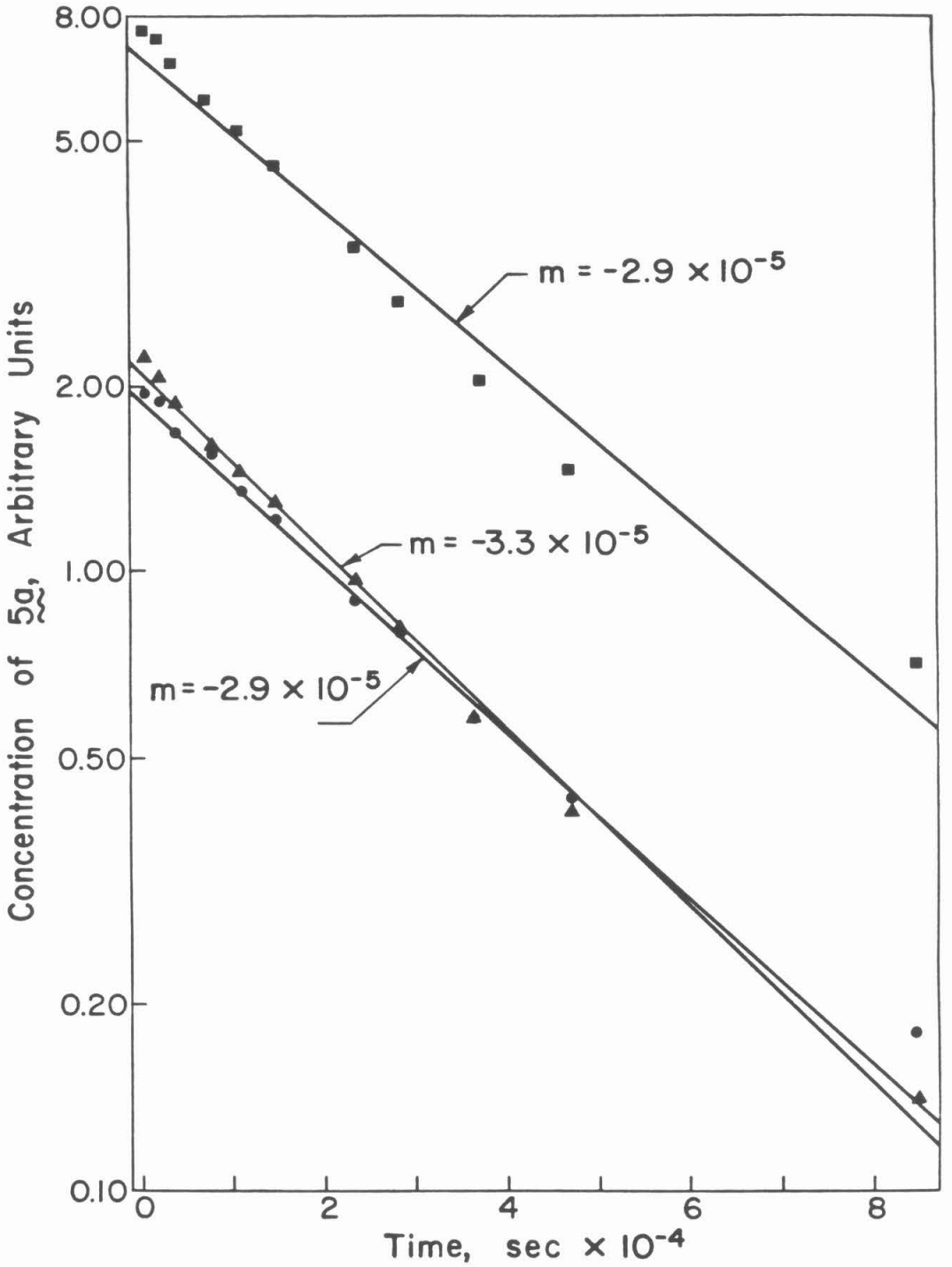

Figure 3. The Rearrangement of **5a** in the Presence of Propene: Kinetic Plots Demonstrating the First-Order Loss of **5a** in the Presence of 0 (●), 2.1 (▲), and 9.7 (■) Molar Equivalents of Propene at 28°C. The loss of **5a** was measured as described for Figure 1.

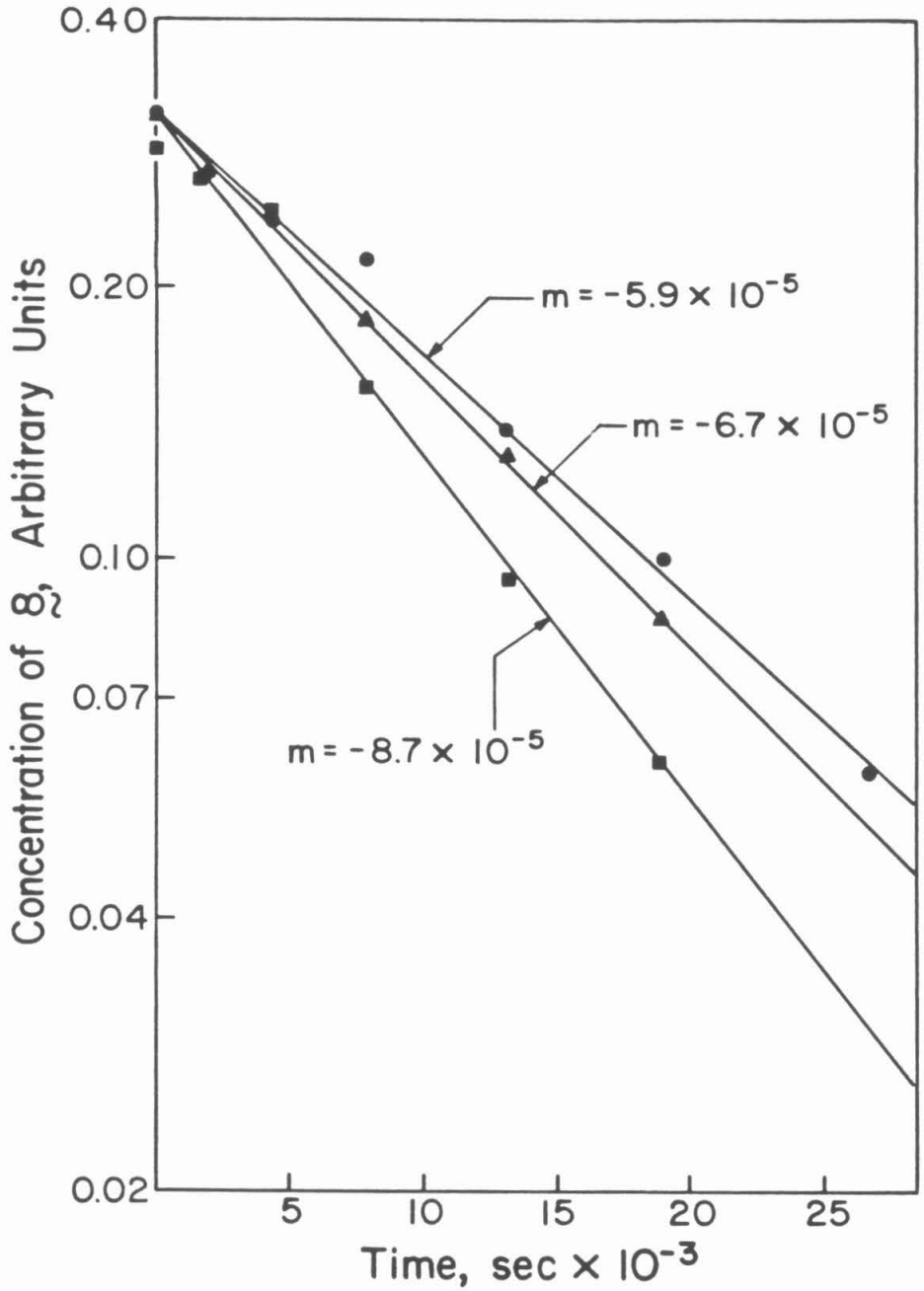

Figure 4. The Rearrangement of **8** in the Presence of Propene: Kinetic Plots Demonstrating the First-Order Loss of **8** in the Presence of 0 (●), 2.2 (▲) and 8.3 (■) Molar Equivalents of Propene at 79°C. The loss of **8** was measured as described for Figure 2.

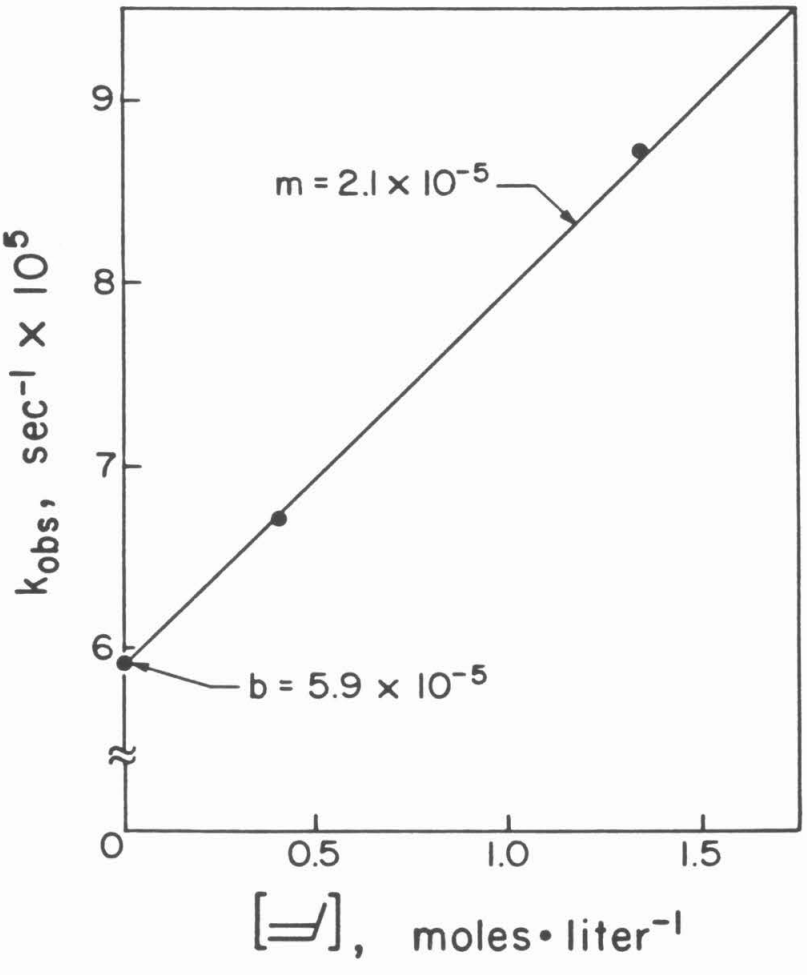

Figure 5. The Rearrangement of **8** in the Presence of Propene: Variation of k_{obs} with the Concentration of Added Propene.

competes effectively at the concentration of propene-$\underline{d}_6$ ($\sim$0.4 M) utilized in these experiments ($k = 5.9 \times 10^{-5}$ sec^{-1} vs. k' propene-$\underline{d}_6 \simeq 8.4 \times 10^{-6}$ sec^{-1}), so that the high level of propene-$\underline{d}_6$ incorporation and, especially, the observation that 50% of the available perprotio propene is released before 10% of **8** has been lost, indicates that loss of propene to form intermediate **10** is a key feature in the isomerization of **8** to **9**.

The bis(butenyl) complex $Cp^*_2Zr(CH{=}CHCH_2CH_3)_2$ (**6**) behaves analogously to the bis(propenyl) complex **5a**, rearranging to zirconacyclopentanes **12** and **13** (eq. 18), with **13** as the thermodynamic, and ultimately only,

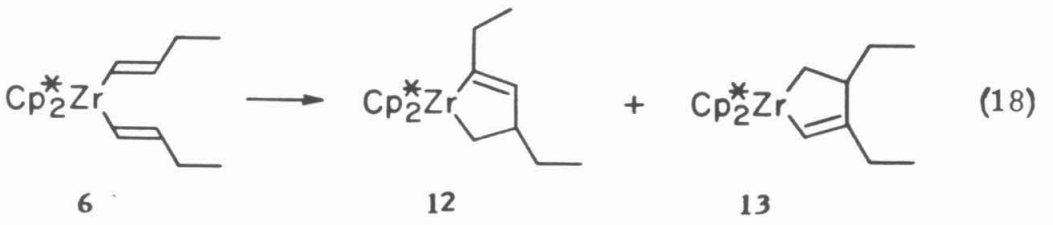

6 **12** **13** (18)

product. The rate is qualitatively similar to that observed for the isomerization of **5a**. However, the energy difference between the activation barriers for the kinetic ring **12** and the thermodynamic ring **13** is less, with **13** accounting for approximately one quarter of the initially observed ring products ($\Delta E_a \simeq 0.6$ kcal·mol^{-1}).

Reactions with CO and H_2. Facile insertion of CO into Zr-C and Hf-C bonds has been previously observed for alkyl derivatives of permethylzirconocene and permethylhafnocene.[10a,b] Both the bis(propenyl) derivatives $Cp^*_2Zr(CH{=}CHCH_3)_2$ (**5a**) and $Cp^*_2Hf(CH{=}CHCH_3)_2$ (**5b**) react quickly with CO at room temperature to yield quantitatively (NMR) the

purple enediolate derivative of permethylzirconocene **14a** (eq. 19) and the red enediolate derivative of permethylhafnocene **14b** (eq. 19). The

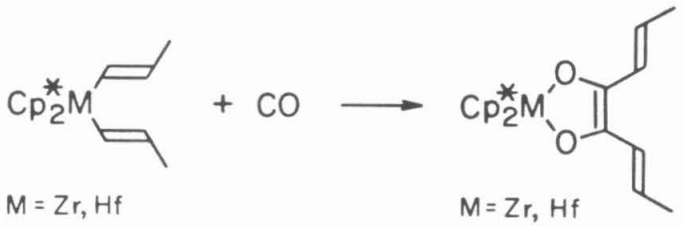

5a 5b **14a 14b** (19)

stoichiometry of two moles CO/mole **5** is confirmed by Toepler pump experiments. Unlike the alkyl analogues, however, the monoinsertion product is never observed.[10b,11] The NMR and IR data (Table I) for **14a** and **14b** are analogous to those observed in similar titanium,[29] zirconium,[5] and hafnium[11] species.

Both zirconacyclopentenes **8** and **9** react with one equivalent of CO at room temperature to yield orange dienolate-hydride derivatives **15** and **16**, respectively (eqs. 20 and 21), in quantitative yield by NMR. Compounds **15** and **16** have been characterized by NMR and IR spectroscopies (Table I) but

8 **15** (20)

9 16 (21)

have not been isolated. The stoichiometry is confirmed by Toepler pump experiments. This reactivity is analogous to that of bis(pentamethylcyclopentadienyl)zirconacyclopentane, which produced an enolate-hydride upon reaction with CO (eq. 22).[10b]

After weeks at room temperature, solutions of compounds **15** and **16** are observed to have undergone apparent sigmatropic [1,5]-hydrogen shifts producing isomers of the original compounds. According to ^{13}C and ^{1}H NMR spectral data, a single isomer results

(22)

from the rearrangement of **15**. The data do not, however, define which of the two possible products, **A** or **B**, is produced. The rearrangement of dienolate-hydride **16** is less clean and was not pursued.

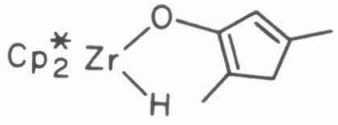

A

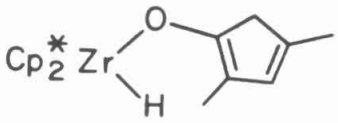

B

The zirconium-alkenyl complexes **5a**, **8** and **9** also react with excess dihydrogen, yielding $Cp^*_2ZrH_2$ and alkane (eqs. 23, 24 and 25). (The hafnium-alkenyl complex **5b** does not react with H_2, however, even after a week at room temperature.) The reaction of the zirconium compound **5a** with H_2 is sufficiently slow that a significant amount of rearrangement to

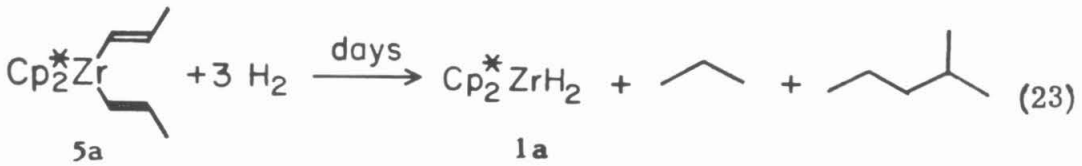

5a 1a (23)

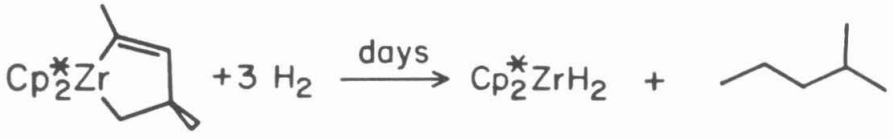

8 1a (24)

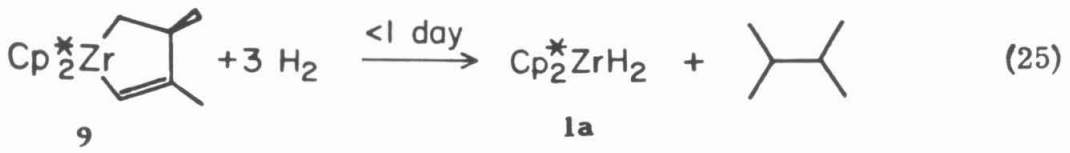

9 **1a** (25)

zirconacyclopentene **8** occurs. Compound **8** then also reacts with H_2, so that a mixture of propane and 2-methylpentane is obtained. In the reactions of zirconacyclopentenes **8** and **9** with H_2, dimethyl substituted butenyl-hydride intermediates can be seen by ^1H NMR. In fact, the NMR spectrum of the alkenyl ligand resulting from the reaction of **9** with H_2 is exactly the one produced when **9** reacts with propyne (eq. 13). This result suggests that H_2 addition occurs across the Zr-sp^3-carbon bond in **8** or **9** in a four-center interaction as proposed by Gell and Schwartz for the hydrogenation of $Cp_2Zr(R)H$.[30] Subsequent steps to yield $Cp^*_2ZrH_2$ and alkane should also be analogous to their proposals.

The reactions of zirconacyclopentenes **8** and **9** with H_2 differ from the reaction of the analogous zirconacyclopentane with H_2 (eq. 26).[24] In the

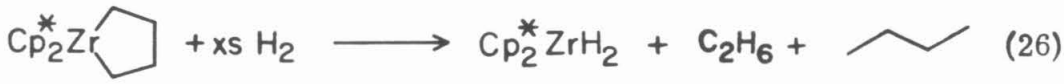

1a (26)

latter reaction, alkane products arise from both the zirconacyclopentane and the bis(olefin) forms of the compound (eq. 27). In the former reactions, the alkane products arise solely from the zirconacyclopentene form, suggesting that the equilibrium between zirconacyclopentene and zirconium(olefin)-

(27)

(acetylene) lies much farther to the side of the zirconacyclopentene.

Reactivity of the Mono(alkenyl) Derivatives of Permethylzirconocene and Permethylhafnocene. The thermal stability of the monoinsertion products $Cp^*_2M(H)(CH{=}CHCMe_3)$ (M = Zr, **2a**; Hf, **2b**) has been previously described.[11] These products are found to be more stable to reductive elimination and other decomposition reactions than the related alkyl-hydride complexes. The monoinsertion products that result from the reaction of 2-butyne with $Cp^*_2ZrH_2$ (**1a**) and $Cp^*_2HfH_2$ (**1b**), however, do not show this same stability.

$Cp^*_2Zr(H)(C(CH_3){=}CH(CH_3))$ (**7a**) rearranges at room temperature in both the solid and solution states. The rearrangement in solution occurs with first-order loss of **7a** to give the crotyl-hydride species **17a** (eq. 28) with a

M = Zr, Hf

7a 7b

M = Zr, Hf

17a 17b

(28)

half-life of 19.3 h at 24°C, corresponding to k_{obs} = 1.0(1) x 10^{-5} sec^{-1} (Fig. 6). The analogous hafnium compound, $Cp^*_2(H)(C(CH_3){=}CH(CH_3))$ **7b**,

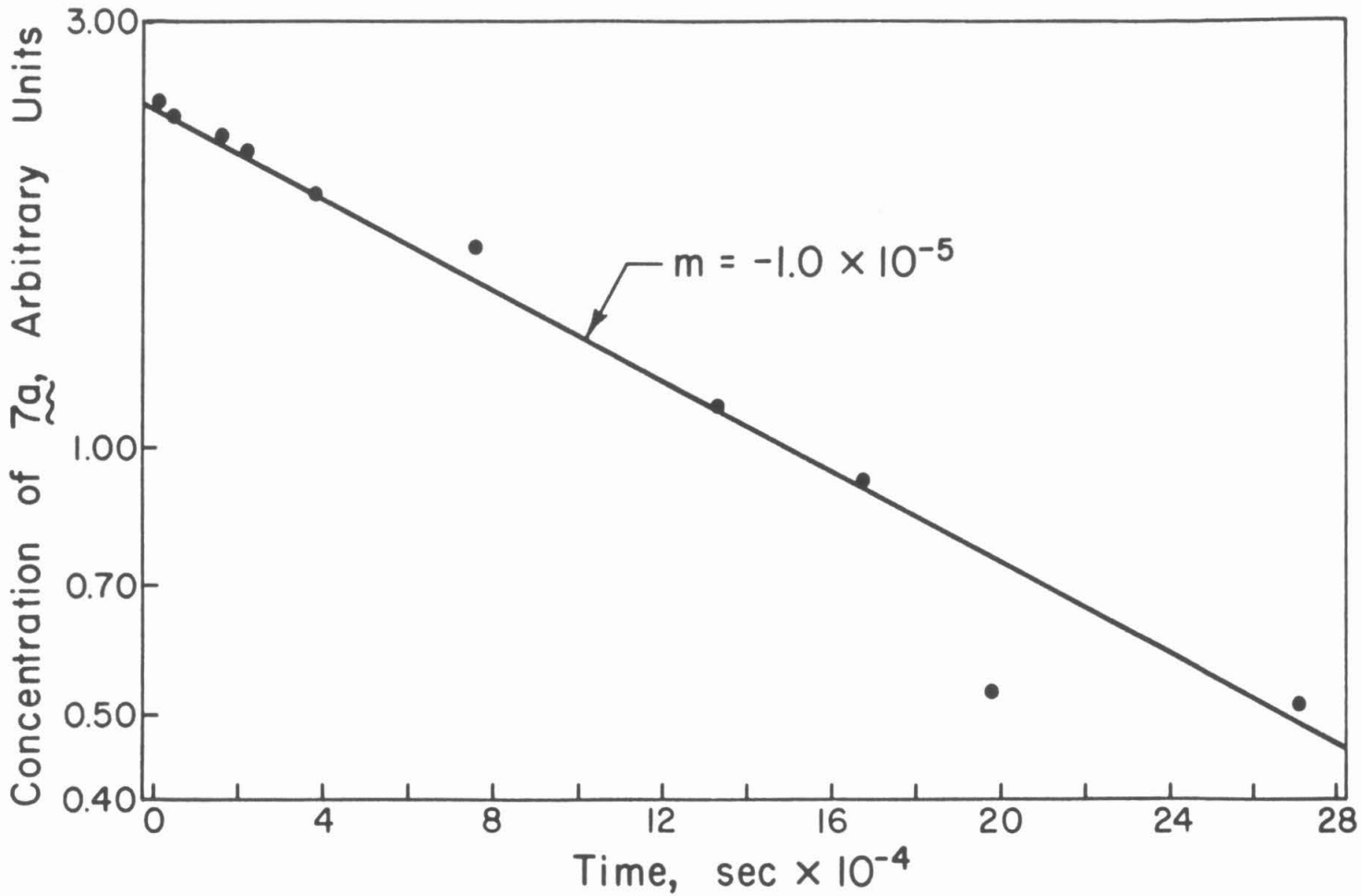

Figure 6. The Rearrangement of **7a:** Kinetic Plot Demonstrating the First-Order Loss of **7a** at 24°C. The loss of **7a** was measured as described for **5a** under Figure 1.

rearranges more slowly and less cleanly, yielding primarily the crotyl-hydride species **17b**. At room temperature, the rearrangement requires weeks and results in three side products. At 80°C, the rearrangement is faster and cleaner, requiring 5 h and resulting in only one observed side product. These side products have not been definitively assigned, but hafnacyclopentanes are indicated by their ^{1}H NMR patterns.

The bisinsertion products $Cp^*_2M(C(CH_3)=CH(CH_3))_2$ have not been observed. However, a second equivalent of 2-butyne does react with the monoinsertion product **7a** to form zirconacyclopentene **18** (eq. 29), which can

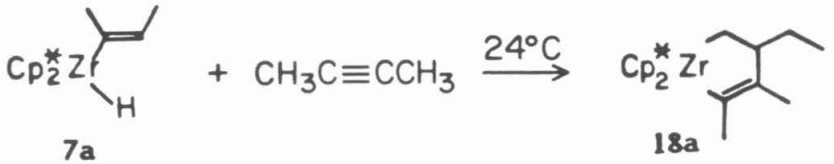

7a **18a** (29)

be isolated as a stable yellow microcrystalline solid. Qualitatively, reactions 28 and 29 proceed at the same rate at room temperature, suggesting a common intermediate derived from **7a**. However, zirconacyclopentene **18a** is not formed in the reaction of the crotyl-hydride species **17a** with 2-butyne. Rather, a 1:1 mixture of zirconacyclopentane **19a** and zirconacyclopentadiene **20a**, identified by comparison with the spectra of actual samples,[19] is obtained (eq. 30). Zirconacyclopentene **18a** does not disproportionate to **19a** and **20a**, even after months at room temperature. Thus, there appear to be two reaction manifolds in these systems. This is supported by the different reactivities of **7a** and **17a** with propyne and diphenylacetylene. While the

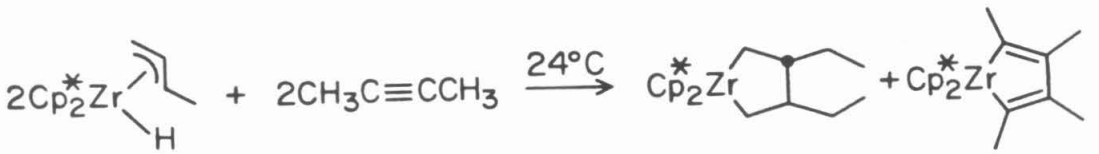

17a **19a** **20a** (30)

products of these reactions have not been unambiguously identified, the reactions of **7a** with each of the alkynes and of **17a** with each of the alkynes produce distinctly different products.

$Cp^*_2Hf(H)(C(CH_3)=CHCH_3)$ (**7b**) also reacts with 2-butyne, forming the hafnium zirconacyclopentene **18b** (eq. 31) in 5 h at 80°C. As before, this reaction is less clean than the zirconium system, producing more free 1-butene, and small amounts (~10%) of crotyl-hydride **17b** and hafnacyclopentadiene **20b.** The reaction of **17b** with 2-butyne has not been explored independently since **17b** has not yet been cleanly isolated. However, the **17b** produced in the reaction of **7b** with 2-butyne reacts over days at room temperature with excess 2-butyne in the NMR tube. Whether **19b** and **20b** are produced cannot be discerned, though, due to overlap with resonances for **18b.**

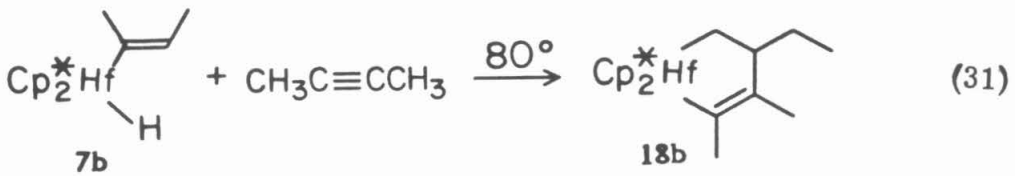

7b **18b** (31)

The Synthesis, Characterization, and Reactivity of Bis(alkynyl) Derivatives of Permethylzirconocene and Permethylhafnocene. The bis(propynyl) derivatives of permethylzirconocene and permethylhafnocene are prepared by treating $Cp^*_2MCl_2$ with two equivalents of propynyl-lithium

(eq. 32) in dimethoxyethane. $Cp^*_2Zr(C{\equiv}CCH_3)_2$ (**21a**) was isolated as a pale yellow solid in 50% yield. $Cp^*_2Hf(C{\equiv}CCH_3)_2$ (**21b**) was isolated as a colorless solid in 70% yield. Both have been characterized by ^{13}C and ^1H NMR and IR spectroscopies (Table I) and microanalyses. The NMR data are analogous to those found for the propynyl ligand of $Cp^*_2Zr(C{\equiv}CCH_3)(CH{=}CHCH_3)$ (**11**).[24] Their IR spectra are diagnostic for disubstituted acetylenes ($\nu_{(C{\equiv}C)}$ = 2090 cm^{-1} and 2102 cm^{-1} for **21a** and **21b**, respectively).[8]

Compounds **21a** and **21b** are remarkably stable, being unreactive with CO, H_2, and $HPPh_2$.[31] Solutions of **21a** darken slowly, but no significant change is noted by ^1H NMR spectroscopy.

$$\underset{M = Zr, Hf}{Cp^*_2MCl_2} + 2LiC{\equiv}CCH_3 \longrightarrow \underset{M = Zr, Hf}{Cp^*_2M(C{\equiv}CCH_3)_2} + LiCl \qquad (32)$$

21a **21b**

Discussion

Whereas the rapid insertion of alkyne into the M-H bonds of $Cp^*_2MH_2$ (M = Zr, Hf) is not surprising in light of previous findings,[5,6] the subsequent rearrangements of the bis(alkenyl) products were unexpected. The results described above lead to the following postulates concerning the mechanism of these reactions, of which the reactivity of **1a** with propyne is representative (Scheme I): (i) the insertion of two equivalents of propyne to afford the bis(propenyl) derivative **5a** is rapid, (ii) the β-hydrogen elimination from an sp^2-carbon in **5a** to afford the propyne adduct of the propenyl-hydride complex occurs, (iii) the reductive elimination of propene follows, (iv) the free propene coordinates to the propyne adduct **10** in orientations conducive to closure to either the kinetic or thermodynamic zirconacyclopentene **8** or **9**, and (v) the ring opening of **8** followed by loss of propene and recoordination of the propene to **10** in the proper orientation for closure to zirconacyclopentene **9** completes the sequence.

The β-hydrogen elimination from the sp^2-carbon proposed in Scheme I is the microscopic reverse of the propyne insertion, but it is not generally recognized as a kinetically accessible reaction; only one report has appeared in the literature.[12,32] The paucity of examples of β-hydrogen elimination from metal alkenyls as compared with the very common β-hydrogen elimination from metal alkyls is probably primarily attributable to the much higher reactivity of the C≡C bond relative to C=C bond rather than to any large difference in metal carbon σ-bond strengths. Indeed, the equilibrium (eq. 33) must lie far to the right for these Group IV alkenyl derivatives, since no alkyne hydride species could be detected in solution for

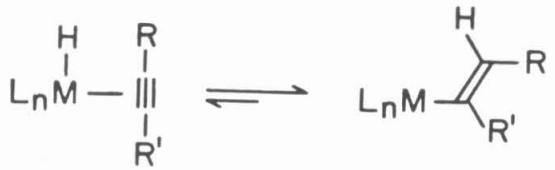

(33)

(34)

any of the alkenyl derivatives. This is also true in the equilibrium between the olefin-acetylene adducts and the zirconacyclopentenes (eq. 34), as evidenced by the reactivity of these compounds with H_2 to produce only C_6 alkanes. Bis(pentamethylcyclopentadienyl)zirconacyclopentane, in contrast, yields both C_2 and C_4 alkanes (eq. 27).

In the case of the bis(alkenyl)zirconium derivatives, the irreversible reductive elimination of alkene that follows β-hydrogen elimination provides the modus operandi for their rearrangements. Whereas the magnitudes of the deuterium isotope effects for **5a**-$(\beta\underline{d})_2$ (4.9(5)) and **5a**$(\alpha\underline{d})_2$ (1.03(10)) could be taken as evidence of a rate-limiting β-hydrogen elimination, the initial rapid generation of **5a** from ($Cp^*_2Zr(H)(CH{=}CHMe)(HC{\equiv}CMe)$) suggests a pre-equilibrium regime with slow reductive elimination of propene. Hence, the deuterium isotope effect for **5a**-$(\beta\underline{d})_2$ is likely to be a composite of a thermodynamic effect on the pre-equilibrium and a primary kinetic effect on the slow reductive elimination. The stability of the hafnium derivative **5b** to these same rearrangements is probably due less to sluggish β-hydrogen elimination than to its reluctance to undergo reductive elimination to afford a

Hf(II) species.[11,33]

Incorporation of propene-$\underline{d}_6$ into zirconacyclopentene **8** when the rearrangement of **5a** is carried out in its presence suggests that propene is lost entirely from the coordination sphere of zirconium following the reductive elimination. The alternative, wherein propene remains coordinated to zirconium during reductive elimination, would appear to involve considerable strain. Similarly, the release of 50% of the available propene-$\underline{d}_0$ from zirconacyclopentene **8** before 10% of **8** has been thermolyzed indicates that propene can also be lost from the coordination sphere of zirconium following ring opening (vide infra). The existence of other stable 16-electron alkyne adducts of permethylzirconocene[23] further supports the intermediacy of the Zr(II)-alkyne adduct **10**.

The mechanism of propene coordination to **10** and ring closure is similar to that described for the formation of zirconaindans[21a,b] and zirconacyclopentadienes,[21c] for which a stereospecific, concerted pathway is indicated. The positional preferences of the substituents in the five-membered rings are then determined by the coordination geometry, not by the π^* polarization rule set forth by Stockis and Hoffman.[21e] The difference in activation energies (1.2 kcal·mol^{-1}) for closure to zirconacyclopentenes **8** and **9** favors **8** as the kinetic product. The sterically less demanding 3,4-dimethyl substituted ring **9** is clearly favored thermodynamically, however, as evidenced by its lack of exchange with propene-$\underline{d}_6$ (1 day, 80°C) and unusual reactivity with propyne.

The evidence for propene catalysis of the isomerization of **8** to **9** (eq. 35) contrasts with the effect of added olefin in the rearrangement of

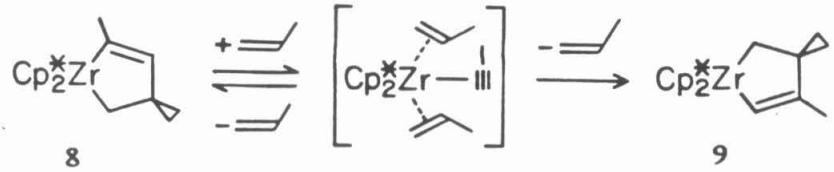

8 9 (35)

zirconaindans.[21c] In those cases, no isomerization is observed; the sterically and, presumably, thermodynamically preferred isomer is the only one obtained. Moreover, exchange of free olefin into the zirconaindan is found to be independent of both the structure and concentration of the added olefin. Only initial rates were measured in this system, but it is possible that the large size of the benzene ring in the zirconaindans and of the sterically demanding added olefins prevents a mechanism in which excess alkene assists in the exchange of free alkene for coordinated alkene (the forward reaction shown in eq. 35).

Although the 2-butenyl-hydride complexes **7a** and **7b** have been studied in less detail, two plausible pathways may be envisioned for their rearrangement to the crotyl-hydride species **17a** and **17b.** The first, and perhaps most obvious, is β-hydrogen elimination from the sp^3(methyl) carbon followed by insertion of methylallene into a metal-hydride bond (eq. 36). This reactivity has been noted for 2-butenyl derivatives of iridium[12] and

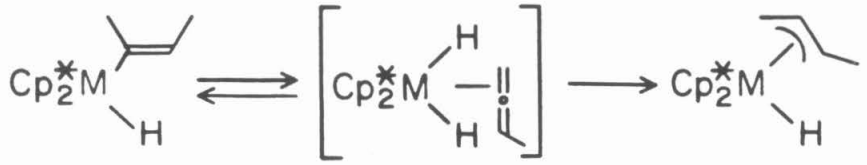

M = Zr, Hf M = Zr, Hf

7a 7b **17a 17b** (36)

molybdenum[35] and is further supported by reaction of **1a** with allene to form $Cp^*_2Zr(H)(\eta^3\text{-}C_3H_5)$.[34]

The alternate pathway available to these systems is a mechanism involving initial reductive elimination of 2-butene followed by re-coordination and tautomerization to **17a** and **17b** (eq. 37). This pathway is supported by

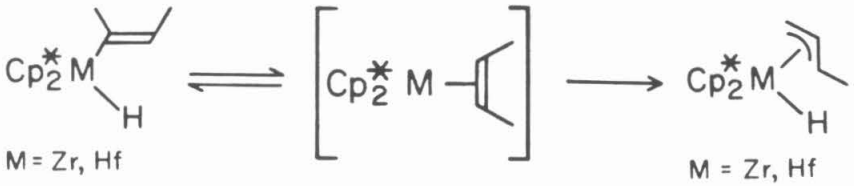

7a 7b **17a 17b** (37)

previous observations that 1-butene and cis- or trans-2-butene react with $\{Cp^*_2ZrN_2\}_2N_2$ to afford the syn-crotyl-hydride species **17a** (eq. 38).[19,34] We favor the former mechanism, nonetheless, since we have shown these alkenyl hydride complexes are quite reluctant to undergo reductive elimination unless induced to do so by added alkyne (Scheme I and ref. 13) or heated to decomposition.[10c,11]

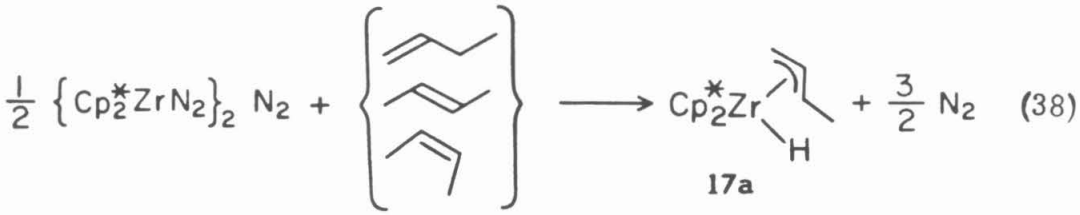

17a (38)

The zirconium-crotyl-hydride species **17a** is known to react with one equivalent of 1- or 2-butene upon heating to yield zirconacyclopentane **19a** (eq. 39).[19,34] That the reaction of **17a** with 2-butyne at room temperature

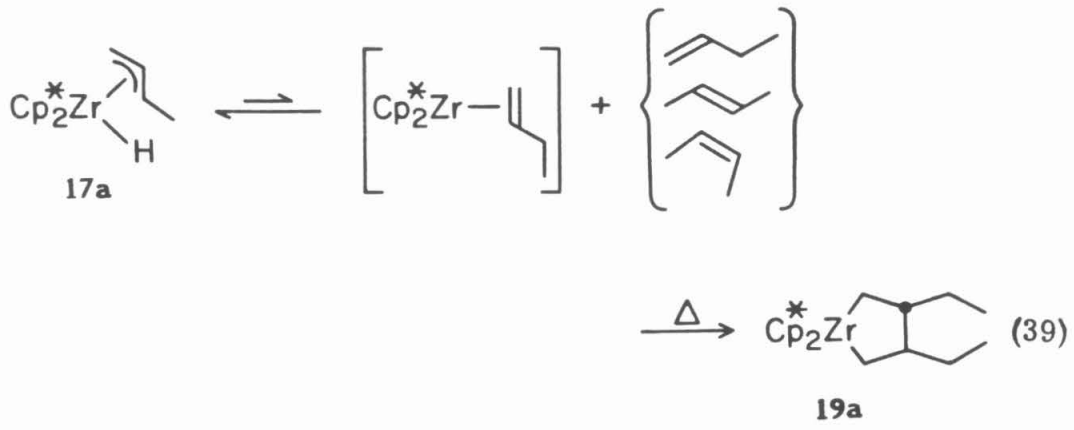

17a

results in formation of one-half equivalent of **19a** and one-half equivalent of zirconacyclopentadiene **20a** while the reaction of **7a** with 2-butyne at room temperature produces zirconacyclopentene **18a** is puzzling, particularly since **7a** isomerizes to **17a** under these conditions and the tautomerization of allyl ligands are known to be facile in these zirconium systems.[34] Thus, neither **17a** nor a tautomer of **17a** can be an intermediate in the reaction of **7a** with 2-butyne.

The mechanistic implications of these results are not clear. The presence of excess 2-butyne with **7a** may induce the alternate reaction pathway of cis-2-butene reductive elimination (eq. 40) and lead to an

7a (40)

intermediate analogous to **10**. To produce **18a**, cis-2-butene must isomerize to 1-butene. This isomerization could occur through a small amount of the "tuck-in" product, $Cp^*_2(C_5Me_4CH_2)ZrH$, from a series of olefin insertion and β-hydrogen elimination steps.[16a,34] This scenario would avoid the allyl reaction manifold, which leads to **19a** and **20a**, but would not explain the observation that the hafnium complex **7b** also forms a hafnacyclopentene **18b**. An alternative, therefore, would involve interaction of 2-butyne with the methylallene-dihydride adduct (eq. 36). Cohen and Bercaw have observed the isomerization of allene to propyne in a titanium system, apparently from a series of steps analogous to those described above for olefin isomerization.[16a] Thus, the methylallene may be isomerized to 1-butyne, which inserts rapidly; 2-butyne then induces reductive elimination of 1-butene (again there exists a difficulty due to the Hf results) and formation of the metallacyclopentene **18**. Obviously there are many possibilities and no clear reasons for **7a** and **17a** to react so differently. Similar reactivity differences have been seen in the reactions of $\{Cp^*_2ZrN_2\}_2N_2$ with the butenes (eq. 38), where trans-2-butene gives **17a** cleanly and **19a** only upon heating while cis-2-butene gives a mixture of **17a** and **19a** at room temperature. These allyl systems, then, are very complex and require a more complete understanding before the reactions observed in this part of our study can be explained satisfactorily.

As noted earlier, the spectroscopic data for the 2-butenyl hydride complexes **7a** and the major isomer of **7b** are unusual by comparison with the alkenyl derivatives with hydrogen at the α carbon. The presence of the minor isomer of **7b** with NMR data similar to those of the alkenyl derivatives

with hydrogen at the α carbon suggests that there are two orientations for the alkenyl ligands in the equatorial plane of the (Cp^*_2M) moiety (C vs. D) and that the more sterically demanding 2-butenyl

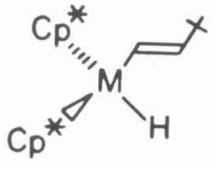

C

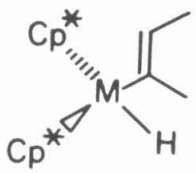

D

ligand preferentially exists in a different orientation than the alkenyl derivatives with hydrogen at the α carbon. An equilibrium mixture of both forms (ca 1:1) has been noted for a similar compound, $Cp^*_2Nb(CO)(C(CH_3)=CHCH_3)$.[36] While nuclear Overhauser effect difference spectroscopy on the major and minor isomers of **7b** failed to reveal which isomer had its vinylic hydrogen closer to its hydride, the irradiation of the hydride signal of **2b** produced a stronger NOE for the β carbon's hydrogen, suggesting C as the preferred orientation of the alkenyl ligand in this compound. By inference, D is suggested as the preferred orientation of **7a** and **7b.**

The reduced carbon-hydrogen coupling constants for the β carbons of **7a** and the major isomer of **7b** indicate a decrease in the s-orbital character at these carbons and may indicate agostic M···H-C interactions. The requisite vacant orbital exists in these coordinatively unsaturated 16-electron complexes (E), and the ^1H and ^{13}C NMR signals of the β-hydrogens and -carbons of **7a** and of the major isomer of **7b** are shifted

upfield, as expected from the alkyl cases documented thus far.[37a] In contrast, the ^{13}C NMR spectrum for the analogous niobium compound

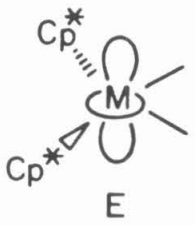

E

$Cp^*_2Nb(CO)(C(CH_3)=CHCH_3)$, which is d^2 and has no vacant orbital, exhibits resonances at δ 136.0 and δ 128.8 with carbon-hydrogen couplings of 156 and 150, respectively, for the β carbons of the two isomers.[36b] However, reduced C-H stretching frequencies in the IR spectra of **7a** and **7b** and significant changes in the isomer ratio upon deuteration of the β carbon position of **7b**, which are also expected, are not observed. Thus, the data could suggest the presence of the agostic interaction of a non-alkylidene[37b] sp^2-hybridized C-H bond, and would be the first such observation, but they are not conclusive.

Conclusion

The most significant result of this study is the demonstration of reversible insertion of acetylenes into group IV transition metal hydride bonds. Indeed, equilibrium 34 may be a general feature of transition metal alkenyls with a β-H that is evidenced only when there is an accessible decomposition pathway from the alkyne-hydride. The bis(alkenyl) derivatives of $(Cp^*_2Zr(IV))$ offer this feature. Moreover, the clean, kinetically well-separated nature of their rearrangements has allowed some of the essential mechanistic details to be elucidated. Such information is important for a more complete understanding of the catalytic and stoichiometric reactions in which such steps may occur.

Experimental Section

General Considerations. All manipulations were performed using glovebox or high vacuum line techniques. Solvents were dried over $LiAlH_4$ and stored over "titanocene".[38] The NMR solvents, benzene-$\underline{d}_6$ and toluene-$\underline{d}_8$, were dried over activated molecular sieves (4 Å, Linde) and stored over "titanocene". Argon, nitrogen, hydrogen, and deuterium gases were passed over MnO on vermiculite and activated molecular sieves.[39]

Propyne, 1-butyne, and propene were purified by several freeze-pump-thaw cycles at -196°C, then vacuum transferred at 24°C. 2-Butyne and $\underline{t}$-butylacetylene were transferred from activated molecular sieves. Propene-$\underline{d}_6$ (Stohler) and 2-butyne-$\underline{d}_6$ (MSD Isotopes) were used as received. Carbon monoxide (Matheson) and ^{13}CO (MRC-Mound) were used directly from the cylinders. $Cp^*_2ZrH_2$ (**1a**),[10c] $Cp^*_2HfH_2$ (**1b**),[13] $Cp^*_2M(CH)(CH{=}CHCMe_3)$ [M = Zr (**2a**), Hf (**2b**)],[11] and $Cp^*_2M(H)(CH{=}CHPh)$ [M = Zr (**3a**), Hf (**3b**)] and $Cp^*_2M(CH{=}CHPh)_2$ [M = Zr (**4a**), Hf (**4b**)][11] were prepared as previously described.

Many reactions were surveyed utilizing NMR spectroscopy. Any experiment described in the body of the chapter but not explicitly listed below was carried out in a sealed NMR tube utilizing ~30 mg of the starting material in ~0.3 mL of benzene-$\underline{d}_6$ containing TMS to which a known amount of the appropriate reagent was added before the tube was sealed at -196°C.

Nuclear magnetic resonance spectra were recorded on Varian EM 390 (90 MHz, ^1H), JEOL FX90Q (89.56 MHz, ^1H; 22.50 MHz, ^{13}C; 13.70 MHz, ^2H) and Brucker WM500 (500.13 MHz, ^1H; 125.8 MHz, ^{13}C; 76.5 MHz, ^2H)

spectrometers and are reported in Table I. ^1H nuclear Overhauser effect difference experiments were performed on the Brucker WM500 using the NOEDIFF pulse program. Infrared spectra were recorded on a Beckman 4240 spectrophotometer and are reported in cm^{-1}. Elemental analyses were determined by Dornis and Kolbe Microanalytical Laboratory, Galbraith Laboratories, Inc., and the Caltech Analytical Facility.

(1) $Cp^*_2Zr(CH{=}CHCH_3)_2$ (5a). $Cp^*_2ZrH_2$ (**1a**) (1.82 g, 5.0 mmol) was placed in a round-bottom flask with petroleum ether (8 mL). Propyne (18.0 mmol) was condensed onto the frozen solvent at -196°C. The blue (due to **1a**) slurry was warmed to -78°C and stirred for 60 min, becoming paler with time. Undissolved free propyne was removed under vacuum at -78°C. A cold filtration, without any warming above -78°C, yielded the off-white microcrystalline solid **5a** (1.49 g, 66%). The air-sensitive solid was refrigerated under N_2. IR (nujol): 1582 (w), 1570 (m), 1490 (w), 1306 (w), 1062 (w), 1023 (m), 994 (m), 974 (w). A microanalysis was not obtained because the compound's thermal instability in solution prevented adequate recrystallization.[40]

(2) $Cp^*_2Zr(CD{=}CHCH_3)_2$ (5a-(α-$\underline{d}$)$_2$). Procedure 1 was followed using $Cp^*_2ZrH_2$ (**1a**) (0.41 g, 1.1 mmol) and $DC{\equiv}CCH_3$ (4.8 mmol) (Procedure 3), resulting in isolation of a light tan solid **5a**-(α-$\underline{d}$)$_2$ (0.09 g, 18% yield). The low yield is due to the high solubility of these compounds in hydrocarbon solvents and the relatively large amount of solvent (8 mL)/amount of **1a** used in this experiment. The solid was characterized by NMR only.

(3) $DC{\equiv}CCH_3$. D_2O was heated throughout the glass vacuum line and Toepler pump system in order to replace H^+ by D^+ at the glass sites.

$LiC{\equiv}CCH_3$ (Aldrich, 1.36 g, 29.6 mmol) was placed in a round-bottom flask. D_2O, which had been degassed by three freeze-pump-thaw cycles, was condensed in at -78°C. The ice was allowed to melt with stirring and the monodeuterated propyne was collected in the Toepler system until no more gas was evolved (~5 h). The propyne was determined to be 90% $DC{\equiv}CCH_3$ by reaction with $Cp^*_2ZrH_2$ (**1a**) and comparison of integrated intensities for the two vinyl positions.

(4) $Cp^*_2Zr(CH{=}CDCH_3)_2$ (5a-(βd)$_2$). Procedure 1 was followed using $Cp^*_2ZrD_2$ (**1a**-d_2) (generated *in situ*, Procedure 5), an excess of $HC{\equiv}CCH_3$, and 4 mL petroleum ether, resulting in isolation of the pale yellow solid **5a**-(βd)$_2$ (0.46 g, 54% yield). The solid was characterized by NMR only.

(5) $Cp^*_2ZrD_2$ (1a-d_2). $\{Cp^*_2ZrN_2\}_2N_2$[10] was placed in a round-bottom flask with petroleum ether (25 mL). D_2 was admitted to the purple solution at 0°C, affording a blue solution after stirring for 1½ h at 0°C. The D_2 atmosphere was removed under reduced pressure. A room temperature filtration removed a small amount of a yellow impurity from the blue solution. The solvent volume was reduced and the solution was used for Procedure 4. Compound **1a**-d_2 was determined to be 90% $Cp^*_2ZrD_2$ by comparison of the integrated intensities of the two vinyl positions in **5a**-(βd)$_2$.

(6) $Cp^*_2Hf(CH{=}CHCH_3)_2$ (5b). $Cp^*_2HfH_2$ (**1b**) (0.90 g, 2.0 mmol) was placed in a glass bomb with petroleum ether (20 mL). Propyne (13.2 mmol) was condensed into the bomb at -196°C. The colorless solution was warmed to room temperature and stirred overnight. The solution was transferred to a

round-bottom flask on a frit assembly. A room temperature filtration removed a pale yellow solid impurity. The solvent volume was reduced and the white solid **5b** collected by cold filtration (3 crops, total yield 0.65 g, 60%). The ^1H NMR spectrum shows a 10% impurity that repeated recrystallization did not remove.[18] IR (nujol): 2100 (w), 1571 (m), 1486 (m), 1152 (w), 1022 (m), 993 (m).

Anal. calcd. for $C_{26}H_{40}Hf$: C, 58.80; H, 7.59. Found: C, 57.96; H, 7.48.

(7) $Cp^*_2Zr(CH{=}CHCH_2CH_3)_2$ (6). $Cp^*_2ZrH_2$ (**1a**) (0.512 g, 1.4 mmol) was placed in a round-bottom flask with petroleum ether (4 mL). 1-Butyne (5.6 mmol) was condensed into solution at -78°C and the solution was stirred at -78°C for 1 h, becoming yellow-green. Since no solid was evident, the excess 1-butyne and solvent were removed under vacuum to yield the pale yellow-green oily solid **6** (isolated yield after scraping from flask, 0.30 g). Compound **6** was identified by ^1H NMR by analogy with **5a**. Because the workup required the solution to warm above -78°C, the product was observed to be contaminated by the zironacyclopentenes **12** and **13** as well as some $Cp^*_2Zr(CH{=}CHCH_2CH_3)(C{\equiv}CCH_2CH_3)$.

(8) $Cp^*_2Zr(H)(C(CH_3){=}CHCH_3)$ (7a). $Cp^*_2ZrH_2$ (**1a**) (0.57 g, 1.6 mmol) was placed in a round-bottom flask with petroleum ether (5 mL). Excess 2-butyne was condensed into the blue solution at -78°C. The slurry became pink, then yellow when warmed just to the point where all the 2-butyne melted. The solution was immediately cooled to -78°C again. A cold filtration with no further warming yielded the pale yellow solid **7a** (0.26 g, 40% yield). The air-sensitive solid was refrigerated under N_2. IR (nujol):

2724 (w), 2528 (w), 2040 (w), 1565 (sh), 1513 (m), 1490 (m), 1183 (w), 1164 (w), 1124 (w), 1106 (w), 1063 (w), 1025 (s), 870 (w), 803 (m), 792 (m), 724 (m), 606 (m), 591 (m), 512 (w), 449 (m). A microanalysis was not obtained because the compound's thermal instability in solution and the solid state prevented adequate recrystallization.

(9) $Cp^*_2Hf(H)(C(CH_3)=CHCH_3)$ (7b). $Cp^*_2HfH_2$ (**1b**) (0.605 g, 1.3 mmol) was placed in a round-bottom flask on a frit assembly. Petroleum ether (20 mL) was condensed onto the white solid at -78°C. 2-Butyne (2.1 mmol) was condensed into solution at -78°C. The solution was allowed to warm to room temperature with stirring for 1.5 h. The pale yellow solution was filtered from a fine white solid (LiCl from the $Cp^*_2HfH_2$ synthesis). After reducing the filtrate volume and cooling the solution to -78°C did not produce a solid product, all the volatiles were removed, leaving the pale yellow solid **7b** (0.546 g, 81%). The solid was too soluble to be recrystallized. It was refrigerated under N_2. By NMR (Table I), two isomers exist in a 90:10 ratio. IR (nujol): 2718 (w), 1568 (s,br), 1486 (m), 1430 (m), 1021 (m), 875 (w), 802 (m).

Anal. calcd. for $C_{26}H_{38}Hf$: C, 57.08; H, 7.58. Found: C, 57.92; H, 7.62.

(10) $Cp^*_2Hf(D)(C(CH_3)=CDCH_3)$ (7b-d_2). Procedure 9 was followed using $Cp^*_2HfD_2$ (**1b-d_2**) (Procedure 11, 0.305 g, 0.7 mmol) and 2-butyne (1.1 mmol). The off-white solid **7b-d_2** was isolated (0.267 g, 76%). ^1H NMR showed the absence of peaks due to the hydride and vinylic hydrogens, which were located in the ^2H NMR spectrum. As for **7b**, two isomers are seen (88:12). IR (nujol): 2718 (w), 1560 (w,br), 1486 (sh), 1150 (sh), 1123 (m,br),

1021 (m), 795 (w).

(11) $Cp^*_2HfD_2$ (1b-d_2). $Cp^*_2HfH_2$ (**1b**) (0.485 g, 1.1 mmol) was placed in a round-bottom flask on a frit assembly. Petroleum ether (∿15 mL) was condensed onto the white solid at -78°C. Deuterium gas (1 atm) was admitted and the solution was stirred at room temperature ∿2 h. The clear solution was then cooled to -78°C, the system was evacuated, and fresh deuterium gas admitted. This procedure was repeated four more times. The solution volume was then reduced (5 mL) and the off-white solid **1b**-d_2 collected by cold filtration (0.327 g, 67%). Residual hydrogen in the hydride position was < 3% by NMR.

(12) $Cp^*_2Hf(H)(C(CD_3)=CHCD_3)$ (7b-d_6). Procedure 9 was followed using $Cp^*_2HfH_2$ (**1b**) (0.212 g, 0.5 mmol) and 2-butyne-d_6 (0.8 mmol). The pale yellow solid **7b**-d_6 was isolated (0.105 g, 42%). ^1H and ^{13}C NMR spectra were recorded to make definitive assignments for **7b**.

(13) $Cp^*_2ZrCH_2CH(CH_3)CH=C(CH_3)$ (8). $Cp^*_2Zr(CH=CH(CH_3))_2$ (**5a**) (1.46 g, 3.3 mmol) was placed in a round-bottom flask with petroleum ether (8 mL). The solution was stirred three days, becoming bright yellow. After a room temperature filtration removed a small amount of fine solid,[40] the solvent volume was reduced (4 mL) and the bright yellow microcrystalline solid was collected by cold filtration (3 crops, total yield 1.09 g, 75%). The solid was pure **8** by NMR, with no evidence of **9**. IR (nujol): 2793 (m), 1554 (w), 1490 (w), 1355 (w), 1299 (w), 1285 (w), 1166 (w), 1113 (w), 1022 (m), 833 (m), 805 (w).

Anal. calcd. for $C_{26}H_{40}Zr$: C, 70.36; H, 9.08. Found: C, 70.23; H, 9.31.

(14) $Cp^*_2ZrCH_2CH(CH_3)_3C(CH_3)=CH$ (9). Zirconacyclopentene **8** (0.80 g, 1.8 mmol) was placed in a small glass bomb with toluene (5 mL). The yellow solution was heated to 80°C with stirring for 22 h. The solution was transferred to a round-bottom flask on a frit assembly. The volatiles were removed under reduced pressure and petroleum ether (5 mL) was condensed in at -78°C. The yellow-orange solution was filtered at room temperature, leaving a small amount of a tan solid impurity. The solvent volume was reduced (2 mL) and the bright yellow microcrystalline solid **9** was collected by cold filtration (2 crops, total yield 0.57 g, 71%). IR (C_6H_6): 2944 (s), 2898 (s), 2856 (sh), 1555 (m), 1450 (sh), 1379 (m), 1356 (m), 1278 (w), 1064 (w), 1013 (w), 809 (w), 725 (w).

Anal. calcd. for $C_{26}H_{40}Zr$: C, 70.36; H, 9.08. Found: C, 70.28; H, 9.13.

(15) $Cp^*_2Zr(H)(\eta^3\text{-}CH_2CHCHCH_3)$ (17). $Cp^*_2ZrH_2$ (**1a**) (1.31 g, 3.1 mmol) was placed in a round-bottom flask with petroleum ether (10 mL). Excess 2-butyne was condensed into the blue solution at -20°C, which rapidly changed to yellow. After ~1 h the volatiles were removed and fresh petroleum ether was condensed onto the yellow solid.[41] The solution was stirred at room temperature for one week. The solvent volume was reduced (3 mL). An oily yellow-brown solid was isolated by cold filtration. Recrystallization from fresh petroleum ether yielded the pale yellow solid **17** (0.45 g, 34%) with NMR spectra identical to those obtained previously.[42]

(16) $Cp^*_2ZrCH_2CH(CH_2CH_3)C(CH_3)=C(CH_3)$ (18). $Cp^*_2Zr(H)(C(CH_3)=CH(CH_3))$ (**7a**) (0.82 g, 2.0 mmol) was placed in a small glass bomb with toluene (5 mL). 2-Butyne (2.5 mmol) was condensed in at -196°C. The

solution was warmed to room temperature and stirred four days. The orange solution was transferred to a round-bottom flask on a frit assembly. The volatiles were removed under reduced pressure and petroleum ether (5 mL) was condensed in at -78°C. The solution was filtered at room temperature, leaving a small amount of pale yellow solid. The solvent volume was reduced (2 mL) and the bright yellow microcrystalline solid **18** was collected by cold filtration (2 crops, total yield 0.62 g, 67%). IR (nujol): 1554 (m), 1490 (sh), 1365 (sh), 1159 (w), 1060 (w), 1021 (m), 921 (w), 928 (w), 706 (w).

Anal. calcd. for $C_{28}H_{44}Zr$: C, 71.27; H, 9.40. Found: C, 71.14; H, 9.05.

(17) $Cp^*_2Zr(C{\equiv}CCH_3)_2$ (21a). $Cp^*_2ZrCl_2$[10] (1.17 g, 2.7 mmol) and $Li(C{\equiv}CCH_3)$ (Aldrich, 0.38 g, 8.3 mmol) were placed in a round-bottom flask. Dimethoxyethane (DME) (20 mL) was condensed into the flask and the solution was warmed to room temperature with stirring. After 4½ h, the volatiles were removed and petroleum ether (15 mL) was condensed into the flask. The LiCl was filtered away. The solvent volume was then reduced and the pale yellow solid **21a** was isolated (2 crops, 0.59 g, 50%). IR (nujol): 2090 (m), 1062 (w), 1023 (m), 970 (m).

Anal. calcd. for $C_{26}H_{36}Zr$: C, 71.00; H, 8.25. Found: C, 70.81; H, 8.23.

(18) $Cp^*_2Hf(C{\equiv}CCH_3)_2$ (21b). $Cp^*_2HfCl_2$[13] (0.83 g, 1.6 mmol) and $Li(C{\equiv}CCH_3)$ (0.20 g, 4.3 mmol) were reacted as in Procedure 17, except the DME solution was refluxed. The white solid **21b** was isolated (2 crops, 0.59 g, 70%). IR (C_6D_6): 2988 (m), 2957 (m), 2909 (s), 2854 (m), 2723 (w), 2102 (s), 1489 (m), 1428 (m), 1379 (m), 1066 (w), 1027 (m), 976 (m).

Anal. calcd. for $C_{26}H_{36}Hf$: C, 59.25; H, 6.88. Found: C, 59.10; H, 6.71.

(19) $Cp^*_2Zr(CH{=}CHCH_3)(C{\equiv}CCH_3)$ (11). $Cp^*_2ZrH_2$ (**1a**) (1.32 g, 3.6 mmol) was placed in a round-bottom flask with toluene (20 mL). A propyne atmosphere was maintained at 760 torr until uptake ceased. All volatiles were removed under vacuum and petroleum ether (10 mL) was condensed in. A cold filtration yielded the pale yellow solid **11** (0.52 g, 33%, not optimized), identified by comparison with spectra obtained previously.[24]

(20) Reactions of 5a, 5a-(βd)$_2$, 8 and 9 with Excess Propyne. These experiments were carried out on NMR samples and the products identified by comparison with the NMR spectra of actual samples, except for the product of the reaction of **9** with propyne, which was identified solely by analysis of its 500 MHz ^1H spectrum. A typical experiment involved: the compound ($\sim$30 mg) was placed in a sealable NMR tube with benzene-$\underline{d}_6$ ($\sim$0.4 mL). Propyne (2-5 equiv) was condensed in at -196°C and the tube was sealed. The tube was warmed to room temperature and its ^1H (and ^2H for **5a**-($\beta\underline{d}$)$_2$) spectrum recorded.

(21) $Cp^*_2\overline{ZrCD(H)CD(CH_3)CH{=}C}(CH_3)$ (8-$\underline{d}_2$)$_A$ and $Cp^*_2\overline{ZrCH(D)CH\text{-}(CH_3)CD{=}C}(CH_3)$ (8-$\underline{d}_2$)$_B$. Zirconacyclopentenes (**8**-$\underline{d}_2$)$_A$ and (**8**-$\underline{d}_2$)$_B$ were formed in NMR tube reactions from **5a**-($\beta\underline{d}$)$_2$ and **5a**-($\alpha\underline{d}$)$_2$, respectively, and identified by ^1H and ^2H NMR. A typical experiment involved: compound **5a**-($\underline{d}$)$_2$ ($\sim$30 mg) was placed in a sealable NMR tube with benzene-$\underline{d}_6$ ($\sim$0.4 mL) and the tube was sealed at low temperature. The tube was brought to room temperature and allowed to react. The reaction kinetics were observed for these systems (Procedure 28).

(22) Reactions of 5a, 8 and 9 in the Presence of Excess Propene-$\underline{d}_6$. These experiments were carried out on NMR samples and the products identified and quantified by ^1H and ^2H spectra. Kinetic measurements were made in similar experiments with perprotio propene (Procedure 29).

(23) Reactions of 5a and 5b with CO. Compounds **5a** and **5b** react with 2 equiv of CO in NMR and bomb reactions to produce enediolates **14a** and **14b**, identified by ^1H and ^{13}C NMR and IR and by analogy to experiments with $Cp^*_2Zr(CH_3)_2$.[10] A typical NMR experiment involved: compound **5** (~30 mg) was placed in a sealable NMR tube with benzene-$\underline{d}_6$ (~0.4 mL). One atmosphere of CO was admitted at -78°C and the tube was then sealed at -196°C. Upon warming, the solution quickly became purple (**14a**) or red (**14b**). The reactions are quantitative by NMR, with no evidence of $Cp^*_2MCO_2$. The stoichiometry of the reaction was checked by Toepler pump experiment: compound **5b** (0.14 g, 2.7×10^{-4} mol) was placed in a glass bomb with toluene (10 mL). CO (1.70×10^{-3} mol, 6.3 equiv) was added to the frozen colorless solution. The solution was warmed to room temperature with stirring. After 3½ h, the red solution was cooled to -78°C and the remaining CO (1.29×10^{-3} mol) was collected by Toepler pump. Analysis indicated that 2.1 equiv of CO were consumed per mole of Hf.

Attempts to isolate **14a** and **14b** have not yielded clean products, probably because insufficient CO pressure was used. An additional problem with the preparation of **14a** is the thermal instability of **5a**. IR (C_6D_6) **14a**: 3017 (m), 2981 (m), 2915 (s), 2854 (m), 2732 (w), 1636 (m), 1603 (w), 1561 (w), 1523 (m), 1440 (m), 1381 (m), 1313 (m), 1291 (s), 1268 (m), 1150 (w), 1092 (w), 1028 (w), 951 (s), 923 (m). IR (C_6D_6) **14b**: 3040 (w), 2978 (m), 2916 (s), 2858

(m), 2734 (w), 1631 (m), 1528 (m), 1495 (w), 1437 (m), 1381 (m), 1315 (m), 1292 (s), 1269 (m), 1092 (w), 1028 (m), 1009 (w), 950 (s), 921 (m), 757 (w).

(24) Reactions of 8 and 9 with CO. Zirconacyclopentenes **8** and **9** react with 1 equiv of CO in NMR reactions to produce dienolates **15** and **16**, identified by ^{1}H and ^{13}C NMR and IR and by analogy to experiments with $Cp^*_2ZrCH_2CH_2CH_2CH_2$.[10] A typical NMR experiment involved: zirconacyclopentene (~30 mg) was placed in a sealable NMR tube with benzene-d_6 (~0.4 mL). CO was condensed in as described in Procedure 23. Upon warming the yellow solutions became orange-brown. The reactions are quantitative by NMR. The stoichiometry of the reaction was checked by Toepler pump experiments as described in Procedure 23: zirconacyclopentene **9** (0.13 g, 3.0×10^{-4} mol), toluene (5 mL), CO (2.6×10^{-3} mol, 8.7 equiv), 1 h stirring, red solution resulted; CO collected (2.31×10^{-3} mol). Analysis indicated that 1.0 equiv of CO was consumed per mole of Zr.

Dienolate **15** has been isolated as follows: zirconacyclopentene **8** (0.20 g, 0.45 mmol) was placed in a small glass bomb with petroleum ether (5 mL). Excess CO was admitted at -78°C. The yellow solution was warmed to room temperature and stirred 20 min. The resulting violet solution was transferred to a round-bottom flask attached to a frit assembly and the solvent volume reduced (2 mL). The lavender solid **15** was isolated by cold filtration (0.09 g, 44%) and characterized by NMR and IR. Attempts to isolate dienolate **16** produced oils and have not been pursued. IR (C_6D_6) **15**: 2980 (m), 2911 (s), 2862 (m), 2760 (w), 2734 (w), 1942 (m), 1845 (m), 1638 (s), 1593 (m), 1579 (w), 1488 (m), 1446 (m), 1388 (m), 1347 (s), 1301 (w), 1243 (s), 1188 (m), 1141 (m), 1028 (m).

As described in Results, dienolates **15** and **16** rearrange, as observed by ^{1}H NMR. Compound **15** appears to form one new dienolate, but **16** rearranges to more than one product, whose NMR spectra are not readily interpreted.

(25) Reactions of 5a, 8 and 9 with H_2. All three compounds **5a**, **8** and **9** react with excess H_2 to produce $Cp^*_2ZrH_2$ (**1a**) and alkane. A typical NMR reaction involved: compound **8** (~30 mg) was placed in a sealable NMR tube with benzene-$\underline{d}_6$ (~0.4 mL). H_2 was admitted at -196°C and the tube was sealed. The tube was warmed to room temperature and allowed to react. The reaction rate slowed as H_2 was consumed. The reactions were followed by ^{1}H NMR and the products identified by comparison with literature reports.[10,43]

(26) $Cp^*_2Zr(H)(\eta^3$-$CH_2CHCHCH_3)$ (17a) and 2-Butyne. Compound **17a** (0.31 g, 7.4×10^{-5} mol) was placed in a sealable NMR tube with benzene-$\underline{d}_6$. 2-Butyne (7.4×10^{-5} mol) was condensed in and the tube was sealed. After one day the reaction was complete; the products, $Cp^*_2\overline{ZrCH_2CH(CH_2CH_3)\text{-}CH(CH_2CH_3)CH_2}$ (**19a**) and $Cp^*_2\overline{ZrC(CH_3)=C(CH_3)C(CH_3)=C(CH_3)}$ (**20a**), were identified by comparison with spectra of authentic samples.[19]

(27) Kinetic Measurements of the Rearrangement of 5a. The rates of rearrangement were followed by monitoring the decrease in peak height[44] of the Cp* resonance of **5a**, **5a**-($\alpha\underline{d}$)$_2$ or **5a**-($\beta\underline{d}$)$_2$ relative to an internal, nonreacting standard of TMS in simultaneous experiments. Reactions proceeded at the ambient laboratory temperature, which was 24°C and was constant to ±1°C over the day required for the experiments with **5a** and **5a**-($\alpha\underline{d}$)$_2$, and ±2°C over the week required for **5a**-($\beta\underline{d}$)$_2$. EM 390 spectra were recorded at appropriate intervals.

A typical ^1H NMR experiment involved 30 mg of **5a** dissolved in 0.30 mL of benzene-$\underline{d}_6$ containing TMS. The NMR tube was sealed with N_2 (<1 atm). As the rearrangement progressed, the Cp* resonance of **5a** lost intensity, and plots of the decay of the ratio of the Cp* peak height/TMS peak height as a function of time showed first-order behavior for three half-lives.

The observed rate constants were derived from the slopes of the semilog plots (Fig. 1), yielding k_{obs} (**5a**) = 2.12(21) x 10^{-5} sec^{-1} (correlation coefficient r^2 = 1.00), k_{obs} [**5a**-($\alpha\underline{d}$)$_2$] = 2.05(21) x 10^{-5} sec^{-1} (r^2 = 0.99), and k_{obs} [**5a**-($\beta\underline{d}$)$_2$] = 4.38(44) x 10^{-6} sec^{-1} (r^2 = 0.99) and isotope effects of $\underline{k}_H/\underline{k}_{\alpha D}$ = 1.03(10) and $\underline{k}_H/\underline{k}_{\beta D}$ = 4.85(48). Assuming the Eyring equation holds (κ = 1),[26] $\Delta G^{\ddagger}$ (297 K) may be calculated: 23.7(2) kcal·mol^{-1}.

The reactions were not run over a range of temperatures, so $\Delta H^{\ddagger}$ and $\Delta S^{\ddagger}$ cannot be calculated. When **5a** was no longer evident, however, **8** and **9** were observed by NMR. The Arrhenius equation[26] can thus be used to calculate ΔE_a = 1.2 kcal·mol^{-1}, assuming the difference in relative amounts of **8** and **9** is a kinetic effect, i.e., [**8**]/[**9**] = k_8/k_9.

The error given in parentheses above represents one standard deviation estimated from the repetition of some of the experiments. An analysis of residuals for each line always gave a smaller error value.

(28) Kinetic Measurements of the Rearrangement of 8. The rates of rearrangement were followed by monitoring the decrease in peak height[45] of the vinylic resonances of **8** and (**8**-$\underline{d}_2$)$_A$ relative to an internal, nonreacting standard of the residual protons of benzene-$\underline{d}_6$ in simultaneous experiments. Compound (**8**-$\underline{d}_2$)$_B$ was not examined because the vinylic resonance was

absent and no other peak in the ^1H NMR spectrum was sufficiently isolated to monitor. The NMR samples from Procedure 27 were utilized for these experiments. The NMR tubes were heated to 78 ± 1°C in an oil bath. EM 390 spectra were recorded at appropriate intervals by removing the tubes from the oil bath and quickly cooling them to room temperature (24°C), at which temperature the rearrangements are negligibly slow.

The observed rate constants were derived from the slopes of the semilog plots (Fig. 2), yielding k_{obs} (**8**) = 2.97(30) x 10^{-5} sec^{-1} (r^2 = 0.99) and k_{obs} [(**8**-$\underline{d}_2$)$_A$ = 2.78(28) x 10^{-5} sec^{-1} (r^2 = 0.99) and a kinetic isotope effect of 1.07(10). Assuming large error bars (<u>vide supra</u>), this value is not significant but it is in the direction expected (see Results). Again assuming the Eyring equation holds (κ = 1), $\Delta G^{\ddagger}$ (351 K) = 27.9(13) kcal·mol^{-1}.

(29) Kinetic Measurements of the Rearrangements of 5a and 8 in the Presence of Propene. Procedures analogous to those of Procedures 27 and 28 were used, except none of the labeled compounds were used. A typical ^1H NMR experiment involved ∿30 mg of **5a** or **8**, weighed accurately and placed in a sealable NMR tube. Propene (∿0, 2 or 10 equiv) was expanded into a calibrated gas volume, then condensed into a calibrated liquid volume containing benzene-$\underline{d}_6$ with TMS (∿0.4 mL). The volume of this solution was measured at room temperature and the solution was then transferred to the NMR tube, which was subsequently sealed under N_2 (3 atm).

The EM 390 spectra were recorded at appropriate intervals as the reactions proceeded at ambient laboratory temperature, 28 ± 1°C, for **5a** and 79 ± 1°C for **8**. The reactions were first order in **5a** for three half-lives and in **8** for two half-lives. The observed rate constants were derived from the

slopes of the semilog plots (Fig. 3 for **5a** and Fig. 4 for **8**), yielding k_{obs} (0 equiv)=2.87(21) x 10^{-5} sec^{-1} (r^2 = 0.99), k_{obs} (2.1 equiv) = 3.26(21) x 10^{-5} sec^{-1} (r^2 = 1.00), and k_{obs} (9.7 equiv) = 2.94(21) x 10^{-5} sec^{-1} (r^2 = 0.98) for **5a** and k_{obs} (0 equiv) = 5.9(6) x 10^{-5} sec^{-1} (r^2 = 0.98), k_{obs}(2.2 equiv) = 6.7(7) x 10^{-5} sec^{-1} (r^2 = 1.00), and k_{obs} (8.3 equiv) = 8.7(9) x 10^{-5} sec^{-1} (r^2 = 0.99) for **8**. Thus the rate determining step in the rearrangement of **5a** is independent of propene concentration, but a plot of the rate of isomeriztion of **8** vs. the concentration of added propene (Fig. 5) yielded a straight line $k_{obs} = k + k'[\text{propene}]$, with k = 5.9(6) x 10^{-5} sec^{-1} and k' = 2.1(2) x 10^{-5} $L \cdot mol^{-1} \cdot sec^{-1}$ (r^2 = 1.00). The error bars represent one standard deviation determined from the the three experiments for **5a**, and an estimated error of 10% for **8**. Analysis of residuals for each line always gave a smaller error value.

(30) Kinetic Measurements of the Rearrangement of 7a. Procedures analogous to those of Procedure 27 were used. Only one experiment was followed. $Cp^*_2ZrH_2$ (**1a**) (0.051 g, 1.40 x 10^{-4} mol) was placed in a sealable NMR tube with benzene-$\underline{d}_6$ and TMS. 2-Butyne (1.40 x 10^{-4} mol) was condensed in and the tube was sealed. $Cp^*_2Zr(H)(C(CH_3)=CH(CH_3))$ (**7a**) was formed instantaneously. The rearrangement proceeded at ambient laboratory temperature (24 ± 1°C). EM 390 spectra were recorded at appropriate intervals. The observed first-order rate constant was determined from the slope of the semilog plot (Fig. 6), yielding k_{obs} = 1.00(10) x 10^{-5} sec^{-1} (r^2 = 0.99). $\Delta G^{\ddagger}$ (297 K) may be calculated by assuming the Eyring equation holds (κ = 1):[26] 24.2(2) $kcal \cdot mol^{-1}$.

References and Notes

(1) A preliminary report of some of this material has appeared. McGrady, N. D.; McDade, C.; Bercaw, J. E. In "Organometallic Compounds: Synthesis, Structure and Theory", Shapiro, B. L. (ed.); Texas A & M University Press: College Station, Texas, 1983, pp. 46-85.

(2) Parshall, G. W. "Homogeneous Catalysis"; John Wiley and Sons: New York, 1980.

(3) (a) Collman, J. P.; Hegedus, L. S. "Principles and Applications of Organotransition Metal Chemistry"; University Science Books: Mill Valley, California, 1980. (b) Heck, R. F. "Organotransition Metal Chemistry: A Mechanistic Approach"; Academic Press: San Francisco, 1974.

(4) For examples see: (a) Otsuka, S.; Nakamura, A. Adv. Organomet. Chem. **1976**, 14, 245-283. (b) Nakamura, A.; Otsuka, S. J. Am. Chem. Soc. **1973**, 95, 7262-7272. (c) Ibid. **1972**, 94, 1886-1894. (d) Longato, B.; Bresadola, S. Inorg. Chem. **1982**, 21, 168-173. (e) Clark, H. C.; Wong, C. S. J. Am. Chem. Soc. **1978**, 100, 7073-7074. (f) Ibid. J. Organomet. Chem. **1975**, 92, C31-C34. (g) Clark, H. C.; Milne, C. R. Ibid. **1978**, 161, 51-59.

(5) (a) Schwartz, J.; Labinger, J. A. Angew. Chem. Int. Ed., Engl. **1976**, 15, 333-340. (b) Hart, D. W.; Blackburn, T. F.; Schwartz, J. J. Am. Chem. Soc. **1975**, 97, 679-680. (c) Labinger, J. A.; Hart, D. W.; Seibert, W. E.; Schwartz, J. Ibid. **1975**, 97, 3851-3852.

(6) Van Horn, D. E.; Negishi, E. J. Am. Chem. Soc. **1978**, 100, 2252-2254.

(7) Wailes, P. C.; Weigold, H.; Bell, A. P. J. Organomet. Chem. **1971**,

27, 373-378.

(8) (a) Jiminez, R.; Barral, M. C.; Moreno, V.; Santos, A. J. Organomet. Chem. **1979**, 182, 353-359. (b) Barral, M. C.; Jiminez, R.; Santos, A. Inorg. Chim. Acta **1982**, 63, 257-260.

(9) (a) Czisch, P.; Erker, G. J. Organomet. Chem. **1983**, 253, C9-C11. (b) Erker, G.; Kropp, K.; Atwood, J. L.; Hunter, W. E. Organometallics **1983**, 2, 1555-1561.

(10) (a) Manriquez, J. M.; McAlister, D. R.; Sanner, R. D.; Bercaw, J. E. J. Am. Chem. Soc. **1978**, 100, 2716-2724. (b) Wolczanski, P. T.; Bercaw, J. E. Accts. Chem. Res. **1980**, 13, 121-127. (c) McAlister, D. R.; Erwin, D. K.; Bercaw, J. E. J. Am. Chem. Soc. **1978**, 100, 5966-5968.

(11) Roddick, D. M. Ph.D. Thesis, California Institute of Technology, 1984.

(12) Only one other report of β-hydrogen elimination from an sp^2-carbon has appeared in the literature. Schwartz, J.; Hart, D. W.; McGiffert, B. J. Am. Chem. Soc. **1974**, 96, 5613-5614.

(13) Roddick, D. M.; Fryzuk, M. D.; Seidler, P. F.; Hillhouse, G. L.; Bercaw, J. E. Organometallics, submitted.

(14) The characterization of **2b** is complete and has been reported.[11] Compound **2a** has been fully characterized. The isolated solid is 92% **2a** and 8% another, unidentified compound (NMR).[15]

(15) Roddick, D. M.; Bercaw, J. E. Unpublished results.

(16) (a) Cohen, S. A. Ph.D. Thesis, California Institute of Technology, 1978. (b) McLain, S. J.; Wood, C. D.; Schrock, R. R. J. Am. Chem. Soc. **1979**, 101, 4558-4570. (c) Wrackmeyer, B. Spectros. Int. J. **1982**,

1, 201-208.

(17) (a) Jolly, P. W.; Mynott, R. Adv. Organomet. Chem. **1981**, 19, 257-304. (b) Chisolm, M. H.; Godleski, S. Prog. Inorg. Chem. **1976**, 20, 299-436. (c) Levy, G. C.; Lichter, R. L.; Nelson, G. L. "Carbon-13 Nuclear Magnetic Resonance Spectroscopy" (2nd ed.); John Wiley and Sons: New York, 1980.

(18) In both ^{13}C and ^{1}H NMR spectra the only impurity peak observed is one assignable to a Cp*, since the chemical analysis figures are good and a weak band appears at 2100 cm^{-1} in the IR, one might postulate $Cp^*_2Hf(H)(C{\equiv}CCH_3)$ as the impurity. A similar suggestion has been made in the formation of $Cp^*_2Hf(H)(CH{=}CHCMe_3)$ (**2b**).[15]

(19) Sanner, R. D. Ph.D. Thesis, California Institute of Technology, 1977.

(20) McDermott, J. X.; Wilson, M. E.; Whitesides, G. M. J. Am. Chem. Soc. **1976**, 98, 6529-6536.

(21) (a) Erker, G.; Kropp, K. J. Am. Chem. Soc. **1979**, 101, 3659-3660. (b) Kropp, K.; Erker, G. Organometallics **1982**, 1, 1246-1247. (c) Skibbe, V.; Erker, G. J. Organomet. Chem. **1983**, 241, 15-26. (d) Erker, G.; Engel, K.; Atwood, J. L.; Hunter, W. E. Angew. Chem. Int. Ed., Engl. **1983**, 22, 494-495. (e) Stockis, A.; Hoffmann, R. J. Am. Chem. Soc. **1980**, 102, 2952-2962 and references cited therein.

(22) The transition state energy difference was calculated using the Arrhenius equation (see Experimental).

(23) Threlkel, R. S. Ph.D. Thesis, California Institute of Technology, 1980.

(24) Threlkel, R. S.; Cohen, S. A.; Bercaw, J. E. Unpublished results.

(25) Since the rates of the reactions were measured only at one temperature, the activation barriers, $\Delta G^{\ddagger}$, were calculated using the Eyring equation. κ (transmission coefficient) was assumed to be unity.[26]

(26) (a) Atkins, P. W. "Physical Chemistry"; W. H. Greeman and Company: San Francisco, 1978, Chapter 26. (b) Hill, C. G., Jr. "An Introduction to Chemical Engineering Kinetics and Reactor Design"; John Wiley and Sons: New York, 1977, Chapter 7.

(27) Lowry, T. H.; Richardson, K. S. "Mechanism and Theory in Organic Chemistry"; Harper and Row: San Francisco, 1976, Chapter 2.

(28) The difference between k_{obs} (no added propene) = 5.9×10^{-5} sec^{-1} for this experiment and k_{obs} (**8**) = 3.0×10^{-5} sec^{-1} result from different preparations in the two sets of experiments. In the propene experiments, nitrogen was condensed in each NMR tube at -196°C before the tube was sealed, resulting in a pressure of $\sim$3 atm. In the isotope labeling experiments, < 1 atm of nitrogen was used in each tube. Thus, some solvent (C_6D_6) reflux could have occurred, resulting in a lower effective temperature. This does not affect the assessment of $\Delta G^{\ddagger}$, however, for a similar value is obtained: $\Delta G^{\ddagger}$ (352 K) = 27.5 kcal·mol^{-1}.

(29) Straus, D. A.; Grubbs, R. H. Personal communication.

(30) Gell, K. I.; Schwartz, J. J. Am. Chem. Soc. **1978**, 100, 3246-3248.

(31) Evans, W. J.; Atwood, J. L. Organometallics **1983**, 2, 709-714.

(32) Another example has since appeared: $Cp^*_2Nb(CO)(C(CH_3)=CH(CH_3))$ loses CO to yield $Cp^*_2Nb(H)((CH_3)C\equiv C(CH_3))$.[1,36]

(33) It has also been observed that the Hf(II) species $\{Cp^*_2HfN_2\}_2N_2$ is much more difficult to make than the zirconium analogue $\{Cp^*_2ZrN_2\}_2N_2$, the difficulty lying in the reduction of the starting $Cp^*_2HfX_2$.[13]

(34) (a) Sanner, R. D.; Erwin, D. K.; Cohen, S. A.; Wood, C.; Messerle, L.; Schrock, R. R.; Bercaw, J. E. Manuscript in preparation. (b) Erwin, D. K. Ph.D. Thesis, California Institute of Technology, 1979.

(35) Bottrill, M.; Green, M. J. Am. Chem. Soc. **1979**, 99, 5795-5796.

(36) (a) Doherty, N. M. Ph.D. Thesis, California Institute of Technology, 1984. (b) McDade, C.; Doherty, N. M.; Bercaw, J. E. Unpublished results.

(37) (a) Brookhart, M.; Green, M. L. H. J. Organomet. Chem. **1983**, 250, 395-408. (b) Schrock, R. R. Accts. Chem. Res. **1979**, 12, 98-104.

(38) Marvich, R. H.; Brintzinger, H. H. J. Am. Chem. Soc. **1971**, 93, 2046-2048.

(39) Brown, T. L.; Dickerhoff, D. W.; Bofus, D. A.; Morgan, G. L. Rev. Sci. Instrum. **1962**, 22, 491-492.

(40) A small amount of insoluble material was always evident when **5a** was placed in benzene-d_6 or was used to synthesize the zirconacyclopentenes **8** and **9**. For kinetics experiments with **5a**, this was centrifuged out of solution to the top of the sealed NMR tube. Compounds **8** and **9** could be isolated cleanly.

(41) If excess 2-butyne is left in the reaction mixture zirconacyclopentene **18** will form (Procedure 16).

(42) Compound **17a** can be formed more rapidly (<1 day) from

{ $Cp^*_2ZrN_2$ }$_2N_2$ and trans-2-butene. Its further characterization has been described.[19]

(43) Pouchert, C. J.; Campbell, J. R. "The Aldrich Library of NMR Spectra", Vol. 1; Aldrich Chemical Company, Inc.: Milwaukee, Wisconsin, 1974.

(44) The peak shape did not change during reaction, and accurate integrations were difficult to obtain due to the proximity of other resonances near the Cp* resonance of the starting compound. Thus, peak heights were adjudged sufficiently accurate for this study.

(45) The resonances due to the Cp* protons of **8** and **9** overlap; only the vinylic resonances were sufficiently separated to monitor. The peak shape did not change during the reaction, but the small size of the resonance made it impossible to get accurate measurements much beyond two half-lives.

CHAPTER III

The Reactions of Aluminum Alkyls with Carbonyl and Hydride Derivatives of Permethylniobocene

Introduction

Aluminum(III) alkyls and halides have many and varied uses, including the synthetically useful formation of C-H, specifically labeled C-D, C-C, and C-O bonds from alkene and alkyne starting materials.[1] Dwarfing these uses, however, is their importance as co-catalysts with early transition metal halides in the Ziegler-Natta polymerization of olefins (eq. 1), which produces

$$CH_2{=}CH_2 \xrightarrow[TiCl_4]{AlR_3} \leftarrow CH_2{-}CH_2 \rightarrow_n \qquad n = 100{,}000 \qquad (1)$$

millions of metric tons of stereoregular polyolefins each year.[2] The desire to better understand the roles of the aluminum and transition metal compounds in the polymerization process has led to substantial investigative efforts surrounding the interactions of aluminum reagents with transition metal compounds, interactions in which the transition metal compound behaves as a Lewis base.

The concept of transition metal basicity was first formalized in the late 1960's as a means of classifying reactions between transition metal compounds and the proton.[3] These reactions generally resulted in transition metal-hydride bonds, with the metal base donating a pair of electrons to the proton. Work on the reactions of transition metal compounds with molecular Lewis acids followed. These reactions were generally proposed to yield transition metal-electrophile bonds analogous to the transition metal-hydride bonds, and some of the proposed structures are supported by X-ray structure determinations.[3-6]

In these studies, the most commonly used molecular Lewis acids have been the alkyl and halide derivatives of Groups IIA (especially Mg), IIIA, and IVA (especially Sn) elements.[4] Of these elements, aluminum(III) is the strongest Lewis acid and, while gallium(III) and indium(III) reagents often form transition metal-Lewis acid metal bonds, only two firm examples of unbridged transition metal-aluminum bonds have appeared in the literature.[5b,c] Indeed, Burlitch and Peterson observed that while $InPh_3$ reacted with an equimolar amount of $[Cp(CO)_3W]^-$ ($Cp \equiv \eta^5$-C_5H_5) to afford a W-In bond, $AlPh_3$ reacted with the same anion to afford a carbonyl-oxygen bound Al adduct,[7] one of the first examples of C- and O-bound carbon monoxide.[8] Thus, the site of coordination of a Lewis acid to a transition metal base depends partly on the nature of the Lewis acid.

The site of coordination also depends on the nature of the ligands attached to the transition metal. While the electron-rich oxygen of transition metal carbonyls is the preferred coordination site of aluminum(III) Lewis acids in many systems,[9] in transition metal carbonyl-halide and -hydride systems aluminum and boron Lewis acids are observed to preferentially coordinate to the halide or hydride ligand. Pan'kowski and coworkers observed the formation of single halide bridges, not carbonyl bridges, in aluminum trihalide adducts of $XMn(CO)_5$ and $CpFe(CO)_2X$ (X = Cl, Br, I).[10a] Similar results were obtained by Powell and Nöth with $(Ph_3Y)Rh(CO)X$ (Y = P, As; X = Br, Cl) and BX_3.[10b] Tebbe proposed a hydride bridge between $Cp_2Nb(H)CO$ and $AlEt_3$ based upon NMR evidence.[11a] Otto and Brintzinger proposed a similar structure for the BF_3 adduct of the same Nb compound based on IR evidence.[11b,12]

Richmond, Basolo and Shriver, in exploring the interaction of aluminum and boron Lewis acids with hydride carbonyl derivatives of Mn, Re, Co, Fe, and Ir, also found the reaction chemistry to be dominated by the behavior of the hydride ligand as a Lewis base, even for such relatively acidic hydrides as $HMn(CO)_5$.[13] Thus, unlike earlier work that had shown the activation of transition metal coordinated CO toward alkyl and aryl migration by molecular Lewis acid coordination of the carbonyl oxygen,[9b,c,d] the thermodynamically less favorable hydride migration was not observed and may even be suppressed by Lewis acid coordination of the potential migrating ligand.

The work presented in this chapter focuses on the reactions of aluminum Lewis acids, with brief excursions to the reactions of other molecular Lewis acids, with carbonyl and hydride derivatives of permethylniobocene. The chemistry of bis(cyclopentadienyl)niobium and -tantalum derivatives has been examined by several groups,[14] and Tebbe has reported the reactions of a series of such compounds, $Cp_2Nb(L)H$ (L = CO, PMe_3, $CH_2{=}CH_2$) and Cp_2MH_3 (M = Nb, Ta), with aluminum, zinc, and hafnium molecular Lewis acids.[11a] The knowledge that substitution of pentamethylcyclopentadienyl ligands can dramatically change the reactivity of a transition metal compound and the prior observation that such differences do exist between niobocene and permethylniobocene derivatives -- in particular the exclusive formation of the <u>endo</u> isomer in olefin-hydride complexes (Fig. 1)[15,16a] and the relatively facile insertion of CO into the Nb-alkyl bond of a variety of alkyl-carbonyl derivatives of permethylniobocene (eq. 2)[15,16b] -- encouraged this study. The possible Lewis acid promotion of carbonyl

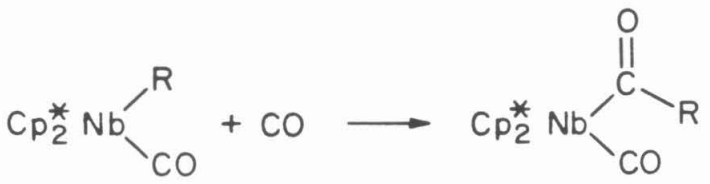

(2)

insertion, seen by Shriver and von Au in some late transition metal systems,[9b,c,d] was of especial interest.[17] The reactions of the carbonyl and hydride derivatives of permethylniobocene with aluminum Lewis acids have indeed yielded results quite different from those of Tebbe[11a] and provide the first example of an aluminum Lewis acid bound to a carbonyl-oxygen in preference to a metal-hydride.

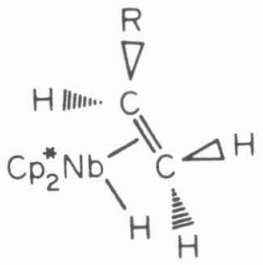

A

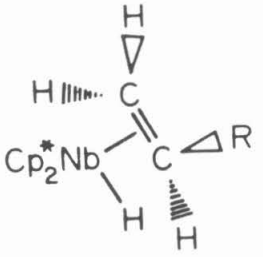

B

Figure 1. Exo (**A**) and Endo (**B**) Isomers of Olefin-Hydride Derivatives of Niobocene.

Results

Synthesis and Characterization of Carbonyl Adducts. The reactions of hydride- and alkyl-carbonyl derivatives of permethylniobocene[15,18] with equimolar amounts of trialkylaluminum reagents occur rapidly in benzene, petroleum ether or petroleum ether/toluene solutions, yielding highly colored products[19] formulated as the carbonyl-oxygen bound aluminum adducts **6–10** (eqs. 3-7). $Cp^*_2Nb(H)(COAlR_3)$ ($Cp^* \equiv \eta^5$-C_5Me_5; R = Me (**6a**), Et (**6b**)),

(3)

1 R = Me **6a**; Et **6b**

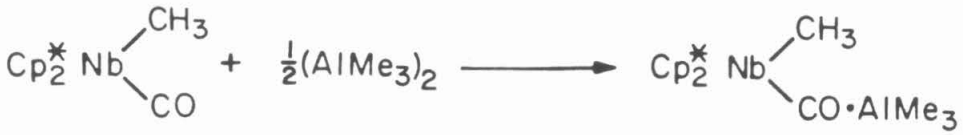

(4)

2 **7**

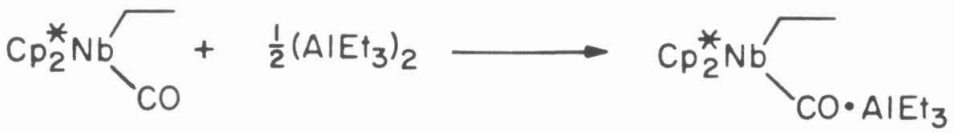

(5)

3 **8**

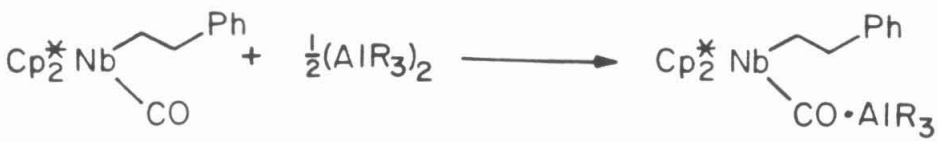

(6)

4 R = Me **9a**; Et **9b**

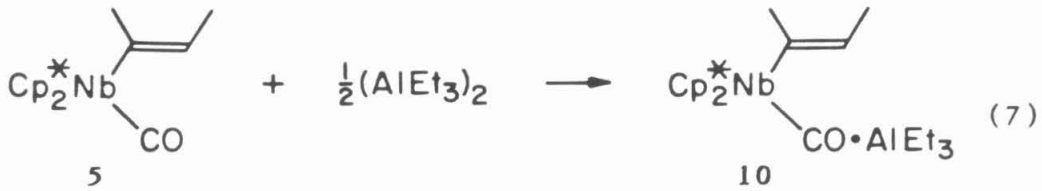

5 10 (7)

$Cp^*_2Nb(CH_3)(COAlMe_3)$ (**7**), and $Cp^*_2Nb(CH_2CH_2Ph)(COAlMe_3)$ (**9a**) have been isolated at -78°C as microcrystalline solids in good to excellent yields[20] and have been fully characterized (NMR, IR, and microanalyses) as 1:1 adducts of the niobium and aluminum reagents. $Cp^*_2Nb(CH_2CH_3)(COAlEt_3)$ (**8**), $Cp^*_2Nb(CH_2CH_2Ph)(COAlEt_3)$ (**9b**), and $Cp^*_2Nb((CH_3)C{\equiv}C(CH_3))(COAlEt_3)$ (**10**) have been prepared in NMR tube experiments and have been characterized by NMR (as well as IR for **10**) and identified by analogy to the isolated products.

The infrared spectroscopic data (Table I) show a significant reduction (>120 cm^{-1}) in the carbonyl stretching frequency of each compound **6a, 6b, 7, 9a** or **10** from that of its precursor **1, 2, 4** or **5.** Furthermore, new bands near 635, 680, and 1180 cm^{-1}, taken as indicative of coordinated trialkylaluminum,[8b] appear in each spectrum (see Experimental Section). The formation of carbonyl adducts **7-10** from the alkyl-carbonyl complexes **2-5** was expected based on the wealth of precedents reported in the literature.[4,8,9a] In each case, the key datum is the large reduction (>65 cm^{-1}) in the carbonyl stretching frequency ν(CO),[8,9] with the opposite result -- a moderate increase in ν(CO) -- taken as primary evidence against CO coordination and for hydride,[11b] halide,[10] or direct metal-aluminum[5bc,7,21] coordination in carbonyl-containing transition metal

Table I. Carbonyl Stretching Frequencies for Nb-CO-Al Adducts and Their Nb-CO Precursors.

Compound	ν(CO), cm^{-1} Nujol Mull	ν(CO), cm^{-1} Solution[a]
$Cp^*_2Nb(H)CO$ (**1**)[b]	1875	1867[c]
$Cp^*_2Nb(H)(COAlMe_3)$ (**6a**)	1721	--
$Cp^*_2Nb(H)(COAlEt_3)$ (**6b**)	1737	1737
$Cp^*_2Nb(CH_3)CO$ (**2**)[b]	1853	1856
$Cp^*_2Nb(CH_3)(COAlMe_3)$ (**7**)	1708	1721
$Cp^*_2Nb(CH_3)(COAlMe_2CH_2CH_2Ph)$ (**14**)	--	1719
$Cp^*_2Nb(CH_2CH_2Ph)CO$ (**4**)[d]	1867	1855
$Cp^*_2Nb(CH_2CH_2Ph)(COAlMe_3)$ (**9a**)	1703	--
$Cp^*_2Nb(C(CH_3)=CH(CH_3))CO$ (**5**)[d]	--	1858[e]
$Cp^*_2Nb(C(CH_3)=CH(CH_3))(COAlEt_3)$ (**10**)	--	1734[e]

[a]Each of these compounds shows a significant amount of uncoordinated Nb compound in equilibrium with the Al adduct in solution. See text. [b]From ref. 18. [c]C_6D_6 solutions unless otherwise specified. [d]From ref. 15. [e]C_7D_8 solution.

complexes. The formation of carbonyl adducts **6a** and **6b** is unexpected; it is supported by the large reduction in ν(CO) for both compounds, especially when compared with "no significant shift in ν(CO)" for $Cp_2Nb(HAlEt_3)$-

CO[11a] and a 30 cm^{-1} increase observed for $Cp_2Nb(HBF_3)CO$.[11b]

The formation of compounds **6-10** as 1:1 carbonyl adducts is further supported by ^1H nuclear magnetic resonance spectroscopy (Table II). Peak position changes are, in general, not dramatic but they are significant. Integration of peak intensities indicates the isolated compounds **6a, 6b, 7** and **9a** have complexed one mole of AlR_3 per mole of Nb precursor. The ^1H NMR spectra are most useful for compounds **6a** and **6b**, where the small (0.8 ppm) downfield shift of the hydride signal for each compound contrasts markedly with the large (5.1 ppm) upfield shift observed for $Cp_2Nb(HAlEt_3)CO$.[11a] Similarly large upfield shifts have also been observed for $Cp_2Nb(HAlEt_3)$-PMe_3,[11a] $Cp_2Nb(HAlEt_3)(C_2H_4)$,[11a] and $[Cp_2Zr(HAlMe_3)H]_2$.[12c]

The use of ^{13}C NMR spectroscopy in these systems has been limited by the quadrupolar broadening effects of both ^{93}Nb ($I = 9/2$) and ^{27}Al ($I = 5/2$). The synthesis of $Cp^*_2Nb(H)(^{13}COAlEt_3)$ (**6b**-^{13}CO) [$\nu(^{13}CO) = 1700\ cm^{-1}$], however, allows a comparison of the O-complexed carbonyl's carbon shift (δ 321.5 ppm) with the uncomplexed carbonyl's carbon in $Cp^*_2Nb(H)(^{13}CO)$ (**1**-^{13}CO) (δ 279.3 ppm) (Table II), and suggests a significant amount of carbenoid character in the μ_2-(C-η^1; O-η^1) carbonyl ligand (Fig. 2).[22]

$$Nb-C\equiv O:\rightarrow Al \longleftrightarrow Nb=C=\ddot{O}:\rightarrow Al \longleftrightarrow Nb\equiv C-\ddot{\underset{\cdot\cdot}{O}}:\rightarrow Al$$

Figure 2. Major Resonance Forms for a μ-(C-η^1; O-η^1) Carbonyl Bridge.

Table II. Nuclear Magnetic Resonance Data.[a]

Compound		Assignment	Chemical Shift, Multiplicity, Coupling Constants
$Cp^*_2Nb(H)CO$ (**1**)[b]	^1H	$C_5(C\underline{H}_3)_5$	1.80 s
		Nb-$\underline{H}$	-5.59 s,br
	$^{13}C\{^1H\}$	$C_5(\underline{C}H_3)_5$	11.6
		$\underline{C}_5(CH_3)_5$	100.4
		Nb-$\underline{C}O$	279.3 $\nu_{1/2}$ = 74 Hz[c]
$Cp^*_2Nb(H)(COAlMe_3)$ (**6a**)	^1H	$C_5(C\underline{H}_3)_5$	1.66 s
		Nb-$\underline{H}$	-4.72 s,br
		Al-$C\underline{H}_3$	-0.14 s
$Cp^*_2Nb(H)(COAlEt_3)$ (**6b**)	^1H	$C_5(C\underline{H}_3)_5$	1.70 s
		Nb-$\underline{H}$	-4.77 s,br
		$AlC\underline{H}_2CH_3$	0.55 q J = 8
		$AlCH_2C\underline{H}_3$	1.43 t J = 8

Table II. Continued.

Compound		Assignment	Chemical Shift, Multiplicity, Coupling Constants
	$^{13}C\{^{1}H\}$	$C_5(\underline{C}H_3)_5$	11.3
		$\underline{C}_5(CH_3)_5$	102.7
		Nb-$\underline{C}$O-Al	321.5 $\nu_{1/2}$ = 95 Hz[c]
		Al$\underline{C}H_2CH_3$	1.7
		Al$CH_2\underline{C}H_3$	10.3
$Cp^*_2Nb(CH_3)CO$ (2)[b]	^{1}H	$C_5(C\underline{H}_3)_5$	1.53 s
		Nb-$C\underline{H}_3$	-0.93 s
$Cp^*_2Nb(CH_3)(COAlMe_3)$ (7)	^{1}H	$C_5(C\underline{H}_3)_5$	1.47 s
		Nb-$C\underline{H}_3$	-0.96 s
		Al-$C\underline{H}_3$	-0.16 s
$Cp^*_2Nb(CH_3)(COAlMe_2CH_2CH_2Ph)$ (14)	^{1}H	$C_5(C\underline{H}_3)_5$	1.45 s
		Nb$C\underline{H}_3$	-0.97 s

Table II. Continued.

Compound		Assignment	Chemical Shift, Multiplicity, Coupling Constants
		$AlC\underline{H}_3$	-0.18 s
		$AlC\underline{H}_2CH_2C_6H_5$	0.81)) AA'XX'
		$AlCH_2C\underline{H}_2C_6H_5$	3.07)
		$AlCH_2CH_2C_6\underline{H}_5$	6.98-7.54
$Cp^*_2Nb(CH_2CH_3)CO$ (3)[d]	^1H	$C_5(C\underline{H}_3)_5$	1.62 s
		$NbC\underline{H}_2CH_3$	-0.03 q J = 8
		$NbCH_2C\underline{H}_3$	1.61 t J = 8
$Cp^*_2Nb(CH_2CH_3)(COAlEt_3)$ (8)[e]	^1H	$C_5(C\underline{H}_3)_5$	1.53 s
		$NbC\underline{H}_2CH_3$	-0.12 q J = 8
		$NbCH_2C\underline{H}_3$	f
		$AlC\underline{H}_2CH_3$	0.36 q J = 8
		$AlCH_2C\underline{H}_3$	1.49 t J = 8

Table II. Continued.

Compound		Assignment	Chemical Shift, Multiplicity, Coupling Constants
$Cp^*_2Nb(CH_2CH_2Ph)CO$ (**4**)[d]	^1H	$C_5(C\underline{H}_3)_5$	1.58 s
		$NbC\underline{H}_2CH_2C_6H_5$	0.02)) AA'XX'
		$NbCH_2C\underline{H}_2C_6H_5$	2.84)
		$NbCH_2CH_2C_6\underline{H}_5$	7.15-7.66
$Cp^*_2Nb(CH_2CH_2Ph)(COAlMe_3)$ (**9a**)	^1H	$C_5(C\underline{H}_3)_5$	1.51
		$NbC\underline{H}_2CH_2C_6H_5$	0.02)) AA'XX'
		$NbCH_2C\underline{H}_2C_6H_5$	2.76)
		$NbCH_2CH_2C_6\underline{H}_5$	7.0-7.6
		$AlC\underline{H}_3$	-0.17 s
$Cp^*_2Nb(CH_2CH_2Ph)(COAlEt_3)$ (**9b**)[e]	^1H	$C_5(C\underline{H}_3)_5$	1.53 s
		$NbC\underline{H}_2CH_2C_6H_5$	-0.03)) AA'XX'
		$NbCH_2C\underline{H}_2C_6H_5$	2.66)
		$NbCH_2CH_2C_6\underline{H}_5$	7.0-7.4

Table II. Continued.

Compound		Assignment	Chemical Shift, Multiplicity, Coupling Constants	
		$AlC\underline{H}_2CH_3$	0.42 q	J = 9
		$AlCH_2C\underline{H}_3$	1.48 t	J = 9
$Cp^*_2Nb(C(CH_3)=CH(CH_3))CO$ (5)[d]	^1H	$C_5(C\underline{H}_3)_5$	1.59[g] s 1.61[h] s	
		$NbC(C\underline{H}_3)=CHCH_3$	1.63 dq[i] 2.30 dq	 J = 1.7, 1.0
		$NbC(CH_3)=CHC\underline{H}_3$	1.81 dq 1.83 dq	J = 6.3, 1.0 J = 6.3, 1.0
		$NbC(CH_3)=C\underline{H}CH_3$	4.76[g] qq 6.12[h] qq	J = 6.3, 1.8 J = 6.3, 1.4
$Cp^*_2Nb(C(CH_3)=CH(CH_3))(COAlEt_3)$ (10)[j]	^1H	$C_5(C\underline{H}_3)_5$	1.49[g] s 1.53[h] s	
		$NbC(C\underline{H}_3)=CHCH_3$	1.40[g] s,br 2.11[h] s,br	
		$NbC(CH_3)=CHC\underline{H}_3$	1.74[g] d 1.69[h] d	J = 6 J = 6

Table II. Continued.

Compound		Assignment	Chemical Shift, Multiplicity, Coupling Constants
		$NbC(CH_3)=C\underline{H}CH_3$	4.49[g] qq J = 6, 1.5 5.97[h] qq J = 6, 1.5
		$AlC\underline{H}_2CH_3$	0.38 q J = 7
		$AlCH_2C\underline{H}_3$	1.34 t J = 7
$Cp^*_2NbH_3$ (11)[b]	^1H	$C_5(C\underline{H}_3)_5$	1.90 s
		$Nb\text{-}\underline{H}_c$	-1.20 br
		$Nb\text{-}\underline{H}_o$	-2.30 d,br J = 3
$Cp^*_2NbH_3 \cdot AlEt_3$ (12)	^1H	$C_5(C\underline{H}_3)_5$	1.91 s
		$Nb\text{-}\underline{H}_c$	-1.44 br
		$Nb\text{-}\underline{H}_o$	-2.13 d,br J = 5
		$AlC\underline{H}_2CH_3$	0.30 q J = 7
		$AlCH_2C\underline{H}_3$	1.17 t J = 7

Table II. Continued.

---

[a] ^{1}H (90 MHz) (T = 34°C) and ^{13}C (22.5 MHz) (T = ambient, ~24°C) NMR spectra taken in benzene-d_6 solution unless otherwise noted. Chemical shifts are reported in ppm relative to internal TMS or residual protons and the carbons in the solvent. Coupling constants are reported in Hz. [b] First reported in ref. 18. [c] Obtained using ^{13}C enriched CO (95%). [d] First reported in ref. 15. [e] C_7D_8 solution. [f] Not observed. [g] Based on relative peak intensities of the mixture of **5a** + **5b** (or **10a** + **10b**) a single isomer, **5a** (or **10a**), gives rise to these signals. [h] The other isomer, **5b** (or **10b**), gives rise to these signals. [i] Coupling obscured by Cp* peak.

Association of the 1:1 adducts in solution was not expected due to the steric bulk of the Cp* ligands and was not observed. The cryoscopically determined molecular weight of **6b** shows it to be monomeric in benzene solution. The other adducts are assumed monomeric by analogy.

Synthesis and Characterization of a Hydride Adduct. The trihydride $Cp^*_2NbH_3$ (**11**) reacts rapidly with an equimolar amount of triethylaluminum in petroleum ether, toluene, or benzene solution yielding a 1:1 adduct **12** (eq. 8). Compound **12** has been isolated at -78°C in moderate yield as a

$$Cp^*_2Nb(H)_3 + \tfrac{1}{2}(AlEt_3)_2 \longrightarrow Cp^*_2Nb(H)_3 \cdot AlEt_3 \qquad (8)$$

11 **12**

microcrystalline, off-white solid and has been fully characterized (NMR (Table II); IR (Table III); microanalysis). The small downfield shift (0.15 ppm) of the ^1H NMR signal of the two outer hydrides and the larger upfield shift (0.35 ppm) of the signal due to the central hydride, while not as dramatic as for $Cp_2TaH_3 \cdot AlEt_3$,[11a] suggest the central hydride is preferentially coordinated to the aluminum. However, a fluxional adduct whose momentary static structure would resemble the bridging structure of $Cp_2WH_2 \cdot AlMe_3$[6a] cannot be ruled out.

Unlike its parent $Cp_2NbH_3 \cdot AlEt_3$,[11a] compound **12** is stable for a day in room temperature solution. Its decomposition is less clean than that of its parent, however. The growth and reduction of four different Cp* signals, the release of ethane, and H/D exchange between at least one of the decomposition products and the methyl group of toluene-$\underline{d}_8$ are observed by

Table III. Niobium-Hydride Stretching Frequencies in Lewis Acid Adducts and Their Nb-H Precursors.

Compound	ν (Nb-H), cm^{-1} [a]
$Cp^*_2NbH_3$ (**11**)	1752, 1697[c]
$Cp^*_2NbH_3 \cdot AlEt_3$ (**12**)	1736, 1706[c]
$Cp^*_2Nb(H)CO$ (**1**)[b]	1700
$Cp^*_2Nb(H)(COAlEt_3)$ (**6b**)	1710
$Cp^*_2Nb(HBF_3)CO$ (**13**)[d]	2390

[a]In nujol mull unless otherwise specified. [b]First reported in ref. 18. [c]The more intense signal of the two. [d]Hydride appears to be in a terminal position on boron (see text).

^1H NMR spectroscopy.

Although not yielding a niobium-hydride-Lewis acid adduct, the reaction between equimolar amounts of $Cp^*_2Nb(H)CO$ (**1**) and the Lewis acid BF_3 in benzene appears to occur at the hydride (eq. 9). The carbonyl stretching frequency of the sparingly soluble bright magenta solid **13** increases

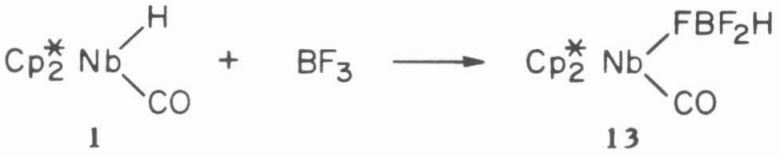

1 **13** (9)

slightly to 1887 cm^{-1} (Table I) and the hydride peak at δ -4.8 ppm is absent in the ^1H NMR spectrum.[23] A broad, medium intensity

band is observed at 2390 cm^{-1} in the IR spectrum (Table III), a region characteristic of terminal B-H bonds.[24,25] Although strong bands at 1170, 1122, 919, 886, and 725 cm^{-1} may not all be definitively assigned as BF bands, they are consistent with bands observed and assigned by Beck and Schloter in L_nMFBF_3 (M = Cr, Mo, W) adducts.[26] Thus, our data support the formulation of **13** as an F-bridged HBF_3 adduct.

The Nature of the Adducts in Solution. While niobium-aluminum adducts **6a, 6b, 7, 9a** and **12** have been isolated from -78°C solution and characterized as 1:1 solids by NMR and IR spectroscopies and microanalyses, variable temperature NMR spectroscopy and solution IR spectroscopy indicate that in solution the adducts exist in equilibrium with the uncomplexed precursors (eq. 10).[27]

$$(AlR_3)_2 \overset{K_{Al}}{\rightleftharpoons} 2\,AlR_3 \qquad (10a)$$

$$Cp^*_2Nb(R')(CO) + AlR_3 \overset{K_{CO}}{\rightleftharpoons} Cp^*_2Nb(R')(CO{\cdot}AlR_3) \qquad (10b)$$

$$Cp^*_2NbH_3 + AlEt_3 \overset{K_H}{\rightleftharpoons} Cp^*_2NbH_3{\cdot}AlEt_3 \qquad (10c)$$

For $Cp^*_2NbH_3 \cdot AlEt_3$ (**12**), significant changes in the position of Cp^*, $AlEt_3$ and Nb-H resonances in the ^1H NMR spectrum occur as the temperature is lowered from 30 to -50°C. The most dramatic changes are those of the hydride signals (Fig. 3). The signal corresponding to the central hydride continues to move upfield and that for the outer hydrides downfield as the temperature is lowered, becoming increasingly similar to the values observed for $Cp_2TaH_3 \cdot AlEt_3$.[11a]

The solution IR spectra of the 1:1 adducts **6–10** always show a moderately sized band assigned to the carbonyl stretching frequency of the starting material **1–5** in addition to the very strong band assigned as ν (CO) of the aluminum adduct. Figure 4 shows an overlay of the carbonyl stretching region for **1** and **6a**. The other compounds showed similar results. As expected in an equilibrium situation, addition of AlR_3 to solutions of $Cp^*_2Nb(R')(COAlR_3)$ reduces the size of the band due to $Cp^*_2Nb(R')CO$.

A quantitative IR spectroscopic analysis of the solution equilibria of compounds **6a** and **6b** in benzene (eqs. 10a and 10b) finds the overall equilibrium constant $K_{Al} \cdot K_{CO}$ on the order of 10^{-2} for both systems (Table IV). Employing literature values of K_{Al} for $(AlMe_3)_2$ and $(AlEt_3)_2$ in benzene solution,[28] we find the adduct formation constant K_{CO} to be $1.1(2) \times 10^5$ M^{-1} for **6a** and $4.5(30) \times 10^3$ M^{-1} for **6b**.[29] The significance of this difference will be considered in the Discussion.

Reactions with Other Lewis Acids. The reaction of the hydride-carbonyl compound **1** with the Lewis acid BF_3 has been described (vide supra). Unlike the trialkylaluminum Lewis acids, BF_3 reacts with the hydride ligand ultimately yielding **13**. With trimethylborate, in contrast, no reaction is

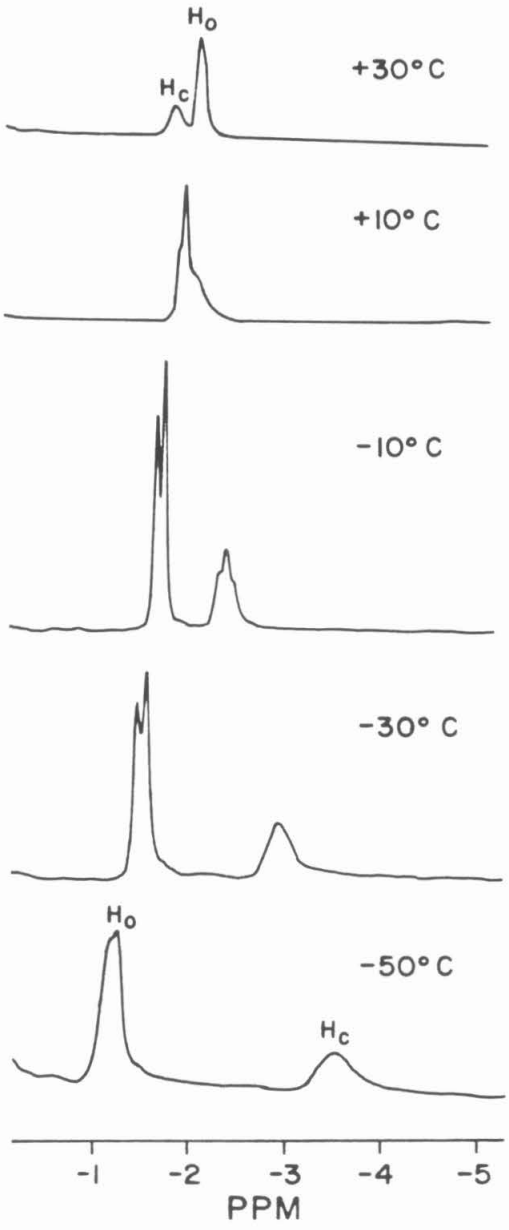

Figure 3. ^{1}H NMR Variable Temperature Experiment for $Cp^{*}_{2}NbH_{3}\cdot AlEt_{3}$ (12). Movement of the Hydride Signals with Temperature.

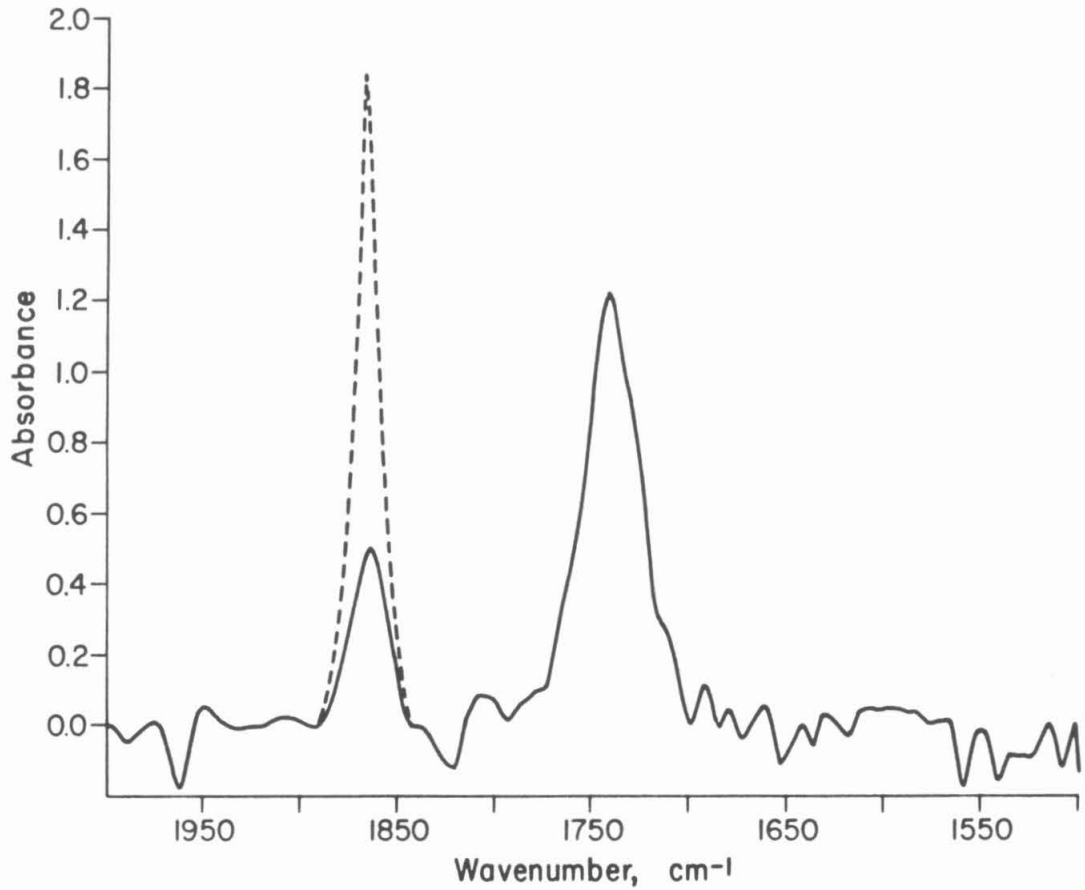

Figure 4. Solution Infrared spectra (Absorbance Mode) Comparing the Carbonyl Region for 0.100 M $Cp^*_2Nb(H)CO$ (**1**) (---) and 0.100 M $Cp^*_2Nb(H)(COAlMe_3)$ (**6a**) (——).

Table IV. Equilibrium Constant Determination for

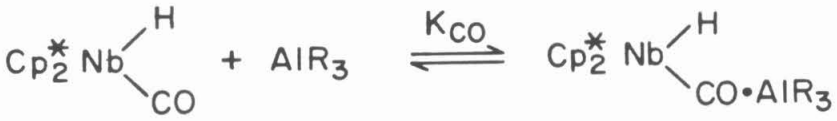

$[Cp^*_2Nb(H)CO]_T$[a]	$[AlR_3]_T$[a]	$K_{Al} \cdot K_{CO}$[b]	K_{CO}[b]
	R = Et		
0.100	0.036	1.1×10^{-1}	5.0×10^3
0.100	0.050	4.4×10^{-2}	2.0×10^3
0.100	0.072	5.1×10^{-2}	2.3×10^3
0.100	0.108	1.9×10^{-1}	8.5×10^3
	R = Me		
0.100	0.100	1.1×10^{-2}	1.2×10^5
0.099	0.099	9.0×10^{-3}	1.0×10^5

[a]Total concentration of reagent in moles·liter^{-1}. [b]Equilibrium constants defined by equations 10a and 10b in the text. Values were determined in two separate experiments.

observed, even after one day at 80°C.

Compound **1** does react instantaneously with $AlBr_3$ in benzene solution, yielding an insoluble dark green solid. The solid does dissolve in dichloromethane-d_2. The resulting purple-red solution[30] contains a mixture with three major products, two of them having inequivalent Cp* rings. Reaction of the alkyl-carbonyl compound **4** with $AlBr_3$ in dichloromethane-d_2

also produces a dark red solution, this one containing a 2:1 mixture of two products. These reactions were not pursued.[31]

Reactivity of the Carbonyl- and Hydride-Aluminum Adducts. The addition of aluminum Lewis acids to hydride- and alkyl-carbonyl complexes **1-5** did not result in CO insertion (alkyl migration). Compounds **3**, **4**, and **5** are known to insert CO when heated in the presence of an excess (~3 atm) of the gas.[15] Their aluminum adducts **8**, **9a**, **9b**, and **10** behave quite differently, however.

Compound **8** is unstable in room temperature solution, reacting in benzene or toluene with a half-life of approximately one day to form **6b** with the release of ethylene (eq. 11).[32] A minor (< 15%) unidentified product

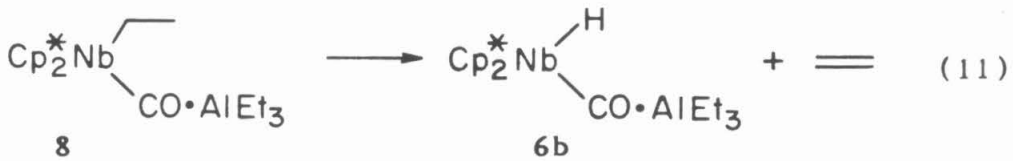

(11)

containing a metal-hydride (δ -2.5, br) and some ethane are also produced in the room temperature reaction. Both the unknown niobium compound and the ethane are absent when the reaction occurs in the presence of excess CO.

Compounds **9a** and **9b** are also unstable at room temperature, both in solution and in the solid state. The trimethylaluminum adduct **9a** cleanly produces the transalkylated product **14** (eq. 12). The reaction is first order in loss of **9a** (Fig. 5) with a half-life of 29.6 min ($k = 3.9(4) \times 10^{-4}$ sec^{-1}) at 34°C.[33] Compound **9b** also transalkylates at room temperature to form compound **15** (eq. 13), but the reaction is complicated by the subsequent loss

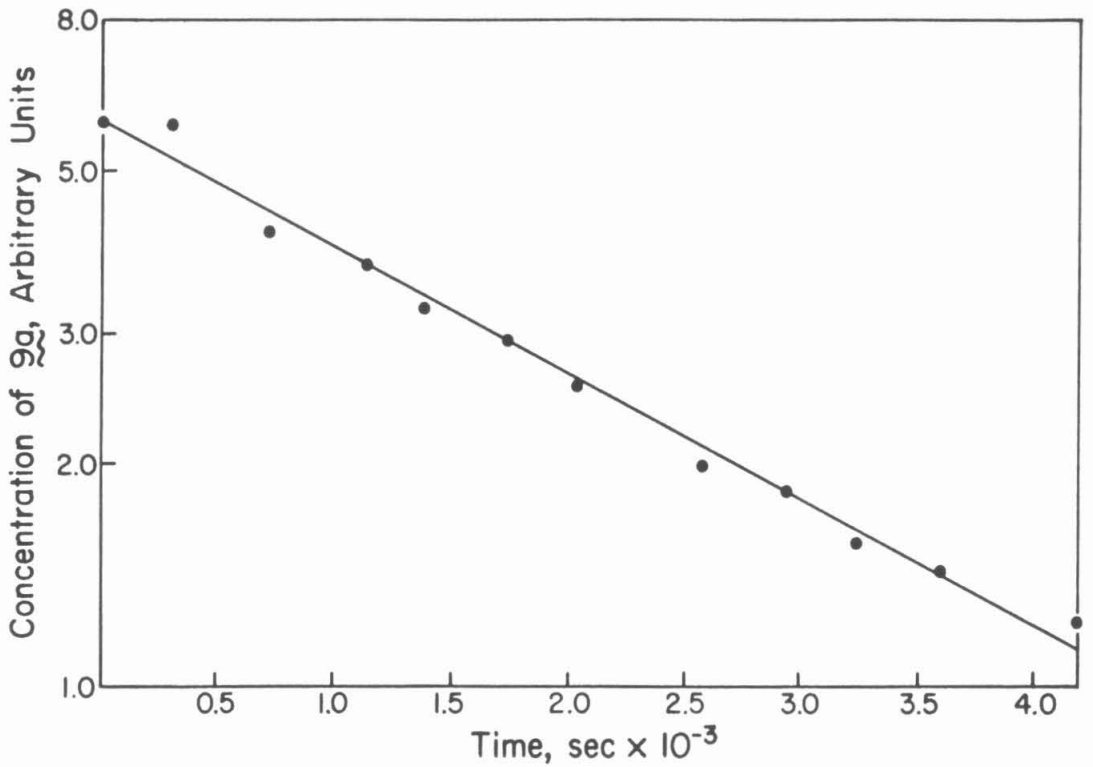

Figure 5. The Transalkylation of **9a** to Form **14:** Kinetic Plot Demonstrating the First-Order Loss of **9a** at 34°C. The loss of **9a.** The loss of **9a** was monitored by measuring the integration of the Cp* resonance relative to the integration of the methyl resonance of added toluene.

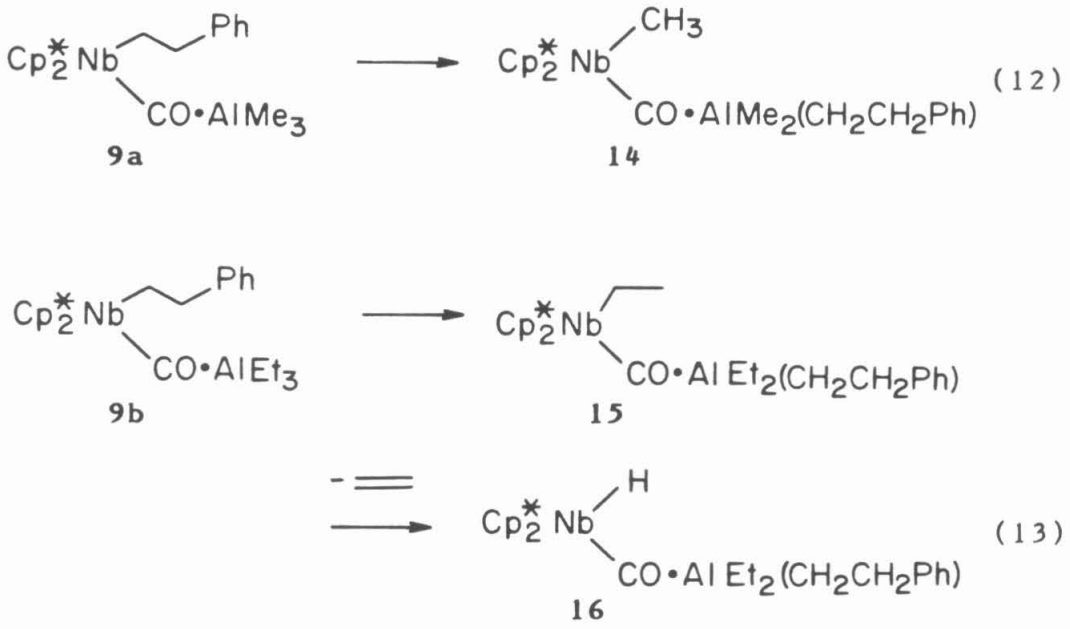

of ethylene (vide supra), which is not kinetically distinct from the trans-alkylation step.[33a] Due to the instability of **9a** and **9b**, no attempt to react either with CO was made.

In contrast to **8**, **9a**, and **9b**, compound **10** is very stable. Like its precursor **5**,[15] **10** exists in two isomeric forms (Fig. 6) that interconvert slowly. Unlike **5**, which loses CO over days in room temperature solutions not maintained in the dark (eq. 14), compound **10** is stable for weeks in solution.

Figure 6. The Two Isomers of Compound **10**.

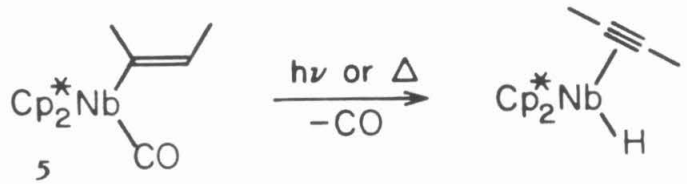

5 (14)

Compound **5** can be heated (120°C) in the presence of excess CO to produce an inserted and rearranged product.[15] When **10** is handled under identical conditions, however, the only observed niobium product (^{1}H NMR) is **5**. Free ethane and ethylene are also observed; no $AlEt_3$ remains.

An unidentified orange oil is formed in the NMR tube reaction described above. This oil also appears when **7** is heated (80°C) in the presence of CO. The only observed niobium product of this reaction is the precursor **2**, and free ethane and ethylene are observed. Again, no $AlMe_3$ remains. Carbonyl insertion is not found in **2**,[18a] nor is it observed for the niobium compound in this system. Transalkylation of the triethyl analogue of **7** does occur (eq. 15), but it proceeds much more slowly and less cleanly

(15)

than in **9a** and **9b**. As observed for **9b**, the reaction is complicated by the elimination of ethylene. The ultimate product does not appear to be the diethylmethylaluminum adduct of **1**, however. The only observable hydride signal occurs at δ -1.75 ppm.

Compound **6b** does not react with excess CO either. The blue solution becomes red after five days (This is also observed for solutions

of **6** that have stood for greater than one week at room temperature), but no significant changes are observed in the ^1H NMR spectrum. Compound **6b** does react with H_2, however, rapidly producing **1** and ethane in melting benzene (eq. 16). The presumed aluminum product, AlH_3, is expected to be

6b **1** (16)

polymeric in benzene. No solid is observed, but a broad lump under the Cp* resonance is observed by ^1H NMR spectroscopy. Compound **6a** is much less reactive towards H_2, producing methane after days at 80°C with some decomposition evident (^1H NMR peak at δ -2.2 ppm).[34]

The transalkylation reaction of **9a** (eq. 12) provides a new route to **2**. Preliminary experiments with poly(4-vinylpyridine-co-styrene) produce moderate yields of **2** from **14** (eq. 17). The previously reported synthesis of **2**

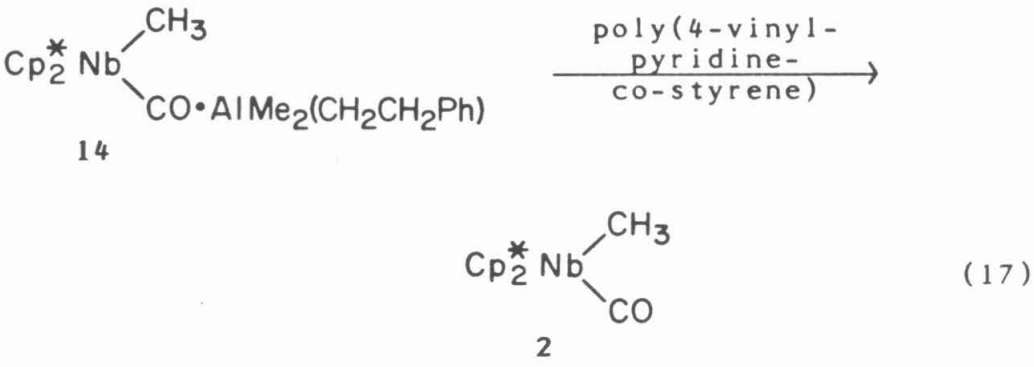

14 **2** (17)

requires one less step from $Cp^*_2NbH_3$ (**11**),[18a] but the final two steps of that synthesis have been reproduced only sporadically.

The decomposition of the hydride-aluminum adduct **12** has been described (vide supra). Compound **12** reacts with CO at 80°C to produce a red solution of the hydride-carbonyl-aluminum adduct **6b**. While these conditions are the same employed to produce **1** from $Cp^*_2NbH_3$ (**11**), the reaction time is shorter (ca. 3 h vs. ca. 12 h).

Discussion

A number of niobium-carbonyl-aluminum adducts have been synthesized. It is expected that a hard Lewis acid such as Al(III) should interact with the hard basic oxygen of a transition metal carbonyl.[35] However, the formation of the carbonyl-aluminum adducts **6a** and **6b** contrasts sharply with the precedent established by the parent compound, $Cp_2Nb(H)CO$, which preferentially forms a hydride-aluminum adduct.[11a]

The substitution of the two pentamethylcyclopentadienyl rings for two cyclopentadienyl rings has two consequences. The Cp* ligands are both more electron-releasing and more sterically demanding than the Cp ligands. The effect of the additional electron donation to the metal center is clearly seen in its effect on ν(CO), which decreases 25-50 cm^{-1} (Table V) indicating increased backbonding from the metal center. The effect on ν(Nb-H) is less clear, however, with an increase in one case, a decrease in another, and very little change in the hydride-carbonyl complexes (Table V).

The increased basicity at the carbonyl-oxygen coupled with virtually no change in the basicity of the hydride, as determined by the changes in IR spectra, may be an important factor in determining the site of aluminum coordination to **1**. However, the importance of the steric effect cannot be overlooked. Steric hindrance was cited by Shriver and coworkers when neither $AlBr_3$ nor BCl_3 reacted with $H_3Re_3(CO)_{12}$ yet both effected halide exchange with $HRe(CO)_5$.[13] In early transition metal bent-sandwich complexes, the bulk of the Cp* ligands is sufficient to stabilize otherwise highly reactive 14- and 16-electron species.[17a,36] In the niobium system, the steric demands of the (Cp^*_2NbR) fragment limit coordination to the small rod-like

Table V. Comparison of ν(CO) and ν(Nb-H) for Cp and Cp* Substituted Niobium Complexes.

Compound	ν (CO), cm^{-1}	ν(Nb-H), cm^{-1}
$Cp_2Nb(H)CO$[a]	1900	1695
$Cp^*_2Nb(H)CO$ (**1**)[b]	1875	1700
$Cp_2Nb(R)CO$[c]	1895-1905	
$Cp^*_2Nb(R)CO$[d]	1853-1867	
Cp_2NbH_3[a]		1710, 1670
$Cp^*_2NbH_3$ (**12**)[b]		1752, 1697
$Cp_2Nb(C_2H_4)H$[a]		1735
$Cp^*_2Nb(C_2H_4)H$[b]		1710
$Cp_2Nb(H)PMe_3$[a]		1625

[a]Ref. 14e. [b]Ref. 18. [c]Ref. 14b. [d]Ref. 15.

ligands CO, CNMe and NCMe, with phosphines apparently too bulky to enter the coordination sphere of the metal.[15] Thus, coordination of aluminum to the carbonyl rather than the hydride in **1** may occur because the trialkylaluminum compound is too bulky to approach the hydride that is screened by the methyl groups of the Cp* ligand. In contrast, the carbonyl-oxygen is

more distant from the steric bulk and therefore more accessible (Fig. 7).

Two results suggest the steric factor is more important than the electronic factor. First, the formation constant K_{CO} for equation 10b is two

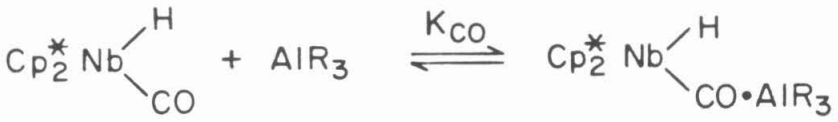

(10b')

orders of magnitude larger when R=Me than when R=Et. Steric factors dominate the formation and stability of aluminum dimers and donor-acceptors complexes;[1] these values for K_{CO} demonstrate steric factors are equally important in the niobium system. $AlMe_3$ is able to form a stronger CO adduct because its smaller size allows a closer approach. Second, compound 1 does react with the smaller Lewis acid BF_3 at the hydride ligand; there is no evidence of prior coordination to the carbonyl ligand. This result

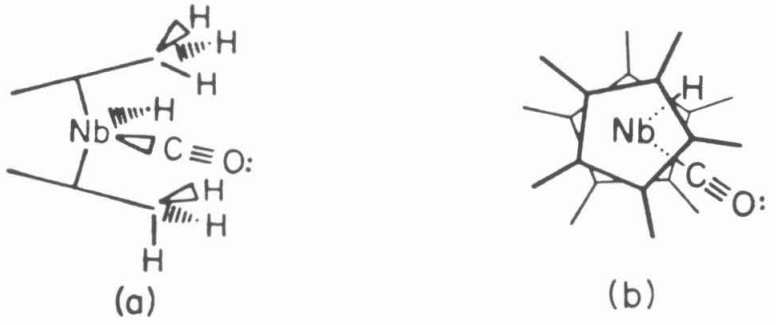

Figure 7. Steric Constraints of the Pentamethylcyclopentadienyl Ligands in $Cp^*_2Nb(H)CO$ (1). (a) Side View. (b) Top View.

suggests the hydride ligand remains the more basic site, although this suggestion must necessarily be tempered by the lack of evidence for Nb-H-B adduct formation prior to halide-for-hydride exchange. The very different reactivity of 1 with $AlBr_3$ (vs. AlR_3) may also result from the smaller $AlBr_3$ coordinating to the hydride and then, due to its higher Lewis acidity, reacting further. Trimethylborate is too large to react at the hydride site and apparently too weak a Lewis acid to coordinate to a terminal carbonyl ligand.

Shriver and coworkers observed that $AlBr_3$ activated coordinated carbon monoxide toward alkyl migration in Mn, Fe, and Mo alkyl carbonyls even in the absence of added CO. Aluminum alkyls did not promote the CO insertion.[9c] Von Au and coworkers obtained a similar result in a Re system.[9d] In the niobium systems described in this study, $AlBr_3$ is too strong to react cleanly, and the alkylaluminum compounds do not promote CO insertion even in the presence of added CO. The ability of an electron-rich bromine atom to fill the vacant site left by formation of the acyl group is an important factor in the success of $AlBr_3$ promotion of CO insertion and may be a factor in the lack of success with the niobium systems. Metal-alkyl-aluminum electron-deficient bonds are known for Ti, Sc, V and a number of lanthanides.[37] These systems are all unsaturated, so the formation of such alkyl bridges in these saturated niobium systems is not expected to be a driving force for CO insertion.

It might be expected that the presence of equilibrium amounts of uncomplexed niobium compounds would influence the reactivity of **6-10** and **12**. Only **12**, though, produces the same product upon reaction with CO that its precursor **11** does, yet **12** does this more rapidly than **11**. The other

compounds behave quite differently than their precursors. Compound **8** reacts in room temperature solution to give **6b** while its precursor **3** is stable until heated in solution at 80°C, whence it decomposes to yield a greater amount of $Cp^*_2Nb(C_2H_4)H$ than **1**. The apparent β-hydrogen elimination, if written in the usual manner (eq. 18), would result in a 20-electron intermediate, which is unlikely. The presence of a significant amount of an impurity (<15%) except in the presence of CO suggests that the reaction mechanism is not simple.

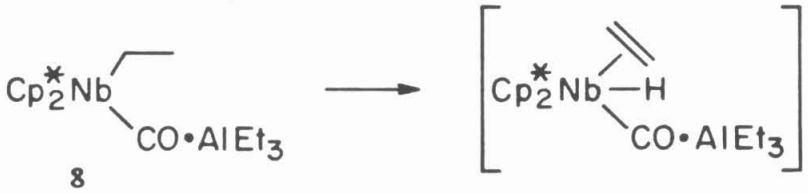

(18)

The stability of compound **10**, which like **7** appears to act as a catalyst for the decomposition of AlR_3 in the presence of CO,[38] suggests that the equilibria in equation 19 must lie far to the right. Otherwise, an observable (^1H NMR or IR) amount of the 2-butyne-hydride complex would be seen. While it is not, IR spectroscopy does demonstrate the presence of some **5** in solution.

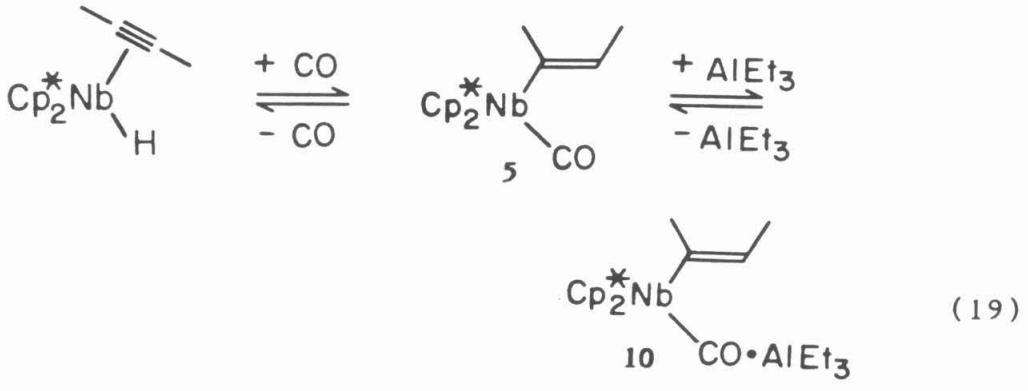

(19)

The transalkylation reactions observed for **9a** and **9b** are the most unusual reactions in these niobium systems. Alkylaluminum compounds have long been used as alkylating agents in organic and inorganic chemistry,[1] but the reactions usually occur between aluminum alkyls and metal-halides[39] or occur as equilibria among metal alkyls that produce statistical product distributions.[1] These transalkylations do neither, irreversibly exchanging Nb-alkyl and Al-alkyl'. The first order loss of **9a**[40] and production of **14**[33b] suggests an intermediate or transition state similar to that proposed for alkyl-halide exchange (Fig. 8 (a)). Any intermediate or transition state in which the aluminum remains coordinated to the carbonyl oxygen (Fig. 8 (b)) would appear to involve considerable strain. An intermediate having two alkyl bridges (Fig. 8 (c)) is a possibility,[37] although any intermediate must have a very short lifetime since **14** is produced at the same rate **9a** is lost and there is no noticeable induction period. The formation of the very stable aluminum adducts of **1** and **2** appears to be the driving force for these reactions.

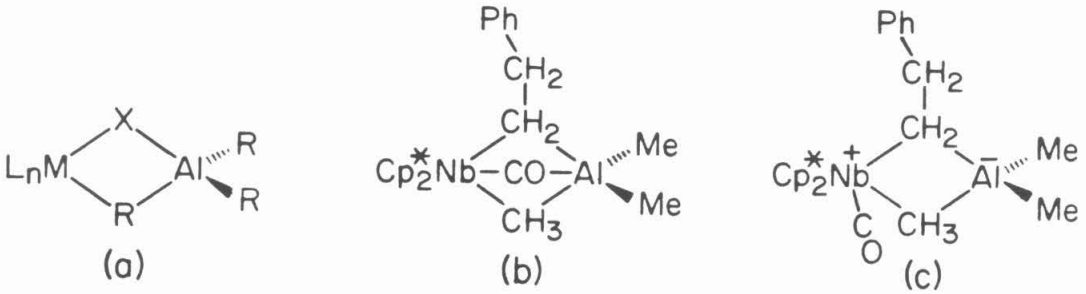

Figure 8. Proposed Reaction Intermediates. (a) Transmetallation reactions. (b) and (c) The transalkylation reaction.

Conclusion

The study of the reaction of aluminum Lewis acids with permethylniobocene complexes has led to the first example of carbonyl-oxygen-aluminum coordination preferred over metal-hydride-aluminum coordination. The steric bulk of the Cp* ligands is proposed to play the deciding role.

We have also observed that CO insertion is not promoted by the addition of aluminum alkyls to the alkyl-carbonyl derivatives of permethylniobocene and that one of the products, **10**, is instead stabilized by aluminum coordination. Similar stabilization was also noted by Tebbe.[11a]

Compounds **7**, **8**, and **9** react, but by alternate pathways that always leave the carbonyl linkage intact. Compound **8** undergoes a net β-hydrogen elimination and compounds **7** and **9** transalkylate. The transalkylation of **9a** provides a useful new synthetic route that is limited by the stability of the resulting alkyl-carbonyl permethylniobocene complex in the presence of the aluminum alkyl.

Experimental Section

General Considerations. All manipulations were performed using glovebox or high vacuum line techniques. Solvents were dried over $LiAlH_4$ or Na/benzophenone and stored under vacuum over "titanocene".[41] The NMR solvents, benzene-$\underline{d}_6$ and toluene-$\underline{d}_8$, were dried over activated molecular sieves (4 Å, Linde) and stored over "titanocene". Argon, nitrogen, and hydrogen gases were passed over MnO on vermiculite and activated molecular sieves.[42] Carbon monoxide (Matheson) and ^{13}CO (MRC-Mound) were used directly from the cylinders. Trimethylaluminum (Aldrich) was used as a 2 M solution in toluene. Triethylaluminum (Aldrich) was used as a neat liquid. Tribromoaluminum (Aldrich) was sublimed under vacuum and stored under nitrogen. Boron trifluoride (Research Organic/Inorganic Chemical) was used directly from the cylinder. Trimethylborate (Aldrich) was degassed and stored over activated molecular sieves. $Cp^*_2Nb(H)CO$ (**1**),[18] $Cp^*_2Nb(CH_3)$-CO (**2**),[18b] $Cp^*_2Nb(CH_2CH_3)CO$ (**3**),[15] $Cp^*_2Nb(CH_2CH_2Ph)CO$ (**4**),[15] Cp^*_2-Nb(C(Me)=CHMe)CO (**5**),[15] and $Cp^*_2NbH_3$ (**11**)[18] were prepared as previously reported.

Many reactions were surveyed using NMR spectroscopy. Any experiment described in the body of this chapter but not explicitly listed below was carried out in a sealed NMR tube utilizing $\sim$0.3 mL of benzene-$\underline{d}_6$ containing TMS to which a known amount of the appropriate reagent was added before the tube was sealed at -196°C.

Nuclear magnetic resonance spectra were recorded on Varian EM390 (90 MHz, ^1H), JEOL FX90Q (89.56 MHz, ^1H; 22.50 MHz, ^{13}C) and Bruker WM500 (500.13 MHz, ^1H) spectrometers utilizing standard parameters and

are reported in Table II. Routine infrared spectra were recorded on a Beckman 4240 spectrophotometer using KBr windows and are reported in cm^{-1}. Equilibrium infrared spectroscopic studies employed the Mattson Sirius 100 FTIR with the Starlab UNIX data system. Elemental analyses were determined by the Caltech Analytical Facility and Dornis and Kolbe Microanalytical Laboratory.

(1) $Cp^*_2Nb(H)(COAlMe_3)$ (6a). $Cp^*_2Nb(H)CO$ (1) (0.548 g, 1.40 mmol) was placed in a round-bottom flask. Petroleum ether (∿7 mL) was condensed onto the red solid at -78°C. An $AlMe_3$/toluene solution (0.72 mL, 1.44 mmol) was added to the cooled solution by syringe. The reaction mixture was allowed to warm to 24°C with stirring for ∿1 h. A bright purple solid was immediately evident. The solution volume was reduced (∿3 mL) and the bright purple microcrystalline solid **6a** was collected by cold (-78°C) filtration (0.560, 1.20 mmol, 85.7%). The solid was refrigerated under N_2. IR (nujol): 1877 (m), 1721 (s), 1424 (w), 1381 (m), 1183 (s), 1064 (w), 1023 (m), 794 (w), 679 (m), 619 (w), 548 (w), 519 (m), 474 (m) 389 (m).

Anal. calcd. for $C_{24}H_{40}OAlNb$: C, 62.06; H, 8.68; Al, 5.81. Found: C, 62.11; H, 8.65; Al, 5.90.

(2) $Cp^*_2Nb(H)(COAlEt_3)$ (6b). Compound 1 (0.640 g, 1.63 mmol) was placed in a round-bottom flask with petroleum ether (∿5 mL) and $AlEt_3$ (230 μL, 1.69 mmol). The red solution immediately became deep blue. The solution volume was reduced (∿2 mL) and the deep blue microcrystalline solid **6b** was collected by cold filtration (0.586 g, 1.16 mmol, 71.2%). The solid was refrigerated under N_2.

IR (nujol): 1875 (m), 1736 (s), 1408 (w), 1381 (m), 1228 (w), 1185 (m), 1067 (w), 1026 (m), 986 (m), 944 (m), 916 (w), 794 (w), 690 (w), 632 (m,br), 472 (w), 389 (w).

Anal. calcd. for $C_{27}H_{46}OAlNb$: C, 64.02; H, 9.15; Al, 5.33. Found: C, 64.10; H, 9.18; Al, 5.43. MW calcd. (found, cryoscopic): 506.56 (515).

(3) $Cp^*_2Nb(CH_3)(COAlMe_3)$ (7). $Cp^*_2Nb(CH_3)CO$ (2) (0.125 g, 3.07 x 10^{-4} mol) was placed in a round-bottom flask. Petroleum ether (~10 mL) and $AlMe_3$/toluene (2.0 M, 0.15 mL, 3.07 x 10^{-4} mol) were added as described in Procedure 1. The green solution immediately became aqua. The cornflower blue microcrystalline solid **7** was collected as described above (0.050 g, 1.04 x 10^{-4} mol, 33.9%).[20] IR (nujol): 1853 (m), 1708 (s), 1178 (m), 1149 (w), 1063 (w), 1021 (m), 795 (w), 676 (m), 611 (w).

Anal. calcd. for 73% $C_{25}H_{42}OAlNb$ and 23% $C_{22}H_{33}ONb$:[43] C, 63.37; H, 8.67. Found: C, 63.59; H, 8.68.

(4) $Cp^*_2Nb(CH_2CH_3)(COAlEt_3)$ (8). $Cp^*_2Nb(CH_2CH_3)CO$ (3) (22 mg, 5.23 x 10^{-5} mol) was placed in a sealable NMR tube with toluene-d_8 (~0.3 mL). $AlEt_3$ (7.1 µL, 5.23 x 10^{-5} mol) was added by syringe and the green solution immediately became deep blue. The NMR tube was evacuated and sealed at -196°C. The subsequent reaction to form **1** and C_2H_4 was monitored by ^1H NMR.

(5) $Cp^*_2Nb(CH_2CH_2Ph)(COAlMe_3)$ (9a). $Cp^*_2Nb(CH_2CH_2Ph)CO$ (4) (0.290 g, 5.84 x 10^{-4} mol) was placed in a round-bottom flask with petroleum ether (~3 mL). An $AlMe_3$/toluene solution (0.30 mL, 5.84 x 10^{-4} mol) was added by syringe to the green solution, which had been cooled to -78°C. The slurry was stirred at -78°C for ~½ h, becoming more blue with time. A cold

filtration yielded the robin's egg blue microcrystalline solid **9a** (0.129 g, 2.27×10^{-4} mol, 51.2%). The solid was refrigerated under N_2. The solid becomes a bright blue oil if left for >30 min at room temperature (see Procedure 10). IR (nujol): 1867 (w), 1774 (sh), 1703 (s), 1598 (m), 1580 (m), 1173 (s), 1100 (m), 1062 (m), 1019 (s), 682 (s), 616 (w), 549 (w), 517 (w), 452 (m).

Anal. calcd. for $C_{32}H_{48}OAlNb$: C, 67.59; H, 8.51. Found: C, 67.70; H, 8.47.

(6) $Cp^*_2Nb(CH_2CH_2Ph)(COAlEt_3)$ (9b). Compound **4** (24 mg, 4.83×10^{-5} mol) was placed in a sealable NMR tube with toluene-d_8 (∿0.3 mL). $AlEt_3$ (6.6 μL, 4.83×10^{-5} mol) was added by syringe and the green solution immediately became aqua. The NMR tube was evacuated and sealed at -196°C and the subsequent reactions (see Results) were followed by ^1H NMR.

(7) $Cp^*_2Nb(C(Me)=CH(Me))(COAlEt_3)$ (10). $Cp^*_2Nb(C(Me)=CH(Me))CO$ (**5**) (35 mg, 7.84×10^{-5} mol) was placed in a sealable NMR tube with toluene-d_8 (∿0.3 mL). $AlEt_3$ (10.7 μL, 7.84×10^{-5} mol) was added by syringe and the green solution immediately became blue. The NMR tube was evacuated and sealed at -196°C. The only reactivity observed by ^1H NMR was a slow change in isomer ratios from 33:67 to 50:50. The rate of isomerization increases with increased temperature.[44] IR (C_7H_8): 2888 (s), 2853 (s), 2794 (w), 2722 (w), 1858 (m), 1734 (s), 1612 (m), 1407 (m), 1378 (m), 1229 (w), 1186 (w), 1023 (m), 984 (m), 947 (m), 916 (w), 789 (m), 634 (s,br).

(8) $Cp^*_2NbH_3 \cdot AlEt_3$ (12). $Cp^*_2NbH_3$ (**11**) (0.485 g, 1.32 mmol) was placed in a round-bottom flask with petroleum ether

(∿4 mL) and $AlEt_3$ (180 μL, 1.31 mmol). The off-white solid **12** was collected by cold filtration (0.279 g, 5.80×10^{-4} mol, 43.9%). The solid was refrigerated under N_2. IR (nujol): 1736 (sh), 1706 (m), 1600 (br), 1484 (m), 1425 (sh), 1406 (w), 1221 (w), 1173 (w), 1064 (s), 1024 (m), 980 (m), 943 (m), 893 (w), 842 (w), 769 (m).

Anal. calcd. for $C_{26}H_{48}AlNb$: C, 64.98; H, 10.07. Found: C, 64.89; H, 10.18.

(9) $Cp^*_2Nb(CO)(FBF_2H)$ (13). Compound 1 (0.125 g, 3.19×10^{-4} mol) was placed in a round-bottom flask with benzene (∿1 mL). BF_3 (1.1 equiv) was condensed into the flask at -196°C. The flask was allowed to warm to 24°C and stirred ½ h. The solution became dark magenta with time. The volatiles were removed under vacuum leaving a magenta solid. IR (nujol): 2390 (m,br), 1887 (s), 1678 (w), 1241 (w), 1170 (s), 1122 (s), 1020 (s), 919 (m), 886 (s), 725 (s), 670 (w), 467 (m).

(10) $Cp^*_2Nb(CH_3)(COAlMe_2(CH_2CH_2Ph))$ (14). Compound **4** (0.226 g, 4.55×10^{-4} mol) was placed in a round-bottom flask with toluene (∿10 mL). An $AlMe_3$/toluene solution (235 μL, 4.70×10^{-4} mol) was added by syringe to the green solution, which had been cooled to -78°C. The solution was allowed to warm to 24°C with stirring. After 14 h the volatiles were removed leaving an aqua oil. Petroleum ether (∿4 mL) was condensed onto the oil. Solid was observed at low temperature, but it became an oil at 24°C. The volatiles were removed and petroleum ether (∿5 mL) condensed onto the oil again. The robin's egg blue microcrystalline solid **14** was isolated by cold filtration (0.111 g, 1.95×10^{-4} mol, 42.9%). IR (C_6D_6): 2912 (m,br), 2018 (w), 1954 (w), 1857 (m), 1719 (s), 1601

(m), 1493 (m), 1380 (m), 1181 (m), 1117 (w), 1024 (m), 730 (m), 694 (m).

Anal. calcd. for $C_{32}H_{48}OAlNb$: C, 67.59; H, 8.51. Found: C, 67.70; H, 8.47.

(11) $Cp^*_2Nb(CH_3)CO$ (2). Compound **14** (0.093 g, 1.64×10^{-4} mol) was placed in a round-bottom flask with poly(4-vinylpyridine-co-styrene) (10% styrene, 0.265 g). Toluene (~7 mL) was condensed in at -78°C and the solution warmed to 24°C with stirring. After 4.5 h the volatiles were removed and petroleum ether (~10 mL) added. The polymer beads and a yellow solid were filtered from a green solution. The solvent volume was reduced (~4 mL) and the green solid **2** was isolated by cold filtration (0.025 g, 6.14×10^{-5} mol, 37.2%-not optimized). The solid was identified by spectral comparisons with previously obtained samples.[18]

(12) Reactions with CO. Each sample was prepared analogously by placing ~30 mg of the compound in a sealable NMR tube with benzene-d_6 containing TMS. Carbon monoxide was admitted to the tube at -78°C. The tube was closed, cooled to -196°C, and sealed. Control experiments using **1-3** and **5** were carried out at the same time and under the same conditions as experiments with **6-8** and **10.**

(13) Reactions with H_2. Each sample was prepared as above, except the step at -78°C was omitted; the H_2 was admitted to the tube at -196°C.

(14) Equilibrium Constant Evaluation for 6a and 6b.[45] A 1.00 M stock solution of $Cp^*_2Nb(H)CO$ (**1**) in benzene was used to prepare solutions from 0.025 to 0.100 M for calibration of the instrument. The calibration curves (the experiment was repeated once) using $\nu(CO) = 1863\ cm^{-1}$ did not follow Beer's Law over the entire concentration range (peak absorbance values and

peak integration values both give the same result). The actual calibration curves were used to determine the concentration of uncomplexed **1** in solutions of **6a** and in solutions of **1** with varying amounts of $AlEt_3$ added. Analysis was based on equations 10a and 10b and their sum, with $K_{Al} = [AlR_3]^2_{eq}/[(AlR_3)_2]_{eq}$, $K_{CO} = [\mathbf{6}]_{eq}/[\mathbf{1}]_{eq}[AlR_3]_{eq}$ and $K_{Al} \cdot K_{CO} = [\mathbf{6}]_{eq}[AlR_3]_{eq}/[\mathbf{1}]_{eq}[(AlR_3)_2]_{eq}$. The value of $[\mathbf{6}]_{eq}$ was determined by subtraction of $[\mathbf{1}]_{eq}$ from the known total concentration of niobium compound added. The values of $[AlR_3]_{eq}$ and $[(AlR_3)_2]_{eq}$ were determined by using the relationship $[AlR_3]_T - [\mathbf{6}]_{eq} = 2 \times [(AlR_3)_2]_{eq} + [AlR_3]_{eq}$, assuming $[AlR_3]_{eq} \simeq 0$ to determine $[(AlR_3)_2]_{eq}$ and then using that value in the equation for K_{Al} ($K_{Al} = 8.99 \times 10^{-8}$ M for $AlMe_3$ in benzene; 2.22×10^{-5} M for $AlEt_3$ in benzene)[28] to determine $[AlR_3]_{eq}$. Generally, $[(AlR_3)_2]_{eq} \simeq 10^{-2}$ and $[AlR_3]_{eq} \simeq 10^{-4}$ so the approximation is reasonable.

(15) Kinetic Study of the Transalkylation Reaction of 9a. Compound **9a** (~30 mg) was placed in a screw-capped NMR tube with benzene-$\underline{d}_6$ containing TMS and toluene (1.4 equiv). The tube was kept at -78°C until it was placed in the probe of the EM390, which is maintained at 34°C. The loss of **9a** was monitored by measuring the integration of the Cp* resonance relative to the integration of the methyl resonance of the toluene, yielding a first-order rate constant of $3.9(4) \times 10^{-4}$ sec^{-1} ($r^2 = 0.99$). The production of **14**, which is also first-order, was monitored by measuring the integration of the Cp* resonance and the Nb-CH_3 resonance relative to the integration of the methyl resonance of toluene, yielding rate constants of $3.5(4) \times 10^{-4}$ sec^{-1} ($r^2 = 0.98$) and $4.3(4) \times 10^{-4}$ sec^{-1} ($r^2 = 0.93$), respectively. The error is

estimated based on past experience with NMR kinetic experiments. An analysis of residuals gave a much smaller value.

References and Notes

(1) (a) Eisch, J. J. "Aluminum" in "Comprehensive Organometallic Chemistry", Wilkinson, G.; Stone, F. G. A.; Abel, E. W. (eds.); Pergamon Press: Oxford, 1982. (b) Mole, T.; Jeffery, E. A. "Organoaluminum Compounds"; Elsevier Publishing: New York, 1972.

(2) Parshall, G. W. "Homogeneous Catalysis"; J. Wiley & Sons: New York, 1980.

(3) (a) Kotz, J. C.; Pedrotty, G. D. Organomet. Chem. Rev. A **1969**, 4, 479-547. (b) Shriver, D. F. Accts. Chem. Res. **1970**, 3, 231-238 and references cited therein.

(4) Hsieh, A. T. T. Inorg. Chimica Acta **1975**, 14, 87-104 and references cited therein.

(5) Some more recent examples include: (a) Green, M. L. H.; Mackenzie, R. E.; Poland, J. S. J. Chem. Soc., Dalton Trans. **1976**, 1993-1994. (b) Burlitch, J. M.; Leonowics, M. E.; Peterson, R. B.; Hughes, R. E. Inorg. Chem. **1979**, 18, 1097-1105. (c) Mayer, J. M.; Calabrese, J. C. Organometallics **1984**, 3, 1292-1298.

(6) Two compounds that were originally thought to contain a transition metal-Lewis acid metal bond but were later shown by X-ray structure determination not to contain such an interaction are: (a) $Cp_2WH_2 \cdot AlMe_3$: Bruno, J. W.; Huffman, J. C.; Caulton, K. G. J. Am. Chem. Soc. **1984**, 106, 444-445; and (b) $(CpW(CO)_3AlMe_2)_2$: Gainsford, G. J.; Schrieke, R. R.; Smith, J. D. J. Chem. Soc., Chem. Commun. **1972**, 650-651.

(7) Burlitch, J. M.; Peterson, R. B. J. Organomet. Chem. **1970**, 24, C65-C67.

(8) The first C- and O-bonded carbon monoxide, at a bridging carbonyl group, was reported by Shriver and coworkers in the previous year.[8a] Kotz and Turnipseed provided the first example of Lewis basicity at a terminal carbonyl's oxygen.[8b] (a) Nelson, N. J.; Kime, N. E.; Shriver, D. F. J. Am. Chem. Soc. **1969**, 91, 5773-5174. (b) Kotz, J. C.; Turnipseed, C. D. J. Chem. Soc., Chem. Commun. **1970**, 41-42.

(9) (a) Shriver, D. F.; Alich, A. Coord. Chem. Rev. **1972**, 8, 15-20. (b) Richmond, T. G.; Basolo, F.; Shriver, D. F. Inorg. Chem. **1982**, 21, 1272-1273. (c) Butts, S. B.; Straus, S. H.; Holt, E. M.; Stimson, R. E.; Alcock, N. W.; Shriver, D. F. J. Am. Chem. Soc. **1980**, 102, 5093-5100. (d) Lindner, E.; von Au, E. Angew. Chem. Int. Ed., Engl. **1980**, 19, 824-825.

(10) (a) Pan'kowski, M.; Demerseman, B.; Bouquet, G.; Bigorgne, M. J. Organomet. Chem. **1972**, 35, 155-159. (b) Powell, P.; Noth, H. J. Chem. Soc., Chem. Commun. **1966**, 637-638.

(11) (a) Tebbe, F. N. J. Am. Chem. Soc. **1973**, 95, 5412-5414. (b) Otto, E. E. H.; Brintzinger, H. H. J. Organomet. Chem. **1979**, 170, 209-216.

(12) Examples of M-H-Al bridges in compounds not containing carbonyls also exist: (a) Ref. 6a. (b) Ref. 11b. (c) Wailes, P. C.; Weigold, H.; Bell, A. P. J. Organomet. Chem. **1972**, 43, C29-C31. (d) Lobkovskii, E. B.; Soloreichik, G. L.; Sisov, A. I.; Bulychev, B. M.; Gusev, A. I.; Kirillova, N. I. J. Organomet. Chem. **1984**, 265, 167-173.

(13) Richmond, T. G.; Basolo, F.; Shriver, D. F. Organometallics **1982**, 1,

1624-1628.

(14) (a) Serrano, R.; Royo, P. J. Organomet. Chem. **1983**, 247, 33-37. (b) Klazinga, A. H. Ph.D. Thesis, University of Groningen, 1979. (c) Schwartz, J.; Labinger, J. A. J. Am. Chem. Soc. **1975**, 97, 1596-1597. (d) Guggenberger, L. J.; Meakin, P.; Tebbe, F. N. Ibid. **1974**, 96, 5420-5427. (e) Tebbe, F. N.; Parshall, G. W. Ibid. **1971**, 93, 3793-3795. (f) Siegert, F. W.; De Liefde Meijer, H. J. J. Organomet. Chem. **1970**, 23, 177-183.

(15) Doherty, N. M. Ph.D. Thesis, California Institute of Technology, 1984.

(16) (a) Klazinga, A. H.; Teuben, J. H. J. Organomet. Chem. **1980**, 194, 309-316. (b) Labinger, J. A. "Niobium and Tantalum" in "Comprehensive Organometallic Chemistry", Wilkinson, G.; Stone, F. G. A.; Abel, E. W. (eds.); Pergamon Press: Oxford, 1982; Vol. 3.

(17) (a) Wolczanski, P. T.; Bercaw, J. E. Accts. Chem. Res. **1980**, 13, 121-127. (b) Moore, E. J. Ph.D. Thesis, California Institute of Technology, 1984.

(18) (a) Threlkel, R. S. Ph.D. Thesis, California Institute of Technology, 1980. (b) Cohen, S. A. Ph.D. Thesis, California Institute of Technology, 1982.

(19) The most dramatic color change results from the reaction of dark red (by reflected light) **1** with AlR_3 to produce a bright violet (R = Me, **6a**) or a royal blue (R = Et, **6b**) microcrystalline product. The green alkyl-carbonyl compounds **2-5** react with AlR_3 to produce bright blue products.

(20) The reactions are quantitative by NMR, but their high solubility in

petroleum ether, even when isolated at -78°C, reduces the isolated yields. The high solubility was particularly troublesome in the $AlMe_3$ reactions, which were carried out in petroleum ether/toluene mixtures. The high volatility of $AlMe_3$ and the solution equilibrium between adduct and starting materials (vide infra) prevented any solvent change.

(21) Karlin, K. D.; Johnson, B. F. G.; Lewis, J. J. Organomet. Chem. **1978**, 160, C21-C23.

(22) Similar lowfield values have been observed in tungsten[22a] and iron/zirconium.[22b] systems whose structures show clear M=C bonds: (a) Cotton, F. A.; Schwotzer, W. J. Am. Chem. Soc. **1983**, 105, 4955-4957. (b) Berry, D. H. Ph.D. Thesis, California Institute of Technology, 1984.

(23) Only the Cp* signal (δ 1.60 ppm) is evident in the ^1H NMR spectrum. The B-H signal is apparently too broad to be observed at the saturation concentration of **13** in C_6D_6.

(24) (a) Marks, T. J.; Kolb, R. A. Chem. Rev. **1977**, 77, 263-293. (b) Baker, M. V.; Field, L. D. J. Chem. Soc., Chem. Commun. **1984**, 996-997. (c) For comparison, $Cp^*_2NbBH_4$ has two terminal [$\nu(B\text{-}H_t)$ = 2428 cm^{-1}, 2452 cm^{-1}] and two bridging [$\nu(B\text{-}H_b)$ = 1620 cm^{-1}, 1728 cm^{-1}] B-H bands.[18]

(25) Otto and Brintzinger report only the carbonyl stretch for $Cp_2Nb(HBF_3)CO$,[11b] so it is not possible to assess whether they actually have a hydride bridge or a fluoride bridge as proposed in this work.

(26) Beck, W.; Schloter, K. Z. Naturforsch. B **1978**, 33B, 1214-1222.

(27) The existence of solution equilibria has also been noted by Kotz and Turnipseed,[8c] Burlitch and coworkers,[5b] and Mayer and Calabrese.[5c]

(28) Smith, M. B. J. Organomet. Chem. **1974**, 70, 13-33.

(29) Burlitch and coworkers have measured the adduct formation constant for $(n\text{-}Bu)_4N^+W(CO)_2(COAlPh_3)Cp^-$ in CH_2Cl_2 by a similar technique and report a value of 1×10^3 M^{-1}.[5b]

(30) Dichloromethane will react with these niobium compounds, but the reaction is quite slow. Dark green solids that yield deep red or purple solutions have been observed before in this laboratory. Manriquez, J. M.; Bercaw, J. E. J. Am. Chem. Soc. **1974**, 96, 6229-6230.

(31) Reaction of another compound, $Cp^*_2Nb(C_2H_4)H$, with $AlMe_2Cl$ also produces intractable products. Chapter IV of this thesis.

(32) Compound **3** is stable for weeks in solution. Decomposition at 80°C results in more $Cp^*_2Nb(C_2H_4)H$ than **1**. Doherty, N. M. Unpublished results.

(33) (a) Free styrene is never observed by ^1H NMR spectroscopy. Unlike reactions of styrene with alkylaluminums, which produce a 76:24 ratio of 1-phenethyl:2-phenethyl tris(phenethylaluminum), only one isomer is observed. The AA'XX' pattern observed in the ^1H NMR spectrum supports the 1-phenethyl linkage. Natta, G.; Pino P.; Mazzanti, G.; Longi, P.; Bernardini, F. J. Am. Chem. Soc. **1959**, 81, 2561-2563. (b) The rate of formation of **14**, measured by the rate of increase in the Cp* or Nb-CH_3 resonances, is also first-order. The rate constants determined from these data agree well with the rate constant determined by the rate of decrease in the Cp* resonance of **9a**

($k = 3.5(4) \times 10^{-4}\ sec^{-1}$ and $4.3(4) \times 10^{-4}\ sec^{-1}$, respectively). Capellos, C.; Bielski, B. H. J. "Kinetic Systems: Mathematical Description of Chemical Kinetics in Solution"; Wiley-Interscience: New York, 1972.

(34) Compound 1 is known to be unreactive toward H_2 under these conditions.[18b]

(35) Pearson, R. G. J. Am. Chem. Soc. **1963**, 85, 3533-3539.

(36) Thompson, M. E.; Bercaw, J. E. Pure & Appl. Chem. **1984**, 56, 1-11.

(37) (a) Holton, J.; Lappert, M. F.; Ballard, D. G. H.; Pearce, R.; Atwood, J. L.; Hunter, W. E. J. Chem. Soc., Dalton Trans. **1979**, 45-53. (b) Ibid., 54-61.

(38) Both produce an orange oil with loss of all ^1H NMR signals due to $AlMe_3$ or $AlEt_3$. In a control experiment, $AlMe_3$ and CO did not react even after weeks at 80°C.

(39) These reactions are known as transmetallations. Seyferth, D.; Weiner, M. A. J. Am. Chem. Soc. **1961**, 83, 3583-3586.

(40) The unimolecular nature of the reaction has not been checked by crossover experiments.

(41) Marvich, R. H.; Brintzinger, H. H. J. Am. Chem. Soc. **1971**, 93, 2046-2048.

(42) Brown, T. L.; Dickerhoff, D. W.; Botus, D. A.; Morgan, G. L. Rev. Sci. Instrum. **1962**, 22, 491-492.

(43) The microanalysis was performed on a small sample prepared from **2** (Procedure 11) and $AlMe_3$ that was 73% **7** and 27% **2** (^1H NMR). The incomplete reaction resulted from the difficulty of handling very small

amounts of the highly volatile $AlMe_3$.

(44) Compound **5** was isolated as a 41:59 ratio of isomers. The starting ratio of 33:67, observed after three months of refrigeration, was the same before and after addition of $AlEt_3$.

(45) (a) Rossotti, F. J. C.; Rossotti, H. "The Determination of Stability Constants"; McGraw-Hill: New York, 1961; Chapter 13. (b) Colthup, N. B.; Daly, L. H.; Wiberley, S. E. "Introduction to Infrared and Raman Spectroscopy", 2nd ed.; Academic Press: New York, 1975.

CHAPTER IV

The Reaction of Aluminum Alkyls with Bis(pentamethylcyclopentadienyl) Ethylene Hydride Niobium (III). Evidence for a Niobium-Ethylene-Aluminum Bridge.

Introduction

Organoaluminum compounds are used to promote the oligomerization of ethylene to long-chain α-olefins. They are also known to promote the dimerization of ethylene when combined with traces of nickel and to promote the stereoregular polymerization of ethylene and higher olefins when combined with early transition metal complexes (Ziegler-Natta catalysis).[1-4] However, despite the commercial importance of these processes little is known about the detailed nature of the catalytic sites when more than one metal compound is involved. It has generally been proposed that the organoaluminum compound both alkylates and reduces the transition metal center and then coordinates to that metal center primarily through halogen bridges.[1,5] The growing number of alkyl-bridged transition metal-aluminum compounds,[6] including the recent X-ray characterizations of $Cp_2M(\mu\text{-}Me)_2AlMe_2$ ($Cp \equiv \eta^5\text{-}C_5H_5$; M = Yb,[6] Y[7]) and $(C_2H_4)_3Ni(\mu\text{-}Et)AlEt_2$,[8] suggests that other alternatives are available.

In the course of studies on the reactions of trialkylaluminum reagents with carbonyl and hydride derivatives of permethylniobocene,[9] we have also examined the reactivity of AlR_3 (R = Me, Et) with $Cp^*_2Nb(H)(C_2H_4)$ (**1**) ($Cp^* \equiv \eta^5\text{-}C_5Me_5$).[10] Reversible insertion of the coordinated ethylene into the Nb-H bond of **1** is observed,[10b,11] so the effect of added trialkylaluminum on the insertion reaction is of interest. Tebbe has obtained the Nb-H-Al adduct $Cp_2Nb(HAlEt_3)(C_2H_4)$ from the reaction of $Cp_2Nb(H)(C_2H_4)$ with $AlEt_3$ and has observed that, under conditions where reaction 1 proceeds to 35% completion, no reaction occurs with $Cp_2Nb(HAlEt_3)(C_2H_4)$.[12] Thus, in contrast to the aluminum/Group IV Ziegler-Natta catalysts, triethyl-

$$Cp_2Nb(H)(C_2H_4) + C_2H_4 \longrightarrow Cp_2Nb(C_2H_5)(C_2H_4) \qquad (1)$$

aluminum deactivates $Cp_2Nb(H)(C_2H_4)$ toward insertion.

The data for the trialkylaluminum adducts of **1** (eq. 2) are quite different than those observed by Tebbe for $Cp_2Nb(HAlEt_3)(C_2H_4)$. Thus,

$$\underset{\mathbf{1}}{Cp^*_2Nb(H)(C_2H_4)} + \tfrac{1}{2}(AlR_3)_2 \longrightarrow Cp^*_2Nb(H)(C_2H_4 \cdot AlR_3) \qquad (2)$$

R = Me, **2a**
= Et, **2b**

we propose that products **2a** and **2b** each contain a niobium-(μ-ethylene)-aluminum bridge and present herein data to support this proposal. A survey of the observed reactivity of **2a** and **2b** is also presented.

Results and Discussion

Synthesis and Characterization. $Cp^*_2Nb(H)(C_2H_4)$ (**1**) reacts rapidly with equimolar amounts of $AlMe_3$ and $AlEt_3$ in benzene, toluene, or petroleum ether solutions, yielding the products **2a** and **2b** (eq. 2). These products are isolated from petroleum ether solutions at -78°C as pale yellow solids[13] and have been characterized by NMR and IR spectroscopies and microanalyses (see Experimental) as 1:1 adducts of the niobium and aluminum reagents.

The ^1H NMR spectra of **2a** and **2b** both show small downfield shifts of the Nb-H resonance relative to the position of that resonance in the spectrum of **1** (δ -2.73 and -2.40, respectively, vs. δ -3.04). This shift contrasts markedly with the large upfield shift observed for the Nb-H-Al product $Cp_2Nb(HAlEt_3)(C_2H_4)$ relative to its precursor $Cp_2Nb(H)(C_2H_4)$ (δ -9.63[12] vs. δ -2.95[14]). Similarly large upfield shifts were observed for $Cp_2Nb(HAlEt_3)(CO)$ and $Cp_2Nb(HAlEt_3)(PMe_3)$.[12] The small downfield shifts for the niobium-hydride resonances of **2a** and **2b** are analogous to those observed for $Cp^*_2Nb(H)(COAlR_3)$ R = Me, **3a**; Et, **3b**)[9] and thus it is proposed that the aluminum reagents coordinate to the ethylene ligand of **1**.

This proposal is supported by the dramatic change in the ethylene ^1H NMR resonances at 90- and 500 MHz (Figs. 1 and 2). Figure 1 shows the AA'MM'X pattern of compound **1** at 25°C.[10b,11] The AA'BB' pattern of compound **2b** is also shown, although it is partly obscured by the quartet due to the methylene protons of $AlEt_3$. The pattern for **2b** varies dramatically with temperature[15] unlike the pattern for **1**, which undergoes only small chemical shift changes as the temperature is lowered. An AA'BB' pattern is

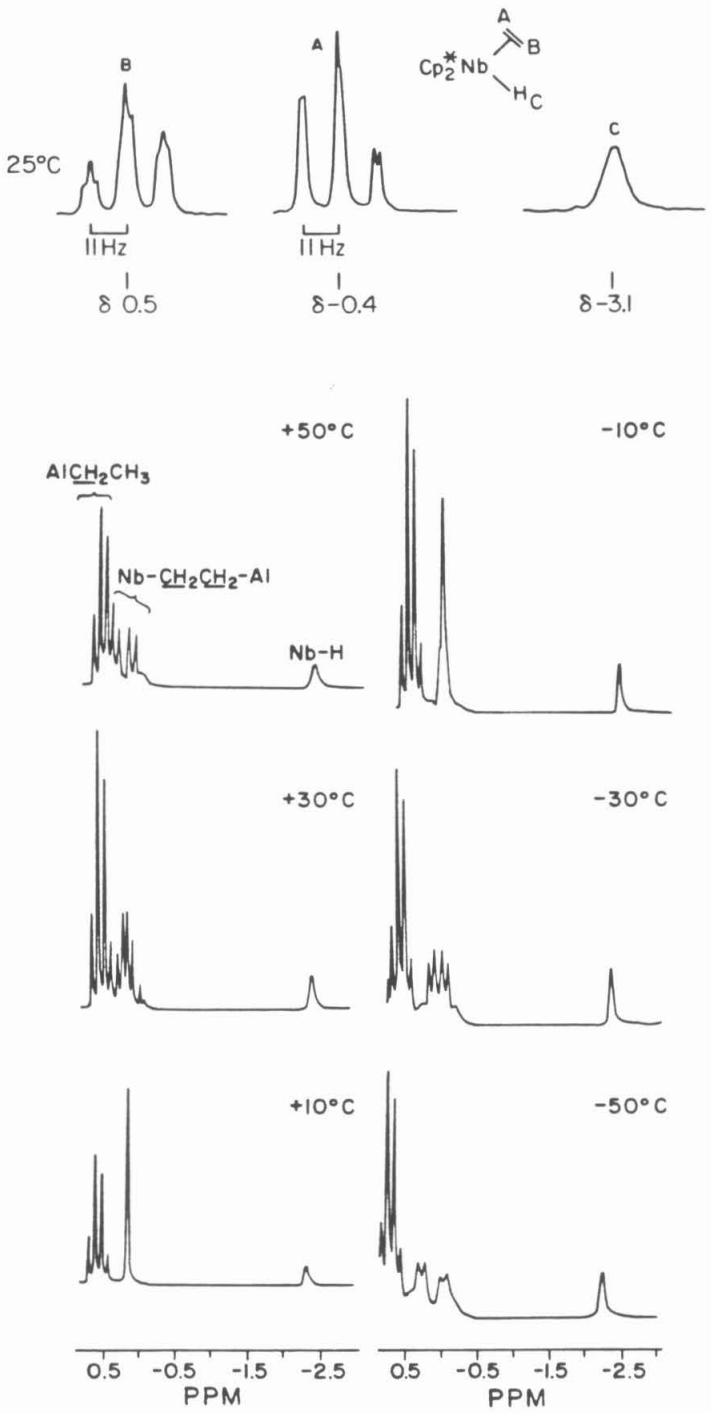

Figure 1. Variable Temperature ^1H NMR (89.6 MHz) spectra for compound **2b**. The spectrum of **1** at 25°C[10b] is shown for comparison. The NMR sample of **2b** also contained CO. (Solvent:toluene-d_8.)

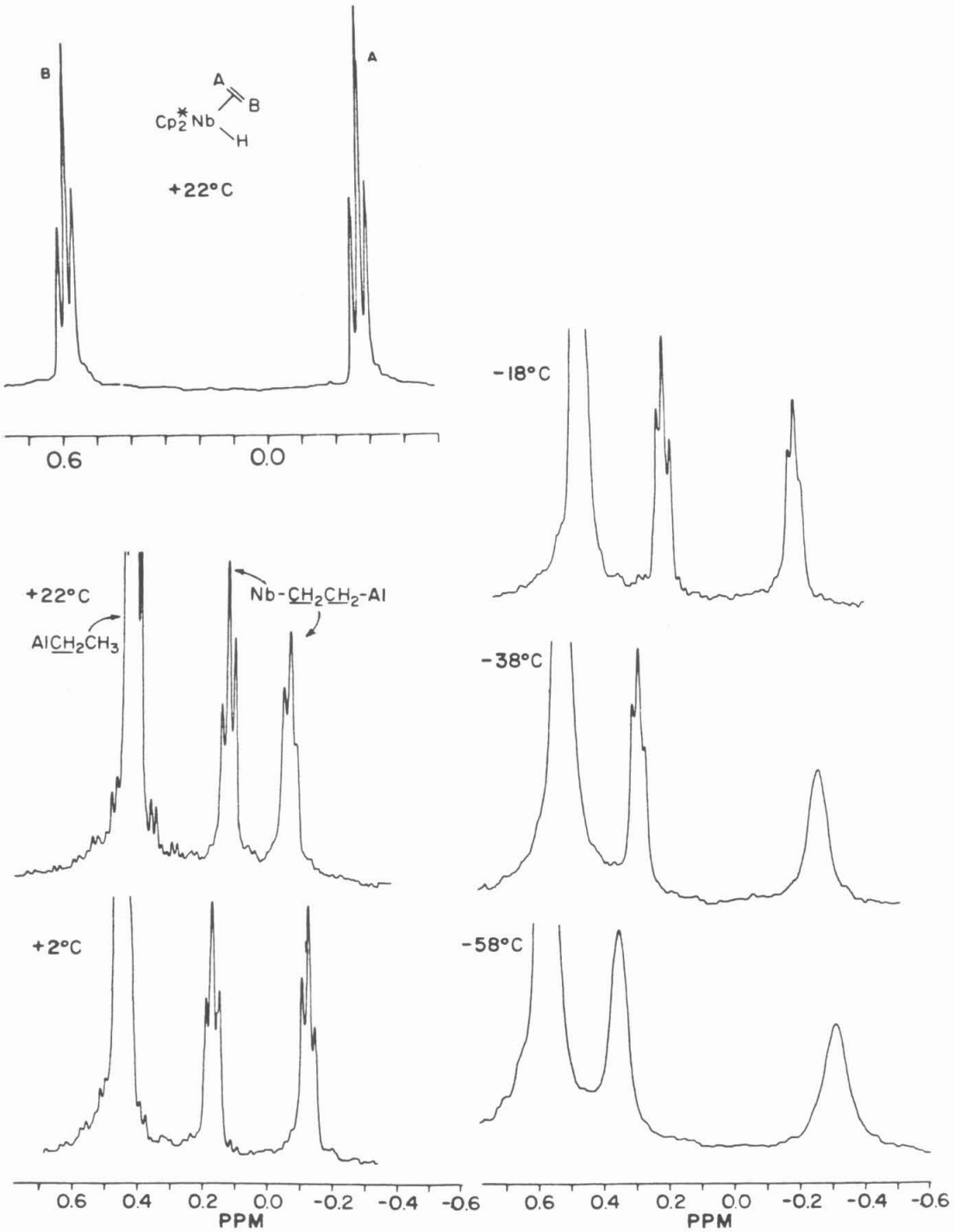

Figure 2. Variable Temperature ^1H NMR (500.13 MHz) Spectra for a Solution of 1 and 1.06 Equivalents $AlEt_3$. The spectrum of 1 at 22°C is shown for comparison. (Solvent: toluene-d_8.)

characteristic for disubstituted ethanes XCH_2CH_2Y in which X and Y have similar electronegativities.[16,17] The AA'BB' pattern observed for **2b** is that obtained when $J_{AB} = J_{AB'}$ and can be analyzed theoretically to obtain values of the coupling constants.[16] However, the spectrum simplifies to a first-order A_2B_2 pattern at 500 MHz (Fig. 2) from which J_{AB} may be obtained directly (10 Hz).[16a]

From Figures 1 and 2, it is clear that the chemical shifts ν_A and ν_B of the $-CH_2CH_2-$ group change with temperature. Similar changes are also observed when varying amounts of the trialkylaluminum reagent are added to solutions of **1**. Thus, equation 2 is better written as an equilibrium between the reagents and the 1:1 adducts **2a** and **2b** (eq. 3).[18] Similar equilibria in other aluminum-transition metal systems have been previously noted.[9,19]

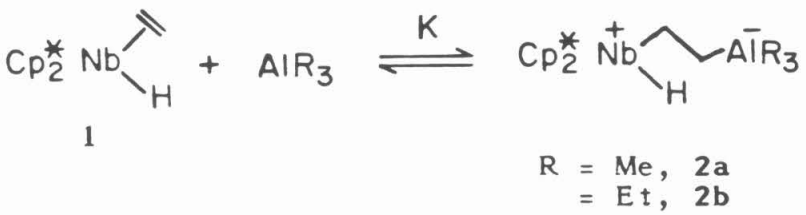

1 (3)

R = Me, **2a**
= Et, **2b**

Figure 3 presents a schematic summary of the chemical shift changes observed in the 500 MHz ^1H NMR resonances of $-CH_2CH_2-$ and Nb-H with changes in temperature (25 to -78°C) and added $AlEt_3$ (0 to 2.59 equiv). The chemical shift changes are approximately linear with added $AlEt_3$ up to 1 equivalent of $AlEt_3$ per mole of **1**. Above 1 equivalent the chemical shift changes level off, although the changes continue for those samples containing aluminum as the temperature is lowered.

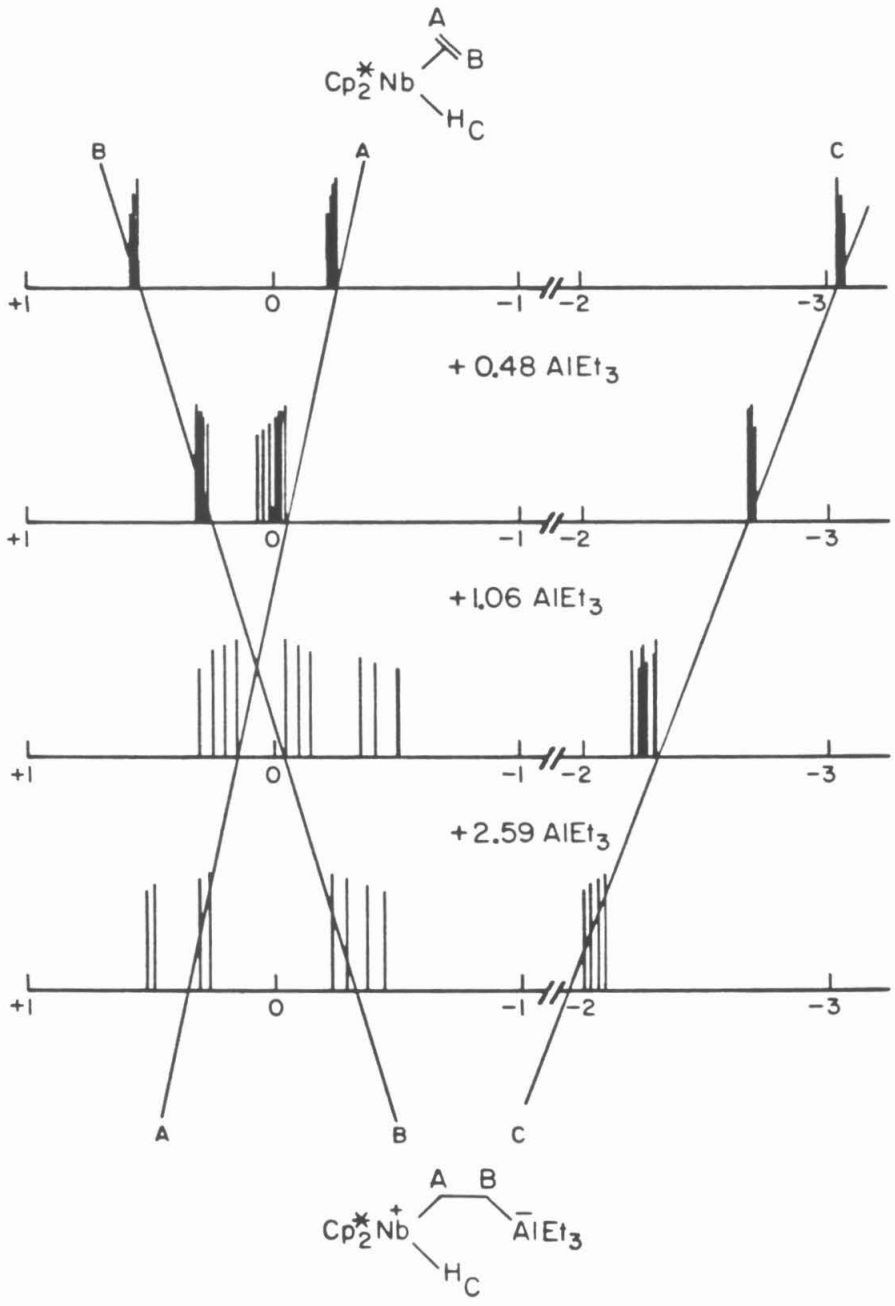

Figure 3. Schematic Representation of the Changes in the 500 MHz ^1H NMR Spectrum for Solutions of **1** and $AlEt_3$ with Added $AlEt_3$ and with Lowered Temperature. Each vertical line represents the position of the resonance at a given temperature (295, 275, 255, 235, and 215 K - the longer lines represent the higher temperatures). The lines labeled A, B and C trace the change in a given resonance's room temperature position with added $AlEt_3$.

The same behavior is observed in a room temperature IR spectroscopic study in which increasing amounts of $AlEt_3$ are added to benzene solutions of **1** (Table I). The IR band for ν(Nb-H) shifts from 1704 to 1760 cm^{-1} upon coordination of the aluminum reagent (Fig. 4). The formation constant K of the adduct **2b** has been determined from the changes in these IR bands with the addition of $AlEt_3$ (eq. 4).[20] The average value of the adduct formation

$$(AlEt_3)_2 \overset{K_{Al}}{\rightleftharpoons} 2\,AlEt_3 \qquad (4a)$$

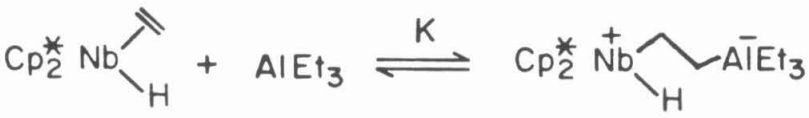

(4b)

$+ AlEt_3$ (4c)

constant K ($2.4(6) \times 10^2$ M^{-1}) is smaller than the formation constants for the carbonyl-aluminum adducts **3a** ($1.1(2) \times 10^5$ M^{-1}) and **3b** ($4.5(30) \times 10^3$ M^{-1})[9] and probably reflects the less basic site of coordination, the ethylene ligand, available to the aluminum reagent. Coordination at the hydride, found in the parent system,[12] is prevented by the steric bulk of the Cp* ligands.[9]

An evaluation of the formation constant K for **2a** has not yet been made. Based on the smaller downfield shift of the niobium-hydride ^1H NMR

Table I. Equilibrium Constant Determination for

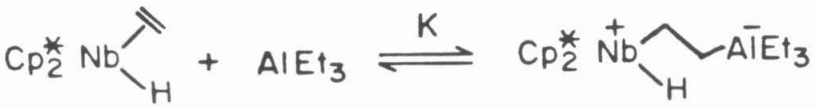

$[Cp^*_2Nb]_T$[a]	$[AlEt_3]_T$[a]	[1][b]	[2b][c]	$K_{Al}\cdot K$[d]	K[d]
0.490	0.244	0.396	0.094	4.1×10^{-3}	1.8×10^{2}
0.472	0.477	0.296	0.176	7.2×10^{-3}	3.2×10^{2}
0.443	0.895	0.268	0.175	5.1×10^{-3}	2.3×10^{2}
0.245	0.243	0.184	0.061	5.2×10^{-3}	2.3×10^{2}

[a]Total concentration of added reagent in moles·liter^{-1}. [b]Concentration of **1** in moles·liter^{-1} determined from the Nb-H peak absorbance measured against a calibration curve. [c]Concentration of **2b** in moles·liter^{-1} determined by subtraction. [d]Equilibrium constants defined by equations 4a, 4b and 4c in the text.

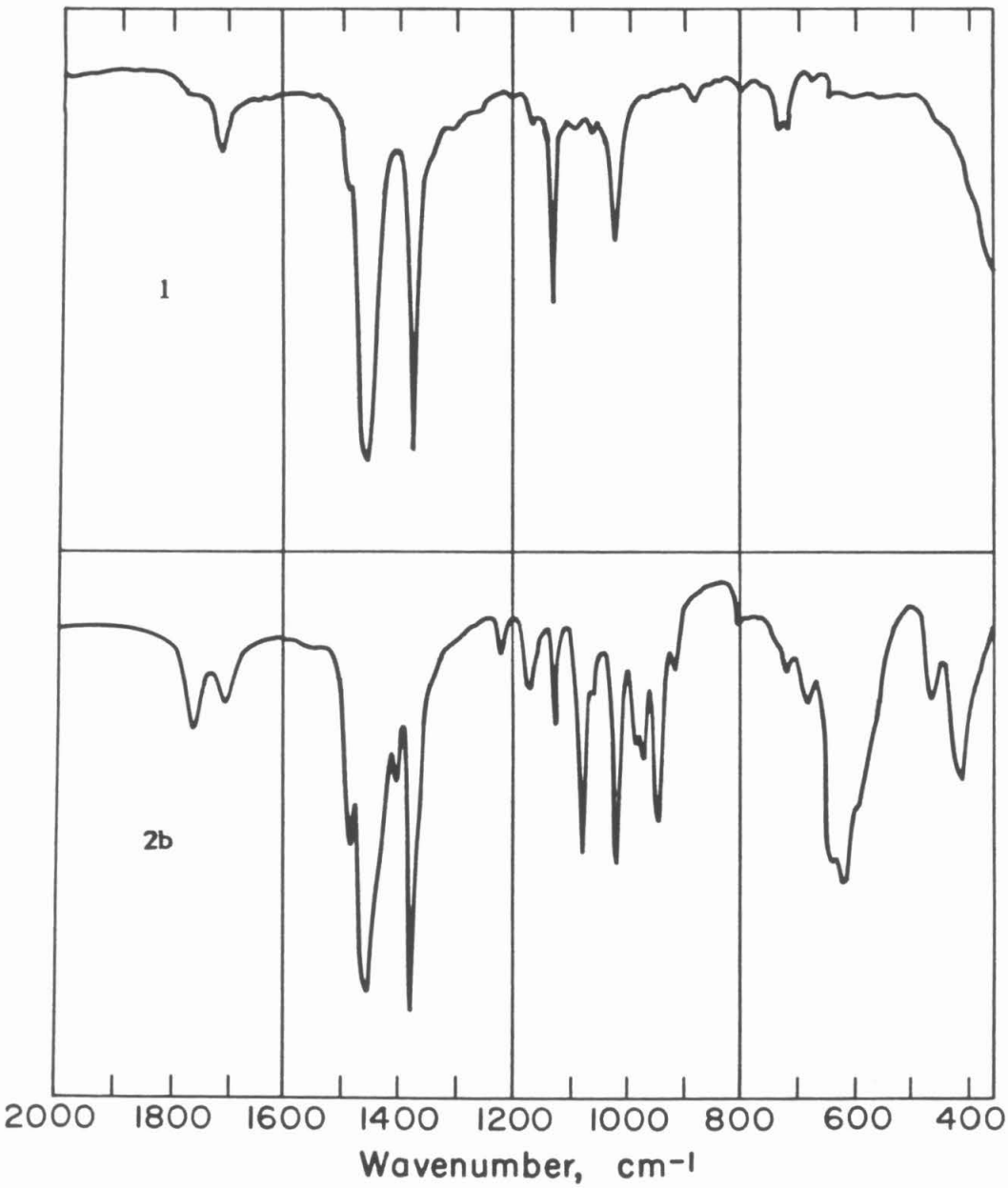

Figure 4. The IR Spectra (Nujol) of Compounds **1** and **2b**. Compound **2b** is sufficiently soluble in nujol to exhibit the equilibrium between itself and **1**.

resonance (vide supra), the overall equilibrium appears to lie even further to the left for **2a** than for **2b**. This was also true for **3a** and **3b**[9] and reflects the relative difficulty of dissociating the trimethylaluminum dimer into its monomer units.[3,20] The formation constant K for **2a** is expected to be larger than that of **2b** by analogy to **3a** and **3b**, where the smaller size of the $AlMe_3$ monomer is important.[9]

The formation of the niobium-ethylene-aluminum bridges in **2a**, and **2b**, the formulation of these complexes as zwitterions, and the suggestion (eq. 3) that the niobium and aluminum centers preferentially exist in the trans conformation have not yet been substantiated by X-ray crystallography. These propositions will be discussed by consideration of the body of NMR and IR data, by comparison to the literature reports of a few similar compounds,[21] and by analogy to the carbalumination reaction.[22]

The AA'BB' (or A_2B_2) nature of the ^1H NMR spectra for the $-CH_2CH_2-$ moieties in **2a** and **2b** is, as mentioned above, characteristic of 1,2-disubstituted ethanes.[16] Such ethanes can exist in three isomeric forms, one trans and two gauche:

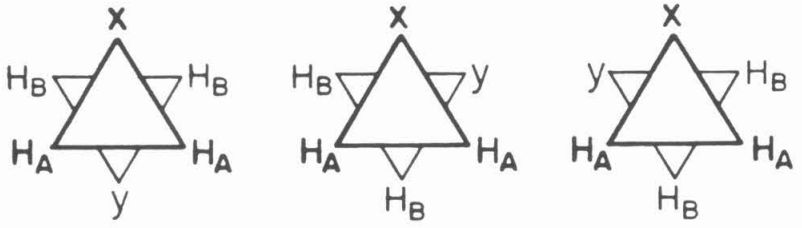

trans gauche gauche

The AA'BB' pattern is applicable to two situations. In an ethane in which rotation is slow on the NMR time scale, it applies only to the trans isomer; the gauche forms will exhibit ABCD patterns. Alternatively, if rotation is fast on the NMR time scale then the chemical shifts and coupling constants of the three forms will average to the AA'BB' pattern. If for a given AA'BB' pattern the chemical shifts and coupling constants are temperature dependent then rapid rotation is indicated. If not, three possibilities remain: 1) rotation is hindered and the trans isomer is preferred; 2) rotation is rapid but the energy difference of the isomers is great, with trans preferred; or 3) there exists such a small energy difference between isomers that changing the temperature does not change the population of each isomer.

Another dynamic process that could be observed in these systems and that would cause changes in the ^1H NMR spectral pattern of the $-CH_2CH_2-$ moiety is rapid inversion of the ethylene-bridge carbon α to the aluminum.[23,24] The changes observed in AA'BB' or analogous AA'XX' spectral patterns with changes in temperature are characteristic and are distinctly different for the rotation and inversion processes.[23a,b] The changes observed in the spectra of **2a** and **2b** (Figs. 1 and 2) are unlike those for rotation or for inversion.

Rather, the ^1H NMR spectra of **2a** and **2b** are dominated by the equilibrium nature of the adducts in solution. The coupling constants are temperature independent until the triplets (500 MHz) begin to broaden (Fig. 2). Chemical shift changes with added aluminum and with decreased temperature can be explained by an increased amount of the 1:1 adduct in solution. The positive charge at niobium in **2a** and **2b** is deshielding and the

negative charge at aluminum is shielding. Thus, the exo ethylene hydrogens of **1** are expected to move downfield while the endo ethylene hydrogens of **1** should move upfield with an increasing proportion of **2a** or **2b** in solution. This is observed (Fig. 3). A limiting ^{1}H NMR spectrum is observed (500 MHz) at -18°C for a sample containing 2.59 equivalents of $AlEt_3$ per mole of **1**. Trialkylaluminum exchange is still fast -- separate peaks for free and complexed $AlEt_3$ are not observed -- but the chemical shifts of Nb-H (δ -2.0) and Nb-CH_2CH_2-Al (δ 0.5 and -0.4, respectively) do not change below -18°C, although the triplet structure of the -CH_2CH_2- resonance is lost.

If the coordination of the aluminum reagent to the ethylene ligand of **1** occurs as pictured in Scheme I, it initially forms the trans isomer **A**. The steric bulk of the Nb and Al substituents could be large enough to prevent rapid rotation to **B**,[23a] but **A** is formally a 16-electron species and no stable 16-electron permethylniobocene compounds are known. Thus, rotational isomer **B**, or its analogue **B'** formed from inversion at the carbon α to the aluminum, is expected to exist for it is an 18-electron species.[25] Isomer **B** or **B'** cannot be the dominant species in solution, though, or an ABCD ^{1}H NMR pattern would be observed for the gauche form. An alternative that is closer to the trans orientation of the Nb and Al centers and contains a formally 18-electron niobium center is one that contains a bridging hydrogen from the ethylene moiety (C in Scheme I).[26] This form cannot be static in solution, however, or an AA'BB' (or A_2B_2) pattern would not be observed.

The syntheses and X-ray characterizations of four compounds

Scheme I. Coordination of AlR_3 to the Nb-Ethylene Ligand. Cp* ligands above and below the reaction plane have been omitted for clarity.

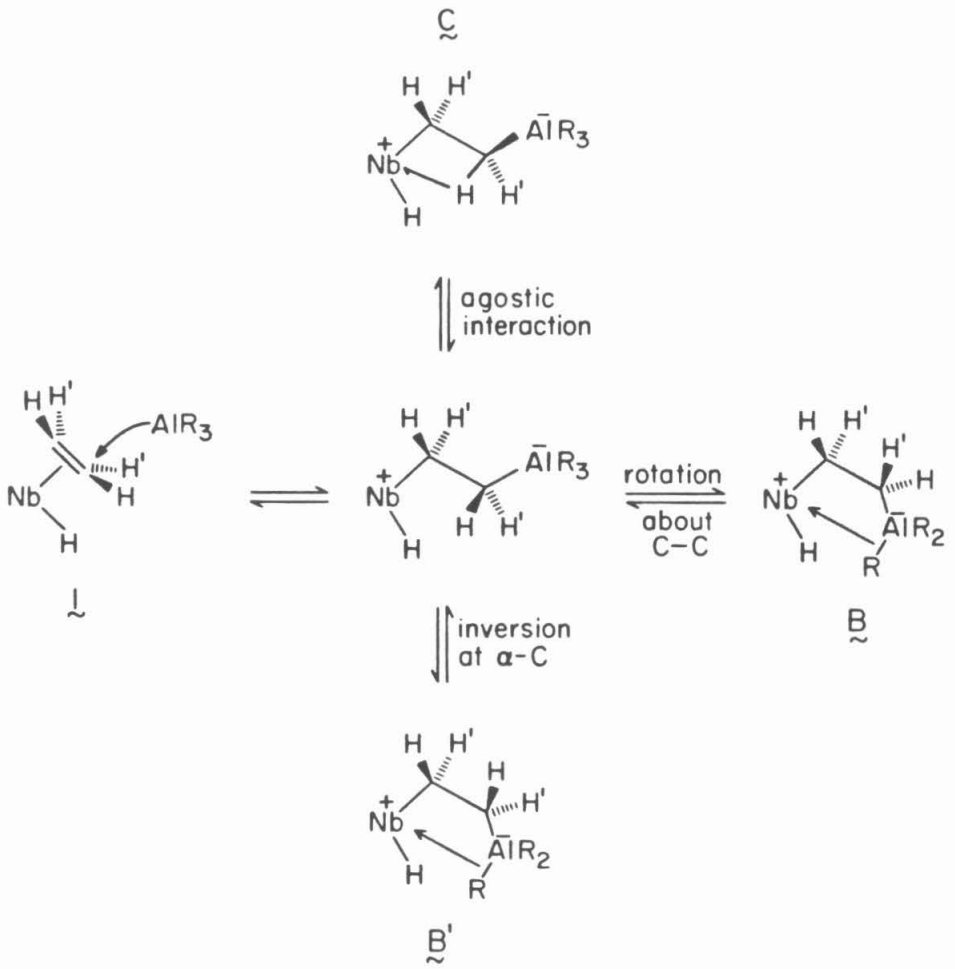

containing ethylene bridges similar to the ones proposed for **2a** and **2b** favor a structure like that of **C** for **2a** or **2b**.[21] Kaminsky and coworkers have reported the X-ray structure of $[(Et_3AlClCp_2Zr)_2(-CH_2CH_2-)]$ (**4**) as well as the structures of two related compounds **5** and **6** (Fig. 5).[21b,e,f] Beck and coworkers have reported the X-ray structure of $[(OC)_5Re)_2(-CH_2CH_2-)]$ (**7**) (Fig. 5).[21g,h] All four show a C-C bond length consistent with their formulation as substituted ethanes (>1.5 Å). Compounds **4** and **7** both show <u>trans</u> disposition of the metals about the C-C bridge. The acute M-C-C angles observed in **4** (and **5** and **6**) (75°) are not observed in **7** (117°) and may indicate that the unsaturated zirconium centers are participating in agostic bonds, as proposed for **C** (Scheme I).[26]

A final piece of evidence that suggests a structure similar to **C** for **2a** and **2b** is the description of the variable temperature ^1H NMR spectra of $(OC)_5ReCH_2CH_2Mn(CO)_5$ (**8**).[21h] Like **2a** and **2b**, compound **8** exists in equilibrium in solution; it easily forms **7** and $Mn(CO)_5^-$ when excess $Re(CO)_5^-$ is added to solution. The ^1H NMR spectral changes for the $-CH_2CH_2-$ moiety in **8** are analogous to those described for **2a** and **2b**, and a similar explanation, a chanage in the chemical shifts ν_A and ν_B with temperature, is given.

Only compound **6** has a formal positive charge on the metal atom. The formal charge separation postulated for **2a** and **2b** also occurs in dialkyl bridge compounds such as $Cp_2M(\mu\text{-}R)_2AlR_2$[6] and is akin to that postulated in the mechanism for carbalumination reactions (eq. 5).[22] Unlike carbalumination, however, the formation of **2a** and **2b** is not slow. Rather,

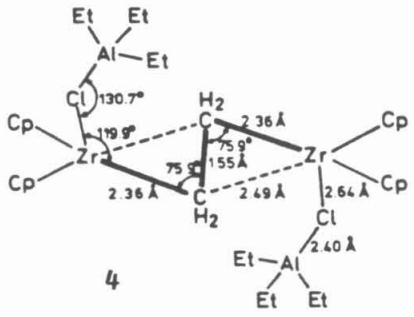

4

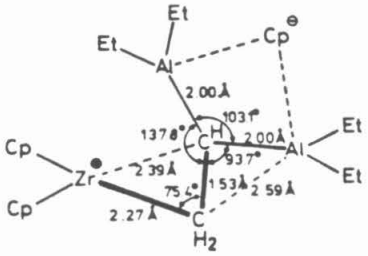

5

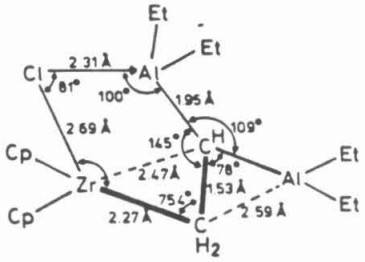

6

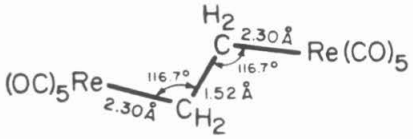

7

Figure 5. Comparison of the Corresponding Structural Elements of Compounds **4**, **5**, **6**[21b] and **7**.[21h]

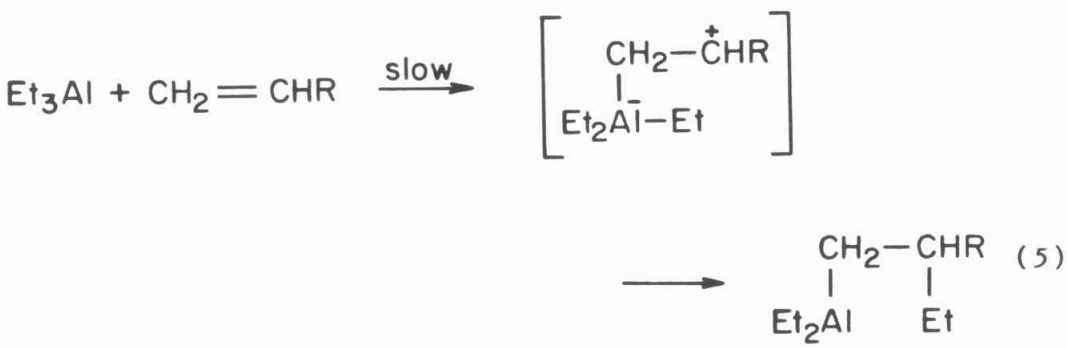

decomposition, which does occur to give ethane, is slow.

Reactivity of 2a and 2b. Compounds **4**, **5**, and **6** react with olefins and, in the presence of excess $AlEt_3$ and H_2O, form good Ziegler-Natta catalysts.[21b] Compounds **2a** and **2b** are less robust. Both decompose slowly to produce methane and ethane, respectively. The niobium product has not been identified since after one month <10% of the adduct has decomposed. Heating solutions of **2a** or **2b** speeds the decomposition, but it is also less clean. Compound **2b** does react with excess ethylene to quickly form an orange solution and solid. The ^1H NMR signals broaden quickly as ethane is formed. The reaction was not followed further.

$Cp^*_2\overset{+}{Nb}(D)(CD_2CD_2\bar{A}l(CH_2CH_3)_3)$ (**2b**-$\underline{d}_5$) was formed from the reaction of $Cp^*Nb(D)(CD_2CD_2)$ (**1**-$\underline{d}_5$) with $AlEt_3$. There was no increase in the size of the ^1H NMR signal of residual H for Nb-CD_2CD_2-Al over the course of one month. Thus, there is no exchange of ligands between the niobium and aluminum centers.

Compound **2b** reacts cleanly with excess CO, ultimately producing $Cp^*_2Nb(H)(COAlEt_3)$ (**7**) (Scheme II). An intermediate is observed (^1H NMR) during the course of the reaction. Although the identity of this intermediate cannot be definitively assigned, the rate of the formation of **7** from the

Scheme II. Alternative Mechanisms for the Production of **7** from **2b**

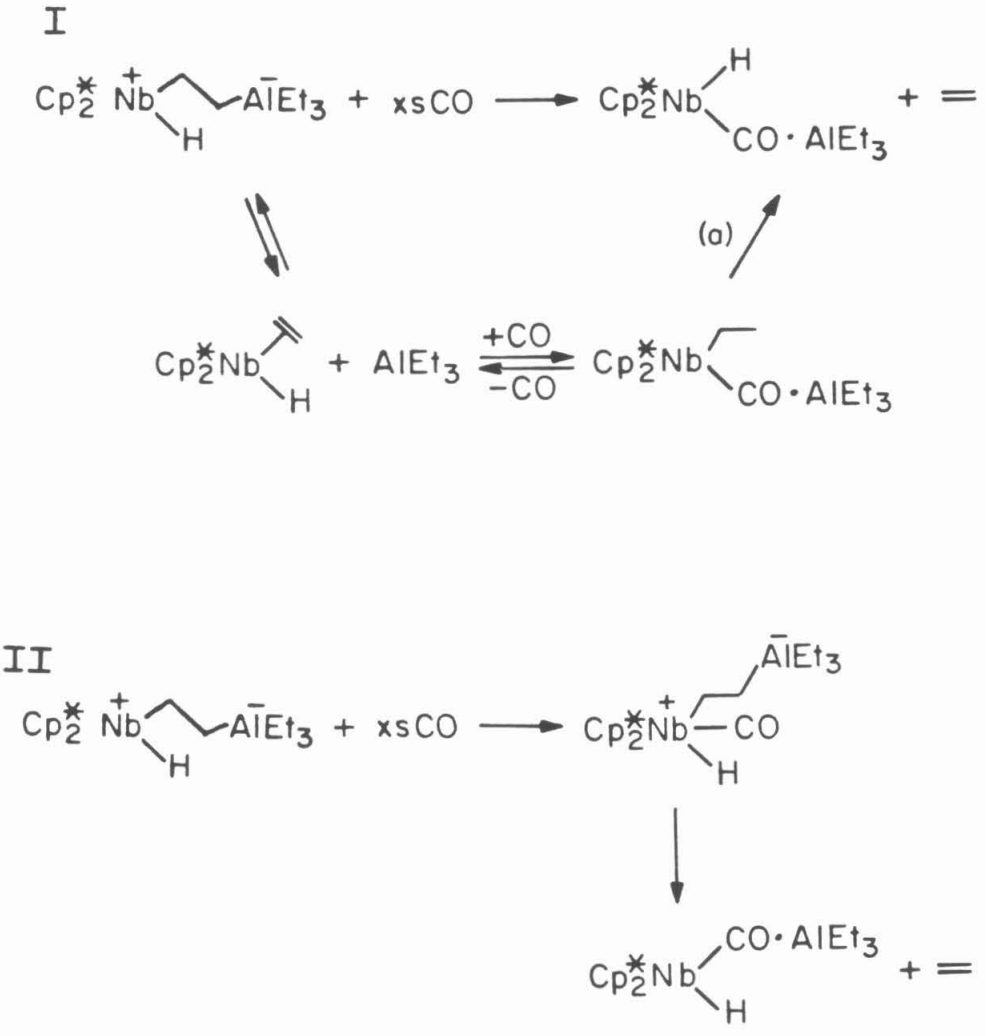

intermediate is qualitatively the same as that for the formation of **7** from $Cp^*_2Nb(CH_2CH_3)(COAlEt_3)$.[9] The independent observation of reaction (a) in Scheme II supports mechanism I over unprecedented alternatives such as mechanism II.

Related Reactions. The coordination of trialkylaluminum compounds to coordinated ethylene encouraged exploration of other Lewis acid and transition metal systems. Changing the Lewis acid was not successful; trimethylborate did not react while BF_3, $AlMe_2Cl$, and $AlBr_3$ all reacted to produce magenta products that are insoluble in benzene.

Triethylaluminum reacts rapidly with the endo-propene adduct $Cp^*_2Nb(H)(CH_2{=}CHMe)$ (**8**). The product of this reaction, **9**, shows a single Cp* resonance and exchange broadened resonances for $AlEt_3$, the $-CH_2CHR-$ resonances, and Nb-H, the latter not seen in the 89.6 MHz ^1H NMR spectrum obtained at 34°C. Cooling the sample sharpens all but the $AlEt_3$ resonances until, at -31°C, the spectrum resembles that of **8** at -40°C.[10b,11] These spectral changes are similar to those observed for **8** alone except that at room temperature ethane (from $AlEt_3$, which decreases in intensity) is evolved and two new niobium products are formed in succession. The first contains a Nb-H resonance at δ -2.4, the second at δ -9.0. Other changes occur, but they are less clearly resolved. Thus, $AlEt_3$ does react with the propene complex **8** but clear evidence for an adduct structure similar to that of **2b** is not observed.

The reactions of $AlMe_3$ and $AlEt_3$ with the styrene complex $Cp^*_2Nb(H)(CH_2{=}CHPh)$ (**10**) are similar. Minor changes in the ^1H NMR spectrum of **10** occur when $AlMe_3$ or $AlEt_3$ is added. Methane and ethane,

respectively, evolve over the course of one day as the Al compound's signals decrease in intensity. Changes observed for the signals due to **10** over this same period are not easily described. Clear evidence for an adduct structure is not observed.

The 2-butyne complex $Cp^*_2Nb(H)(CH_3C{\equiv}CCH_3)$ is unreactive toward $AlEt_3$, even after two days in room temperature solution. No ethane is evolved.

The 16-electron ethylene complex $Cp^*_2Ti(C_2H_4)$ (**12**)[10a] was also reacted with $AlEt_3$. The singlet due to the ethylene protons is shifted upfield (from δ 2.02 to δ 1.73) and the $AlEt_3$ protons are broad. The spectrum changes very little as the temperature is lowered, however. Over the course of two days ethane evolves and the $AlEt_3$ resonances diminish. Since adduct formation was not clearly indicated, the reaction was not followed.

Conclusion

This study has shown the ethylene-hydride compound $Cp^*_2Nb(H)(C_2H_4)$ (**1**) reacts with trialkylaluminum compounds to form 1:1 adducts $Cp^*_2\overset{+}{N}b(H)(CH_2CH_2\bar{A}lR_3)$ (R = Me, **2a**; Et, **2b**) containing $Nb\text{-}CH_2CH_2\text{-}Al$ bridges. A <u>trans</u> structure about the ethylene bridge is proposed. While X-ray structural evidence has not yet been obtained, ^1H NMR and IR data support this proposition. This study has been limited by the inability to obtain other examples of this bonding. The relatively stable nature of **2a** and **2b** has not been observed in the reactions of trialkylaluminum reagents with other early transition metal-olefin compounds, and the niobium-2-butyne compound does not react with AlR_3 either.

The equilibrium nature of the adducts **2a** and **2b** in solution may prevent the acquisition of structure quality crystals. Work is currently underway in the permethyltantalocene system to determine if the tantalum analogues of **2a** and **2b** will be more stable.[28]

Experimental Section

General Considerations. All manipulations were performed using glovebox or high vacuum line techniques. Solvents were dried over $LiAlH_4$ or Na/benzophenone and stored under vacuum over "titanocene".[29] The NMR solvents, benzene-$\underline{d}_6$ and toluene-$\underline{d}_8$, were dried over activated molecular sieves (4 Å, Linde) and stored over "titanocene". Argon was passed over MnO on vermiculite and activated molecular sieves.[30] Carbon monoxide (Matheson) was used directly from the cylinder. Ethylene was purified by three freeze-pump-thaw cycles. Trimethylaluminum (Aldrich) was used as a 2 M solution in toluene. Triethylaluminum (Aldrich) and dimethylaluminum chloride (Aldrich) were used as neat liquids. Aluminum tribromide (Aldrich) was sublimed under vacuum and stored under nitrogen. Boron trifluoride (Research Organic/Inorganic Chemical) was used directly from the cylinder. Trimethylborate (Aldrich) was degassed and stored over activated molecular sieves. $Cp^*_2Nb(H)(C_2H_4)$ (**1**),[10] $Cp^*_2Nb(D)(C_2D_4)$ (**1**-$\underline{d}_5$),[10b] $Cp^*_2Nb(H)$-$(CH_2{=}CHR)$ (R = Me, **8**; Ph, **10**),[10b,11] $Cp^*_2Nb(H)(MeC{\equiv}CMe)$,[10b] and $Cp^*_2Ti(C_2H_4)$[10a] were prepared as previously reported.

Many reactions were surveyed using NMR spectroscopy. Any experiment described in the body of the chapter but not explicitly listed below was carried out in a sealed NMR tube utilizing ~30 mg of the starting material in ~0.3 mL of benzene-$\underline{d}_6$ containing TMS or, for variable temperature experiments, toluene-$\underline{d}_8$ to which a known amount of the appropriate reagent could be added before the tube was sealed at -196°C.

Nuclear magnetic resonance spectra were recorded on Varian EM 390

(90 MHz, ^1H), JEOL FX90Q (89.56 MHz, ^1H) and Bruker WM500 (500.13 MHz, ^1H) spectrometers utilizing standard parameters. Routine infrared spectra were recorded on a Beckman 4240 spectrophotometer using KBr windows and are reported in cm^{-1}. Equilibrium infrared spectroscopic studies employed the Mattson Sirius 100 FTIR with the Starlab UNIX data system. Elemental analyses were determined by the Caltech Analytical Facility.

(1) $Cp^*_2\overset{+}{N}b(H)(CH_2CH_2\bar{A}lMe_3)$ (2a). $Cp^*_2Nb(H)(C_2H_4)$ (1) (0.503 g, 1.28 mmol) was placed in a round-bottom flask. Petroleum ether (∿7 mL) was condensed onto the yellow solid at -78°C. An $AlMe_3$/toluene solution (0.64 mL, 1.28 mmol) was added to the cooled solution by syringe. The reaction mixture was allowed to warm to 24°C with stirring for 15 min. A pale yellow solid was immediately evident. The solution volume was reduced (∿3 mL) and the pale yellow solid **2a** was collected by cold (-78°C) filtration (0.475 g, 1.02 mmol, 79.7%). The solid was refrigerated under N_2. If left at room temperature, the solid slowly becomes orange. ^1H NMR (C_6D_6, 34°C): 1.61 (s, 30, Cp*), 0.18 (AA'BB' m, 4, -$C\underline{H}_2C\underline{H}_2$-), -0.21 (s,br, 9, $AlC\underline{H}_3$), -2.73 (s,br, 1, Nb-$\underline{H}$). IR (nujol): 1769 (w), 1704 (w), 1487 (w), 1172 (m), 1132 (w), 1079 (m), 1022 (m), 934 (w), 799 (w), 688 (m), 650 (m), 607 (m), 509 (w), 470 (w), 411 (m).

Anal. calcd. for $C_{25}H_{44}AlNb$: C, 64.64; H, 9.55. Found: C, 64.40; H, 9.52. MW calcd. (Found, Cryoscopic): 464.52(376).[31]

(2) $Cp^*_2\overset{+}{N}b(H)(CH_2CH_2\bar{A}lEt_3)$ (2b). $Cp^*_2Nb(H)(C_2H_4)$ (1) (0.463 g, 1.18 mmol) was placed in a round-bottom flask with petroleum ether (∿4 mL) and $AlEt_3$ (161 μL, 1.18 mmol). No color change was apparent as all solid went into solution. The solution was cooled to -78°C and the pale

yellow solid **2b** was collected by filtration (0.416 g, 0.82 mmol, 69.5%). The solid was refrigerated under N_2. ^1H NMR (C_6D_6, 34°C): 1.57 (s, 30, Cp*), 1.48 (t, J = 7 Hz, 9, $AlCH_2C\underline{H}_3$), 0.48 (q, J = 7 Hz, 6, $AlC\underline{H}_2CH_3$), 0.11 (AA'BB' m, 4, $-C\underline{H}_2C\underline{H}_2$), -2.40 (s,br, 1, Nb-$\underline{H}$). IR (nujol): 1762 (w), 1703 (w), 1487 (m), 1406 (m), 1224 (w), 1175 (m), 1131 (m), 1081 (m), 1022 (m), 987 (m), 970 (m), 942 (m), 912 (w), 721 (w), 629 (s), 462 (m), 412 (m).

Anal. calcd. for $C_{28}H_{50}AlNb$: C, 66.39; H, 9.95. Found: C, 66.08; H, 9.65.

(3) Equilibrium Constant Evaluation for 2b.[32] $Cp^*_2Nb(H)(C_2H_4)$ (1) (0.398 g) was dissolved in benzene in a 2 mL volumetric flask. This solution (0.507 M) and a solution prepared by diluting 0.5 mL of the first solution to 1 mL in a volumetric flask (0.254 M) were used to calibrate the instrument. The calibration curve using peak absorbance values for ν(Nb-H) = 1703 cm^{-1} followed Beer's Law from 0 to 0.507 M. The calibration curve was used to determine the concentration of uncomplexed **1** in 0.20 mL portions of the 0.507 M solution of **1** to which 6.95, 14.0, and 28.0 μL of $AlEt_3$ had been added and in a 0.20 mL portion of the 0.254 M solution of **1** to which 6.90 μL of $AlEt_3$ had been added. Analysis was based on equations 4a-c with $K_{Al} = [AlEt_3]^2_{eq}/[(AlEt_3)_2]_{eq}$, $K = [\mathbf{2b}]_{eq}/([\mathbf{1}]_{eq}[AlEt_3]_{eq})$ and $K_{Al}\cdot K = ([\mathbf{2b}]_{eq}[AlEt_3]_{eq})/([\mathbf{1}]_{eq}[(AlEt_3)_2]_{eq})$. The value of $[\mathbf{2b}]_{eq}$ was determined by subtraction of $[\mathbf{1}]_{eq}$ from the known total concentration of **1** added. The values of $[AlEt_3]_{eq}$ and $[(AlEt_3)_2]_{eq}$ were determined by using the relationship $[AlEt_3]_T - [\mathbf{2b}]_{eq} = 2[(AlEt_3)_2]_{eq} + [AlEt_3]_{eq}$, assuming $[AlEt_3]_{eq} \approx 0$ to determine $[(AlEt_3)_2]_{eq}$ and then

using that value in the equation for K_{Al} ($K_{Al} = 2.22 \times 10^{-5}$ M for $AlEt_3$ in benzene)[20] to determine $[AlEt_3]_{eq}$. Generally, $[(AlEt_3)_2]_{eq} \simeq 10^{-1}$ and $[AlEt_3] \simeq 10^{-3}$, so the approximation is reasonable.

References and Notes

(1) Parshall, G. W. "Homogeneous Catalysis"; John Wiley & Sons: New York, 1980.

(2) Ziegler, K. In "Organometallic Chemistry", Zeiss, H. (ed.); Reinhold: New York; 1960, pp 194-195, 229-231.

(3) Mole, T.; Jeffery, E. A. "Organoaluminum Compounds"; Elsevier Publishing: New York; 1972, Chapter 15.

(4) Boor, J., Jr. "Ziegler-Natta Catalysis and Polymerization"; Academic Press: New York, 1979.

(5) Jonas, K.; Kruger, C. Angew. Chem. Int. Ed., Engl. **1980**, 19, 520-537.

(6) Holton, J.; Lappert, M. F.; Ballard, D. G. H.; Pearce, R.; Atwood, J. L.; Hunter, W. E. J. Chem. Soc., Dalton Trans. **1979**, 45-53.

(7) Scollary, G. R. Austral. J. Chem. **1978**, 31, 411-414.

(8) Wilke, G. Presented at the 23rd International Conference on Coordination Chemistry; Boulder, Colorado; July 29-August 3, 1984.

(9) Chapter III of this thesis.

(10) (a) Cohen, S. A. Ph.D. Thesis, California Institute of Technology, 1982. (b) Doherty, N. M. Ph.D. Thesis, California Institute of Technology, 1984.

(11) Doherty, N. M.; Bercaw, J. E. J. Am. Chem. Soc. in press.

(12) Tebbe, F. N. J. Am. Chem. Soc. **1973**, 95, 5412-5414.

(13) Unlike the carbonyl compounds described in Chapter III of this thesis, these solids are not microcrystalline.

(14) Tebbe, F. N.; Parshall, G. W. J. Am. Chem. Soc. **1971**, 93, 3793-3795.

(15) (a) The collapse of the AA'BB' pattern to a broad "singlet" is due to accidental overlap of ν_A and ν_B. A similar pattern of collapse has been seen for the disubstituted ethane moiety in benzyl acetone ($Ph\text{-}CH_2CH_2\text{-}COCH_3$) as the solvent is varied. Danyluk, S. S. Can. J. Chem. **1963**, 41, 387-392. (b) The variable temperature ^1H NMR spectrum of **2a** is similar, but the "singlet" occurs at a much lower temperature.

(16) (a) Bovey, F. A. "Nuclear Magnetic Resonance Spectroscopy"; Academic Press: New York, 1969; Chapters 4 and 5 and Appendix D. (b) Pople, J. A.; Schneider, W. G.; Bernstein, H. J. "High Resolution Nuclear Magnetic Resonance"; McGraw-Hill: New York, 1959; Chapter 6 and references cited therein.

(17) The electronegativities of Al and Nb are 1.5 and 1.6, respectively. Disubstituted ethanes in which the electronegativities of X and Y are great result in AA'XX' spectra. See ref. 23.

(18) The structure of **2a** and **2b** is based on the analogy to disubstituted ethanes. It will be discussed further.

(19) (a) Kotz, J. C.; Turnipseed, C. D. J. Chem. Soc., Chem. Commun. **1970**, 41-42. (b) Burlitch, J. M.; Leonowics, M. E.; Peterson, R. B.; Hughes, R. E. Inorg. Chem. **1979**, 18, 1097-1105. (c) Mayer, J. M.; Calabrese, J. C. Organometallics **1984**, 3, 1292-1298.

(20) The method is described in the Experimental Section. K_{A1} in benzene was obtained from: Smith, M. B. J. Organomet. Chem. **1974**, 70, 13-33.

(21) (a) Erker, G.; Kropp, K.; Atwood, J. L.; Hunter, W. E.

Organometallics **1983**, 2, 1555-1561. (b) Kaminsky, W.; Kopf, J.; Sinn, H.; Vollmer, H.-J. Angew. Chem. Int. Ed., Engl. **1976**, 15, 629-630. (c) Kaminsky, W.; Vollmer, H.-J. Liebigs Ann. Chem. **1975**, 438-448. (d) Kaminsky, W.; Sinn, H. Ibid. 424-437. (e) Kopf, J.; Kaminsky, W.; Vollmer, H.-J. Cryst. Struct. Comm. **1980**, 9, 197-201. (f) Kopf, J.; Vollmer, H.-J.; Kaminsky, W. Ibid. 271-276. (g) Beck, W.; Bauer, H.; Nagel, U.; Raab, K.; Olgemöller, B.; Olgemöller, L.; Schloter, K.; Sükel, K.; Urban, G. Presented at the XI International Conference of Organometallic Chemistry; Callaway Gardens, Pine Mountain, Georgia, October 10-14, 1983. (h) Raab, K.; Nagel, U.; Beck, W. Z. Naturforsch. B **1983**, 38, 1466-1476.

(22) (a) Eisch, J. J. "Aluminum" in "Comprehensive Organometallic Chemistry", Wilkinson, G.; Stone, F. G. A.; Abel, E. W. (eds.); Pergamon Press: Oxford, 1982. (b) Eisch, J. J. Adv. Organomet. Chem. **1977**, 16, 67-109. (c) Ref. 3.

(23) (a) Whitesides, G. M.; Witanowski, M.; Roberts, J. D. J. Am. Chem. Soc. **1965**, 87, 2854-2862. (b) Witanowski, M.; Roberts, J. D. Ibid. **1966**, 88, 737-741. (c) Fraenkel, G.; Dix, D. T.; Carlson, M. Tetrahedron Lett. **1968**, 579-582.

(24) This inversion is slowed considerably by the addition of small amounts of ether.[23c] When 0.6 equivalent of ether was added to a toluene-d_8 solution of **2b**, $AlEt_3$ was complexed by the ether and uncomplexed **1** was observed by ^1H NMR. Thus, the effect of ether on the possible inversion cannot be checked in this system.

(25) Alkyl bridges are known,[6] and Wilke has recently presented X-ray

evidence for the coordination of an Al-CH_2CH_3 bonded to a nickel center in a manner analogous to that proposed in B and B'.[8]

(26) Brookhart, M.; Green, M. L. H. J. Organomet. Chem. **1983**, 250, 395-408.

(27) Hogeveen, H.; Jorritoma, H.; Wade, P. A. Tetrahedron Lett. **1974**, 3915-3918.

(28) The tantalum analogue of **2b** has been made. Gibson, V. C.; Bercaw, J. E. Unpublished results.

(29) Marvich, R. H.; Brintzinger, H. H. J. Am. Chem. Soc. **1971**, 93, 2046-2048.

(30) Brown, T. L.; Dickerhoff, D. W.; Botus, D. A.; Morgan, G. L. Rev. Sci. Instrum. **1962**, 22, 491-492.

(31) The molecular weight was determined cryoscopically in benzene. The low value obtained (±80) is probably due to the equilibrium of **2a** in solution producing more molecules in solution.

(32) (a) Rossotti, F. J. C.; Rossotti, H. "The Determination of Stability Constants"; McGraw-Hill: New York, 1961; Chapter 13. (b) Colthrup, N. B.; Daly, L. H.; Wiberley, S. E. "Introduction to Infrared and Raman Spectroscopy", 2nd ed.; Academic Press: New York, 1975.